

## Facilitation of the development of concrete fuse blocks in southern countries

**Auteur :** Achary, Kawthar

**Promoteur(s) :** Epicum, Sébastien

**Faculté :** Faculté des Sciences appliquées

**Diplôme :** Master en ingénieur civil des constructions, à finalité spécialisée en "civil engineering"

**Année académique :** 2023-2024

**URI/URL :** <http://hdl.handle.net/2268.2/20431>

---

### *Avertissement à l'attention des usagers :*

*Tous les documents placés en accès ouvert sur le site le site MatheO sont protégés par le droit d'auteur. Conformément aux principes énoncés par la "Budapest Open Access Initiative"(BOAI, 2002), l'utilisateur du site peut lire, télécharger, copier, transmettre, imprimer, chercher ou faire un lien vers le texte intégral de ces documents, les disséquer pour les indexer, s'en servir de données pour un logiciel, ou s'en servir à toute autre fin légale (ou prévue par la réglementation relative au droit d'auteur). Toute utilisation du document à des fins commerciales est strictement interdite.*

*Par ailleurs, l'utilisateur s'engage à respecter les droits moraux de l'auteur, principalement le droit à l'intégrité de l'oeuvre et le droit de paternité et ce dans toute utilisation que l'utilisateur entreprend. Ainsi, à titre d'exemple, lorsqu'il reproduira un document par extrait ou dans son intégralité, l'utilisateur citera de manière complète les sources telles que mentionnées ci-dessus. Toute utilisation non explicitement autorisée ci-avant (telle que par exemple, la modification du document ou son résumé) nécessite l'autorisation préalable et expresse des auteurs ou de leurs ayants droit.*

---



UNIVERSITY OF LIÈGE  
FACULTY OF APPLIED SCIENCES

---

FACILITATION OF THE DEVELOPMENT OF  
CONCRETE FUSE BLOCKS IN SOUTHERN  
COUNTRIES

---

Master's thesis

completed in order to obtain the degree of Master in Civil Engineering

conducted by ACHARY KAWTHAR

*Supervisor:*  
S. ERPICUM

*Jury:*  
M. PIROTON  
J-F. DEMONCEAU  
N. NERINCX

ACADEMIC YEAR  
2023 – 2024



# Acknowledgements

First and foremost, I am deeply grateful to my supervisor, Mr. Sébastien Erpicum, for the opportunity to work on a subject that is especially meaningful to me. His constant guidance, invaluable advice, and enthusiasm for this topic have been indispensable in my completion of this work.

I would also like to express my sincere gratitude to the team at the Laboratoire d'Hydraulique, particularly Grégory Thonard, Maxime Mathieu, and Claude Lhermerout, whose help was indispensable in carrying out my experimental tests. Their expertise, advice, and encouragement were essential throughout this work.

I am thankful to Clément Delhez and Vincent Schmitz for their valuable advice, encouragement, and reassurance when I needed it.

Heartfelt thanks to my friends for their support during my five years at university. Margaux and Hulya, in particular, have made these years truly enjoyable, and I am especially grateful to Puhia for our mutual support during both joyful and anxious times.

Last but not least, I would like to thank my family for enduring my ups and downs, and in particular my mum, without whom I would not have been able to complete my studies.

# Abstract

The utilization of concrete fuse plugs presents a promising solution for enhancing dam safety and increasing water storage capacity. Developed by the HydroCoop association, this technology addresses critical needs in regions like Burkina Faso, where small dams face significant challenges in water management. Consequently, the development of practical methods to facilitate the implementation of these plugs becomes imperative. This project's primary objective was to contribute to this research.

The methodology involved in this study encompasses a literature review, experimental testing, and analytical modelling.

Experimental tests were conducted on scaled models using blocks with underpressure and varying widths. Two configurations were examined for individual block tilting: when placed alone on the sill, and when adjacent blocks were fixed beside them. These tests revealed parameters affecting block overturning heights, such as the lateral friction effect.

Comparisons of the results with existing formulas highlighted the necessity for a new analytical model, improving the accuracy of block tipping prediction.

A practical design table was developed based on the model. In addition, recommendations derived from literature and tests conducted in this study were formulated to facilitate plug design and installation.

In conclusion, this study provides valuable insights into the design and implementation of fuse plugs for future projects and the development of practical usage guidelines.

# Résumé

L'utilisation de blocs fusibles en béton représente une solution prometteuse pour renforcer la sécurité des barrages et augmenter la capacité de stockage d'eau. Développée par l'association HydroCoop, cette technologie répond à des besoins critiques de régions comme le Burkina Faso, où les petits barrages rencontrent d'importants défis en matière de gestion de l'eau. Par conséquent, le développement de méthodes pratiques pour faciliter la mise en œuvre de ces blocs devient impératif. L'objectif principal de ce projet était de contribuer à cette recherche.

La méthodologie utilisée dans cette étude comprend une revue de la littérature, des tests expérimentaux et la modélisation analytique.

Des essais ont été réalisés sur des modèles réduits à l'aide de blocs avec sous-pression de largeurs variées. Deux configurations ont été examinées pour le basculement individuel des blocs: lorsqu'ils sont placés seuls sur le seuil et lorsque des blocs adjacents sont fixés à côté d'eux. Ces tests ont révélé des paramètres influençant les hauteurs de basculement des blocs, tels que l'effet de frottement latéral.

Les comparaisons des résultats avec des formules existantes ont souligné la nécessité d'un nouveau modèle analytique, améliorant la précision de la prédiction du basculement des blocs.

Une table de conception pratique a été développée sur la base du modèle analytique. De plus, des recommandations issues de la littérature et des discussions de ce travail ont été formulées pour faciliter la conception et l'installation des blocs.

Pour conclure, cette étude apporte des perspectives sur la conception et l'implémentation des blocs fusibles dans les projets à venir, tout en ouvrant la voie au développement de guides pratiques pour leur utilisation.

# Table of Contents

<b>Notation</b>	<b>iii</b>
Abbreviations . . . . .	iv
<b>Introduction</b>	<b>1</b>
<b>1 Background</b>	<b>3</b>
1.1 Definition of fuse plug . . . . .	3
1.2 Scope of use . . . . .	5
1.3 Principle of concrete fuse plug . . . . .	6
1.4 Design of fuse plug . . . . .	8
1.4.1 Fuse plugs without underpressure . . . . .	9
1.4.2 Fuse plugs with underpressure . . . . .	11
1.4.3 Conditions of use of concrete fuse block . . . . .	13
1.5 Construction of fuse plugs . . . . .	14
1.5.1 After tilting . . . . .	14
1.6 Objectives of this work . . . . .	15
<b>2 Methodology</b>	<b>16</b>
2.1 Experimental setup . . . . .	16
2.1.1 Fuse plugs . . . . .	17
2.1.2 Piano Key weir . . . . .	23
2.1.3 Observable zone . . . . .	25
2.2 Measurement devices . . . . .	25
2.2.1 Determination of hydraulic head . . . . .	25
2.2.2 Determination of flow rate . . . . .	28
2.3 Data processing . . . . .	29
2.3.1 Replacement of outliers . . . . .	29
2.3.2 Signal smoothing . . . . .	30
2.3.3 Identification of plateaus . . . . .	31
2.3.4 Result Types . . . . .	33
2.4 Tests . . . . .	35
2.4.1 Configurations . . . . .	35
2.4.2 Procedure . . . . .	37
<b>3 Results</b>	<b>38</b>
3.1 Presentation of results for configurations 1 and 2 . . . . .	38
3.1.1 B10 block . . . . .	38
3.1.2 B20 & B30 blocks . . . . .	40
3.1.3 B40, B50 & B60 blocks . . . . .	41
3.2 Analysis and discussions . . . . .	42
3.2.1 Influence of the position on the sill . . . . .	42
3.2.2 Influence of adjacent blocks . . . . .	43
3.2.3 Influence of friction . . . . .	43

3.2.4	Determination of the tilting head . . . . .	44
<b>4</b>	<b>Analytical model</b>	<b>46</b>
4.1	Formulas from the literature . . . . .	46
4.1.1	Comparison of formulas with experimental results . . . . .	48
4.1.2	Conclusion . . . . .	51
4.2	Development of a new analytical model . . . . .	51
4.2.1	Comparison of the new model with the results . . . . .	54
4.2.2	Adjusting the analytical model based on the results . . . . .	55
4.2.3	Sensitivity analysis . . . . .	57
4.3	Analysis and discussions . . . . .	60
4.3.1	Comparison of the new model with previous formulas . . . . .	61
4.3.2	Pressure diagrams . . . . .	61
4.3.3	Influence of geometric and physical parameters . . . . .	63
4.3.4	Analysis of block B10 results . . . . .	64
<b>5</b>	<b>Application</b>	<b>66</b>
5.1	Practical design table . . . . .	66
5.1.1	Simplified equation . . . . .	66
5.1.2	Design chart definition . . . . .	68
5.2	Recommendations for the design and installation of concrete fuse blocks . . . . .	71
	<b>Conclusion</b>	<b>81</b>

# Notation

$b$	Upstream width of the concrete fuse plug (perpendicular to flow direction)	m
$c$	Block chamfer height and length	m
$e$	Fuse plug length (in flow direction)	m
$i$	Height of the block's lower underpressure chamber	m
$s$	Width of block supports delimiting the lower underpressure chamber	m
$B$	Downstream width of the concrete fuse plug (perpendicular to flow direction)	m
$C_d$	Flow coefficient of the fuse plugs	-
$D_{sensor}$	Distance between the sensor and the water level	m
$H_{dam}$	Maximum head of the dam	m
$H_{PKW}$	Hydraulic head of the Piano Key weir	m
$H_{plug}$	Hydraulic head of the concrete fuse plugs	m
$H_{safe}$	Percentage representing the available distance relative to $H_{dam}$ when the water level reaches the tipping level of the block	m
$H_{tilting}$	Tipping head of a block predicted by the simplified analytical model	m
$H_{th}$	Tipping head of a block predicted by the new analytical model	m
$H_{2007}$	Tipping head of a block predicted by the Hien & Khanh formula	m
$L$	Length of the sill where the blocks are placed	m
$M$	Mass of the fuse plug	kg
$P$	Fuse plug height	m
$P_{dam}$	Height of the block expressed as a percentage of $H_{dam}$	m
$Q_{in}$	Flow rate injected into the model	l/s
$Q_{PKW}$	Flow rate through the Piano Key weir	l/s
$Q_{plug}$	Flow rate spilling over the block	l/s
$V_D$	Volume of water displaced	m <sup>3</sup>
$V_{Distance}$	Voltage expressing the distance between the sensor and the water level	V
$V_{flow}$	Voltage expressing the flow rate injected into the model	V

$\alpha$	Reduction factor of the vertical pressure applied on the fuse plug (for the new analytical model)	-
$\beta$	Reduction factor of the vertical pressure applied on the fuse plug (Hien & Khanh formula)	-
$\Delta_{Density}$	Accuracy of the block density	kg/m <sup>3</sup>
$\Delta_{length}$	Accuracy of the block length	m
$\Delta_{outliers}$	Maximum variation accepted between two consecutive values to determine outliers	m or l/s
$\Delta_P$	Accuracy of the block height	m
$\Delta_{plateau}$	Maximum limit of variation to determine the plateaus of a signal	m or l/s
$\Delta_{Tipping}$	Accuracy of the tipping head	m
$\Delta_{H,max}$	Maximum variation in head over a plateau	m
$\gamma_b$	Specific weight of the concrete fuse plug	N/m <sup>3</sup>
$\gamma_w$	Specific weight of water	N/m <sup>3</sup>
$\rho_b$	Block density	kg/m <sup>3</sup>
$\rho_w$	Water density	kg/m <sup>3</sup>

## Abbreviations

D/S	Downstream
PKW	Piano Key weir
U/S	Upstream

# Introduction

The regions of Africa with small dams face major challenges, such as the significant loss of water storage and the risk of accidents.

Durand et al. point out in their book [Durand et al. 1999] that effective management of water resources is crucial for Africa's development. Indeed, all vital activities such as agriculture, livestock farming, domestic chores and construction are particularly dependent on surface water. For several decades now, small dams have been springing up, providing invaluable help in distributing the water needed.

According to a 2021 report by Kibret and his colleagues [Kibret et al. 2021], there are an estimated 4,907 small dams in Africa's four main river basins: Limpopo, Omo-Turkana, Volta and Zambezi. Many African communities are now reliant on these structures for their water supply.

Burkina Faso has 1453 small dams listed in the African Development Bank (ADB) database maintained by the Directorate General of Hydraulic Infrastructure and Sanitation (DGIRH), as reported by Philippe Cecchi [Cecchi 2006]. This makes Burkina Faso the country with the largest number of such infrastructures. The oldest date from the end of the 19th century and are mainly located in the Bam region. Furthermore, it is on this country that research has partly focused.

Kabore et al. [Kabore et al. 2015] highlight that since the 1970s, the country has faced major changes in rainfall patterns, including prolonged periods of dry weather followed by alternating episodes of droughts and floods, resulting in recurrent famines. In response to these challenges, the government initiated a program to mobilise and store water by constructing small dams, aimed at fostering the development of rural communities.

However, the use of small dams faces a number of challenges.

The first problem is the rising demand for water, mainly due to demographic growth, as asserted by Kabore et al. [Kabore et al. 2015]. This increase in utilisation is leading to insufficient water resources to meet the needs of surrounding activities.

Alongside concerns about water distribution, there are increasing losses from reservoirs, mainly due to the nature of small dams.

Sedimentation represents the primary cause of reduced storage capacity. It occurs when water, carrying sediment, traverses catchment areas [Durand et al. 1999]. These sediments are transported until the water's velocity decreases, leading to their deposition, particularly noticeable when rivers reach reservoirs. This threat becomes pronounced after several decades of structure use.

Lempérière and Vigny [Lempérière and Vigny 2013] underscore the issue of evaporation, resulting in substantial water storage losses in Burkina Faso's dams. Evaporation is closely tied to the water body's surface area, a concern especially relevant for small dams known for their low height and extensive length. The book "Technique des petits barrages en Afrique sahélienne et équatoriale" [Durand et al. 1999] indicates that water loss through evaporation is particularly high in Sahelian regions, where they can average up to two metres per year. In these areas,



reservoirs with a height of less than two or three metres are generally emptied before the start of the rainy season.

In addition to reductions in storage due to external natural factors, Lempérière and Vigny [Lempérière and Vigny 2013] identified a problem linked to the design of dams. The flood flows to be considered are significant, often exceeding  $100 \text{ m}^3/\text{s}$ , and are usually managed by free spillways, which are long and relatively expensive. This makes it possible to preserve a valuable reservoir depth and limit the considerable increase in the volume of the dam. However, serious accidents and dam failures can occur, mainly as a result of flooding.

Moreover, Serge Marlet and his colleagues [Marlet et al. 2016] point out that almost half of these structures (around 47%) are in poor condition, with major maintenance and management problems. There are no clear standards for the design, construction, and maintenance of these structures, and no system for monitoring their condition. Some are now obsolete, damaged by erosion or even destroyed by run-off, while others retain less water or dry out prematurely due to the accumulation of sand or silt. This makes them particularly vulnerable to extreme flooding, especially in the context of climate change.

Having considered these challenges facing certain regions of Africa, it is clear that it is essential to find solutions to improve not only the water storage capacity of dams, but also their safety. It is therefore necessary, on the one hand, to increase the elevation of the spillway crest and, on the other, to allow more effective evacuation of flood flows. In addition, it is crucial to take into account higher flood flows than those currently forecast.

One possible solution to these challenges is to use concrete fuse plugs, a technology developed by the non-profit organisation HydroCoop [Kabore et al. 2015]. This cost-effective system raises the level of the spillway by placing blocks next to each other on the weir, thereby increasing the storage capacity of existing dam reservoirs. What is more, the fusible nature of these blocks makes them safer. Although this solution has been successful, having been implemented in Vietnam and on certain dams in Burkina Faso, there is currently no practical guide available to provide straightforward instructions on sizing these blocks.

The aim of this work is therefore to facilitate the development of concrete fuse plugs by proposing a simplified table for their design, as well as recommendations to complement those already available in the literature. Additionally, this work has the objective to provide a summary of key information, presented in a clear and accessible manner, so that designers can easily understand the steps to be followed and the critical points to consider when designing and installing fuse blocks on a weir.

This project is divided into several parts.

Chapter 1 presents a review of the literature in order to understand what has already been studied about concrete fuse plugs.

Then, chapter 2 points out the methodology applied in this work, including an experimental and theoretical study. The setup of the tests and measurement devices are described. The protocols for processing data and conducting the tests are also explained. The experimental results are presented and discussed in chapter 3. The influence of various parameters on block tipping is demonstrated. In chapter 4, an analytical model describing the tilting of a concrete fusible plug is established. To do this, the previously developed formulas are analysed. Then, an equation adapted to the block studied is determined

These studies are used in chapter 5 to present recommendations for the design and installation of the blocks. Finally, besides a summary of the results, the limitations of the work and the perspectives for future research is outlined in the conclusion.

# Chapter 1

## Background

This chapter aims to review the literature to understand what has already been studied about concrete fuse plugs. Then, the objectives of this work are defined.

### 1.1 Definition of fuse plug

A *fuse plug* can be defined as an element placed on a spillway that has the characteristic of disappearing when the water level in a dam reaches the maximum capacity limit. The fall of the fuse plug increases the dam's spill potential by rapidly releasing water, which is particularly useful for flood management. Since this element is lost during exceptional floods, it must be replaced in the following weeks or months.

F. Lempérière [Lempérière 2017] highlights the integration of fuse plugs, a long-standing component within the broader category of fuse devices, into traditional hydraulic systems like gated or free-flow weirs. These newer technologies offer distinct advantages, notably their cost-effectiveness compared to gated spillways and their flexibility in managing various flood scenarios. Additionally, the combination of fuse devices with free-flow weirs has emerged as a promising solution. This association enhances the efficiency of traditional spillways, particularly in evacuating extreme floodwaters. Furthermore, the integration of fuse plugs with traditional weirs, such as Piano Key Weirs, can significantly increase the flow rate, up to five times, for the same water depth.

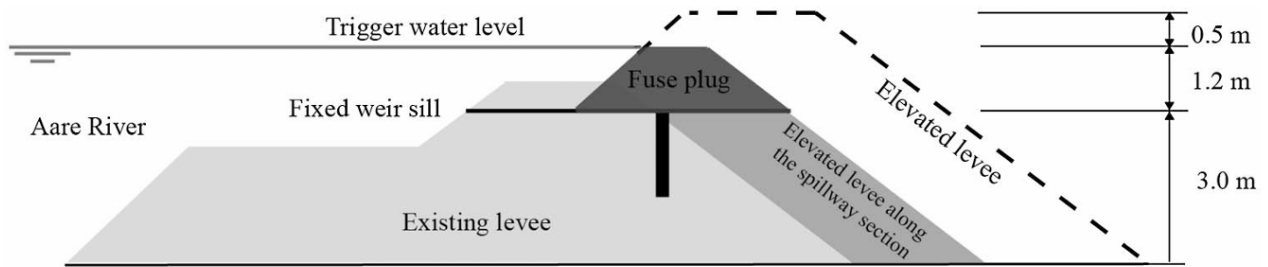
In the literature, the term *fuse plug* is used for two specific purposes.

On the one hand, the designation *fuse plug* refers to a component of a spillway made of erodible materials. This is a construction similar to a conventional embankment dam, but whose composition in terms of materials is particular, as shown in FIGURE 1.1. In 2017, according to F. Lempérière in the article “Dams and Floods” [Lempérière 2017], approximately a hundred earth fuse plugs had been constructed, predominantly during the 1980s in China and the United States. These plugs typically measure between 5 and 10 metres in height and are designed to handle flow rates of several thousand cubic metres per second. According to Johan Lagerlund [Lagerlund 2018], this technology is intended to be used as an emergency measure to protect the dam against overflows. Indeed, when the water level in the tank reaches the crest of the fuse plug, it begins to erode. The water level is predefined to completely wash away the materials in a predictable and controlled manner. The progressive erosion of this particular element makes it possible to increase the evacuation capacity. According to Schmocker et al. [Schmocker et al. 2013], this technology constitutes a safe alternative. Although it is necessary to rebuild the fuse plug once eroded, this is a cost-effective solution that allows for the improvement of existing spillways. In addition, fusible plugs have the advantage of being more natural than fixed concrete or steel structures. However, the success of this device is limited, which can be explained by the specific topography that is required. Furthermore, their long-term effectiveness is not

guaranteed, depending on the material.



(a) Photo of earth fuse plugs at the Warragamba Dam in Australia (from Reid)



(b) Diagram of a fuse plug in erodible materials (from Schmocker et al. [2013])

FIGURE 1.1: Earth fuse plugs

On the other hand, the term *fuse plug* can also be used to refer to concrete elements that can tip over. These type of plugs have been designed by the non-profit association HydroCoop in order to solve the storage problems encountered by small dams. For more than twenty years, this technology has been used. The system is installed at approximately a hundred dams, with evacuation capacities ranging from several hundred to twenty thousand cubic metres per second. Concrete fuse elements come in various shapes, including blocks, as depicted in FIGURE 1.2a, and labyrinth elements known as fuse gates, as illustrated in FIGURE 1.2b. The fusible plugs are an inexpensive solution for raising the level of existing weir crest. According to Lempérière & Vigny [Lempérière and Vigny 2013], they can improve free weirs either by increasing discharge capacity (and thus dam safety against flooding), increasing water storage, or combining these two effects.



(a) Photo of fuse blocks at Wedbila dam in Burkina Faso (from HydroCoop [2013])



(b) Photo of fuse gates at Terminus Dam in the United States (taken by Chris Austin)

FIGURE 1.2: Concrete fuse plugs

This work focuses only on concrete fuse blocks. Therefore, use of the term *fuse plug* will only refer to these blocks.

## 1.2 Scope of use

Fuse blocks can be used in two different situations: on new dams or on existing spillways [ICOLD - CIDGB 2010].

According to ICOLD [ICOLD - CIDGB 2010], in the case of new constructions, the use of fuse blocks makes it possible to double the evacuation rate of extreme floods, with approximately the same quantity of concrete and the same cost as without their use.

Concerning existing spillways, the installation of fuse blocks is an asset to improve their capacity. Indeed, either the crest of the sill is lowered, top diagram of the FIGURE 1.3, and the discharge rate is increased. Or, the crest of the blocks is greater than the initial level of the sill, bottom diagram of the FIGURE 1.3, and the storage of the reservoir is increased. Alternatively, the two solutions can be combined.

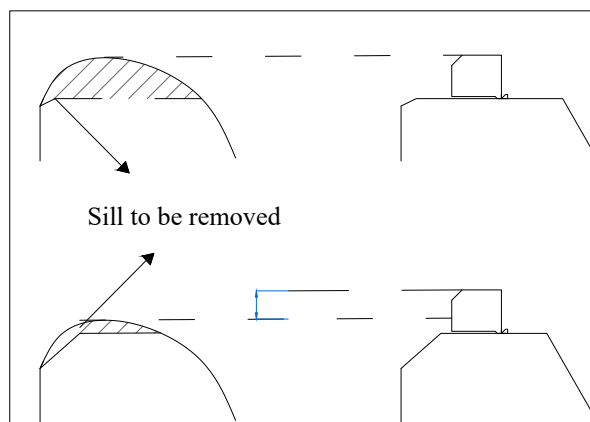


FIGURE 1.3: Representation of the uses of fuse blocks: increased security for the top diagram and increased storage for the bottom diagram (inspired by [ICOLD - CIDGB 2010])

### 1.3 Principle of concrete fuse plug

Fuse blocks are therefore massive concrete elements located side by side on the weir. They are designed to tilt when the water level in the reservoir reaches a certain point.

The operating principle of fuse plugs is based on their stability. The blocks are self-stable and resist water pressure thanks to their weight, FIGURE 1.4a. Then, the water level in the reservoir reaches a certain limit  $H_{plug}$ , FIGURE 1.4b, and the stability is broken. This hydraulic head causes the block to tip over, FIGURE 1.4c. After tilting, the block disappears completely and the weir reverts to a conventional weir, FIGURE 1.4d. This change instantly reduces the water level and increases discharge capacity.

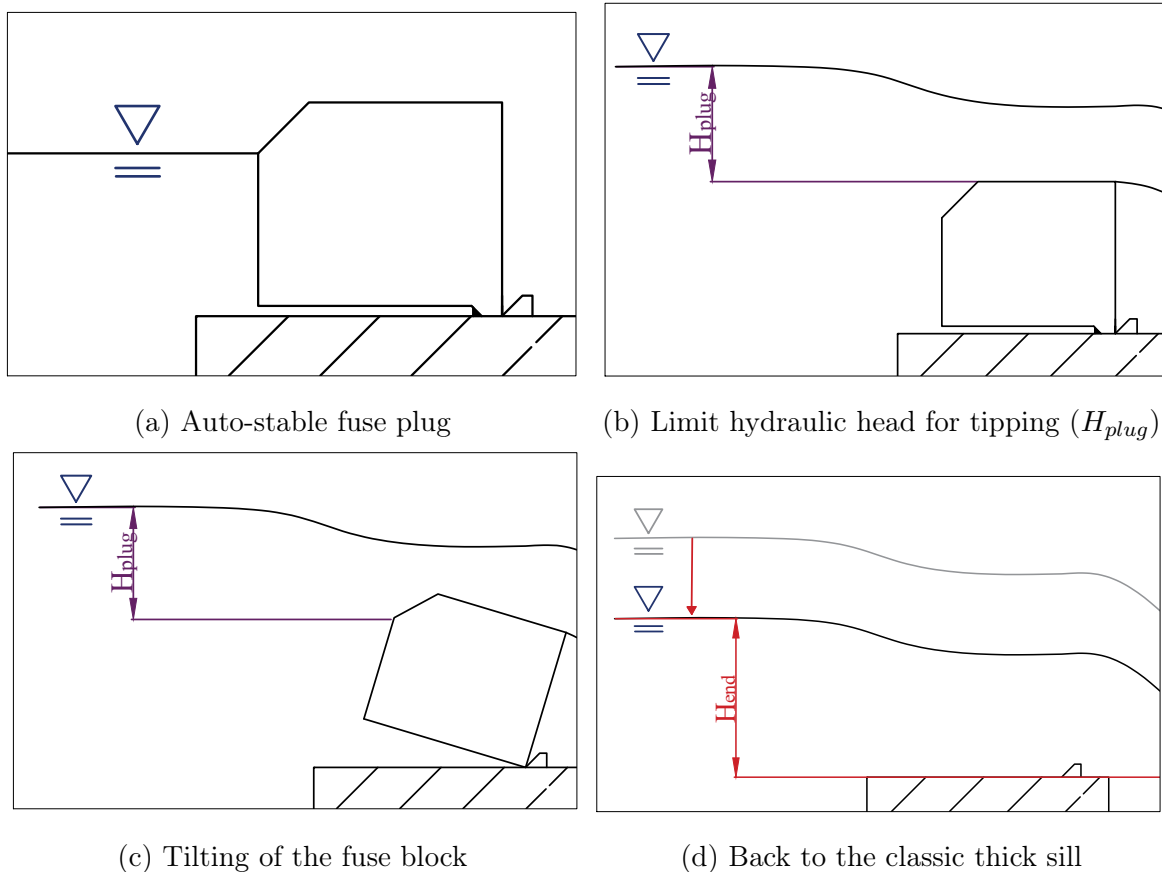


FIGURE 1.4: Operating principle of fuse block

Several factors influence this equilibrium, and are important to understand in order to determine the moment when the equilibrium is broken and the fuse block overturns.

The dimensions of the block itself are crucial in determining the tilting height. The weight of the block plays a stabilizing role in its equilibrium. Typically, elements positioned on the same weir share a common height, but they may vary in length (dimensions parallel to the flow direction), resulting in different weights and thus tipping at distinct water levels. Additionally, ICOLD [ICOLD - CIDGB 2010] suggests employing at least 4 to 5 blocks of varying lengths along a spillway, facilitating gradual tilting as the water level increases.

To improve the accuracy of determining the tipping level, one method is to accurately measure the underpressure exerted beneath the block [Lempérière and Vigny 2013]. This can be achieved by either imposing total or non-existent underpressure. Practically, it involves creating a lower chamber beneath each block. The chamber can either be open at the upstream end and sealed

at the downstream end (total underpressure, see FIGURE 1.5 on the left), or sealed at the upstream end and open at the downstream end (no underpressure, see FIGURE 1.5 on the right).

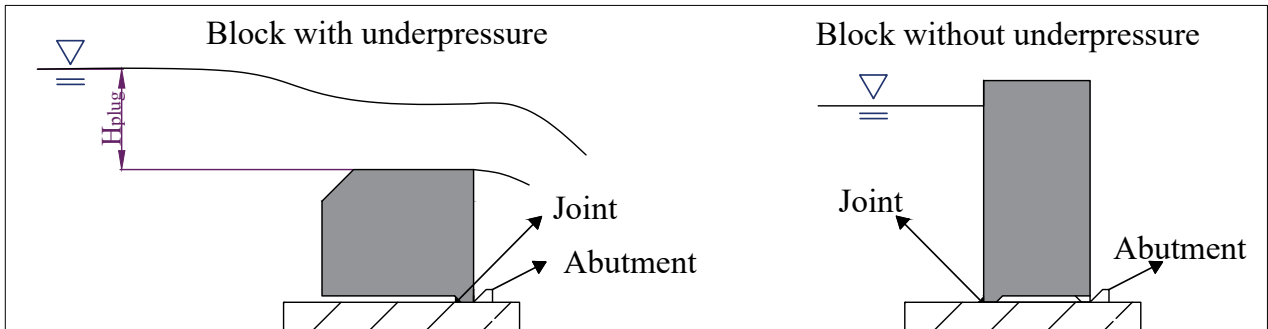


FIGURE 1.5: Diagram of a block with underpressure (left) and a block without underpressure (right) (inspired by Lempérière and Vigny [2013])

The tilting of a block influences the deformation of the water table on adjacent ones. To mitigate this effect, it is beneficial to place a thin vertical wall between two fuse plugs. Moreover, a greater precision on the water level causing the tipping of the remaining blocks is achieved. Numerous experimental tests have been carried out in various countries (France, Algeria, China, Vietnam) and coordinated by HydroCoop [Lempérière and Vigny 2013], demonstrating the benefits of using such dividers. These are especially important when the blocks are of small width (dimension perpendicular to the direction of the flow). The walls are generally fixed in the weir and do not need to be large. Typically, they have the same height as the blocks and a length equivalent to 1.2 times the plug length, as shown in FIGURE 1.6.

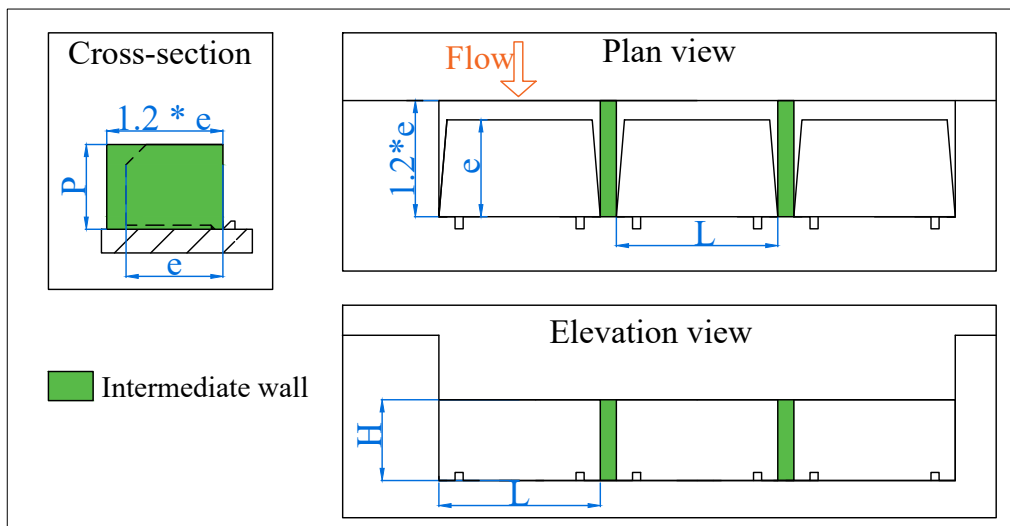


FIGURE 1.6: Diagram of general dimensions of intermediate walls (inspired by Lempérière and Vigny [2013])

To facilitate the overflow of water on the blocks, the upstream upper corners of the blocks can also be chamfered, as illustrated in FIGURE 1.5 to the left.

So that the blocks can tilt, they must be positioned upstream of the abutments. In addition, these elements make it possible to prevent the fuse plugs from sliding under the effect of external

solicitations. The abutments can be two small supports (as illustrated in FIGURE 1.6) fixed downstream on the sill or steel bars anchored into the weir.

According to ICOLD [ICOLD - CIDGB 2010], it is worth mentioning that experiments conducted on scale models have indicated that floating debris does not have a notable impact on water levels causing tipping.

## 1.4 Design of fuse plug

The tilting of the blocks depends on their stability, which is determined by the horizontal and vertical forces applied to them. These forces can be stabilizing or destabilizing and induce a moment of rotation calculated at the downstream abutment. The graph in FIGURE 1.7, defined by Lempérière & Vigny [Lempérière and Vigny 2013], illustrates the theoretical stability curves: the moments induced by horizontal effects (the “MH” curve) and those induced by vertical forces (the “MV” line).

These curves are a function of the water head “W” upstream, with “H” indicating the height of the block on the x-axis. The intersection of these two curves indicates the tilting point of the block. When the block thickness increases by 10%, the vertical moment line shifts to the dotted line “MV’”, indicating that the block is tilting under a higher “W” head.

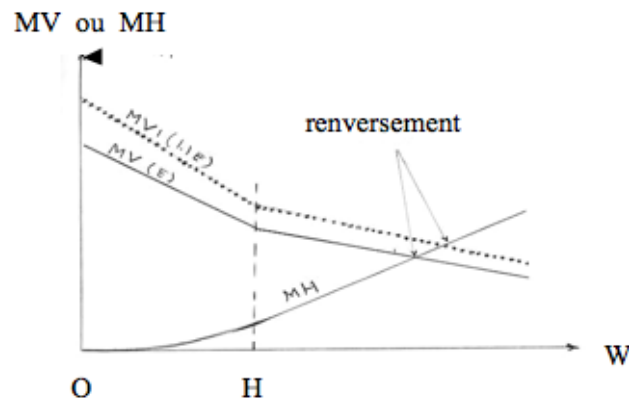


FIGURE 1.7: Stability diagram: evolution of the vertical and horizontal moment curves as a function of the upstream head (W) (diagram from [Lempérière and Vigny 2013])

According to the article "Economie et sécurité des déversoirs du Burkina Faso" [Lempérière and Vigny 2013], theoretical calculations were only sufficient to produce preliminary designs. As a result, it was recommended to carry out scale model tests to accurately determine the thicknesses required for overturning. Post-tilt calculations are complex due to the difficulties in determining the thickness of the water table, the pressure on the upper surface, as well as frictional and dynamic effects.

Since then, research has been carried out to develop simple formulas for designing blocks with or without underpressure.

### 1.4.1 Fuse plugs without underpressure

Lempérière & Vigny [Lempérière and Vigny 2013] have provided information on the dimensions of blocks without underpressure. In this case, the fuse plugs should be relatively taller than they are wide, with a height  $P$  of up to twice the width  $B$ . Additionally, this type of block allows for a reduction in the length  $e$ . Consequently, blocks that can topple over before being submerged serve as a safety barrier when the water height reaches a critical level.

#### Hien & Khanh (2006)

Researchers Hien & Khanh from Hô-Chi-Minh University of Technology conducted a study on blocks without underpressure, as illustrated in FIGURE 1.8 [Hien and Khanh 2006]. The main objective of this research was to compare the measured and calculated water levels at which simple concrete blocks tip, in two distinct scenarios:

- Tipping one block while keeping the other adjacent blocks stationary.
- Tipping the blocks successively according to their weight.

The aim of the study was to demonstrate that fuses are easily designed, reliable, and can be economically used as auxiliary spillways for small dams.

The researchers determined the calculated water levels ( $H_{plug}$ ) at which the blocks would topple over using the equilibrium of moments equation. The general formula used is as follows:

$$H_{plug} = \sqrt{\frac{3 \cdot M \cdot e}{\rho_w \cdot B}}^3 \quad (1.1)$$

where

- $H_{plug}$  is the upstream water depth above the block [m];
- $M$  corresponds to the mass of the block [kg];
- $e$  is the length of the block [m];
- $B$  is the upstream width of the block [m];
- $\rho_w$  is the density of water [kg/m<sup>3</sup>].

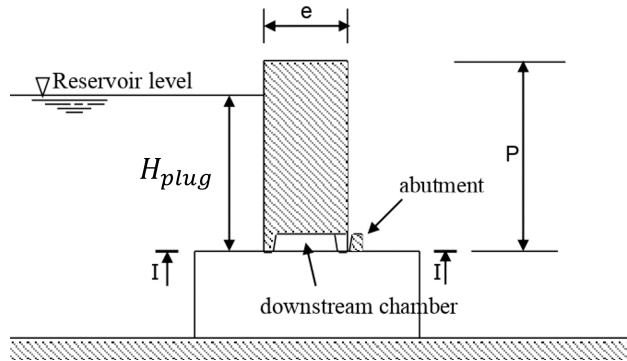


FIGURE 1.8: Diagram of the block geometry from [Hien and Khanh 2006]

Experimental tests were carried out in a 34-metre-long glass laboratory channel with a rectangular cross-section. The channel has a width of 0.60 metres, a side wall height of 0.65 metres and no bottom slope. Concrete blocks of different lengths, in a parallelepiped shape, were specially designed so that they would not be submerged before tipping over. The depths upstream of the blocks were measured using a piezometric device located 2 metres in front of the fuses.

#### Conclusions of this work

- From the results of the tests, it was found, by the researchers, that the measured and calculated water levels at which the fuses trip generally agree satisfactorily.



- However, under static conditions, the observed water levels tend to be slightly lower than the expected values. This observation could be attributed to a small uplift under the fuse plugs, suggesting a possible imperfection at the upstream horizontal junction.
- In addition, the correlations are less precise for the blocks located near the side walls, where the measured water levels are significantly lower than the calculated values, probably due to the dissymmetry of flows next to these walls.
- Furthermore, it was noted that there was no significant difference between the calculated and measured water levels leading to the tipping of a block, before and after the tipping of adjacent blocks.

Thus, according to Hien & Khanh's analysis, the proposed fuse plugs appear to be an attractive solution for auxiliary spillways in small dams because of their simplicity, moderate cost and reliability.

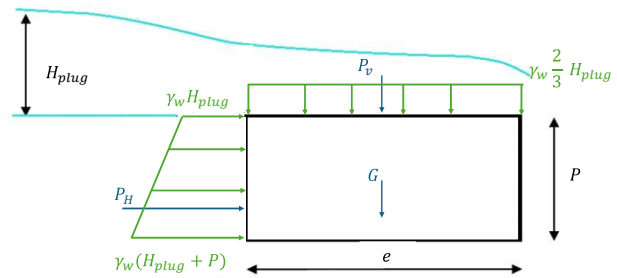
### Master's Thesis of Khezzar (2019)

In her master's thesis at Mohamed Khider University in Biskra, Khezzar [Khezzar 2019] investigated blocks without underpressure. This work led to the development of a formula for sizing this type of fuse plugs. Her study started with a theoretical analysis of predesigning these blocks, focusing on the principle of limit stability when they are positioned on the weir. The diagram of forces applied to the block is provided in FIGURE 1.9. This analysis resulted in the development of a mathematical relationship. It determines the length ( $e$ ) of the fuse plugs relative to the height of water above them. This relationship is expressed as follows:

$$e = P \cdot \sqrt{\frac{P + 3 \cdot H_{plug}}{3 \cdot \frac{\gamma_b}{\gamma_w} \cdot P + 2 \cdot H_{plug}}} \quad (1.2)$$

where

- $e$  is the length of the block;
- $P$  is the height of the block;
- $H_{plug}$  is the height of water upstream above the block crest;
- $\gamma_b$  is the specific weight of the block;
- $\gamma_w$  is the specific weight of water.



In FIGURE 1.9,  $P_H$  is the horizontal hydrostatic pressure,  $P_v$  is the vertical pressure and  $G$  is the block self-weight.

FIGURE 1.9: Diagram of forces applied to the block (inspired by [Khezzar 2019])

In this research, an experimental study was carried out to verify the validity of the theoretical relationship. The tests were performed on a physical scale model. A channel 12 m long, 1.2 m high and 1 m wide was used to simulate a watercourse. The experiments were conducted on four fuse blocks of different widths.

The results showed that the flow behaviour over the blocks was similar to that over a broad crest weir. It was also observed that the fuse plug tipping head increases rapidly with a larger width.

A comparison between the theoretical and experimental results indicated relatively good agreement.

## 1.4.2 Fuse plugs with underpressure

### Lempérière & Vigny (2013)

Lempérière & Vigny worked on fuse plugs with underpressure [Lempérière and Vigny 2013]. They provide recommendations on the dimensions of blocks capable of being submerged before tipping over. The overturning of these blocks can be carried out by a significant height of water “ $h$ ”, which can reach up to twice the height  $P$  of the fuse plug. In this context, the blocks are relatively long and thick in relation to their height ( $B/P$  up to 10;  $e/P$  up to 3) and may be chamfered upstream to facilitate water flow.

According to Lempérière & Vigny, measures must be taken at the extremities of the blocks to avoid friction during tilting. Friction can occur as a result of irregularities or defects in verticality during manufacture. This can be prevented by slightly reducing the width of the downstream face of the fuse plug. This gives a trapezoidal shape, minimising the risk of contact with other blocks or dividing walls.

Tests on models have demonstrated the reliability of the relationship between the length  $e$  of a block and the height of water ( $h$ ) required to tip it. For a preliminary study, the article by Lempérière & Vigny proposes an approximate formula for a block:

$$h = e - 0.4 \cdot P. \quad (1.3)$$

This indicates that a block whose length is equal to one and a half times its height ( $e = 1.5P$ ) will tip over when the water reaches approximately its height ( $h = P$ ).

### Hien & Khanh (2007)

In 2007, Hien and Khanh carried out research into underpressure blocks [Hien and Khanh 2007]. The major difficulty is to accurately determine the water level that would cause the fusible plugs to tip over. Laboratory tests aimed to clarify this issue by assessing the influence of plug width and the usefulness of dividing walls. The report also proposes a simplified calculation method.

The blocks examined have a similar geometry to that proposed by HydroCoop. Several fuse plugs of different lengths were tested in a glazed laboratory channel 34 m long, 0.6 m wide and 0.65 m high with a zero bottom slope. The upstream depth  $H_{plug}$  above the plug crest was measured using a piezometer device (vertical tube), installed close to the channel and located 1.2 m upstream of the concrete fusible plugs.

The researchers also developed a formula based on block stability, assuming that the fuse plug will tip when the destabilising moment exceeds the stabilising moment. The equation is as follows:

$$H_{plug} = \frac{-6Me + \rho_w(P - i) \cdot [2B(P - i) \cdot (P + 2i) + 3(B + b)e^2]}{3\rho_w \cdot [-2B \cdot (P^2 - i^2) + (\beta - 1)(B + b)e^2]} \quad (1.4)$$

where

- $H_{plug}$  is the upstream water depth above the block;
- $M$  corresponds to the mass of the fuse plug;
- $\rho_w$  is the density of water;
- $\beta$  is a reduction factor [-];

- $i$  is the height of the underpressure chamber;
- $B$  is the downstream width of the block;
- $b$  is the upstream width of the block;
- $P$  is the height of the block;
- $e$  is the length of the block.

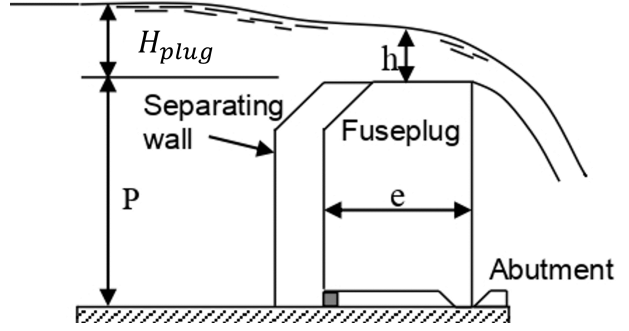


FIGURE 1.10: Diagram of the block geometry from [Hien and Khanh 2007]

### Conclusions of this work

- According to this study, it has been shown that the width of the blocks has no influence on their tipping height when they have an identical cross-section.
- The dividing walls ensure that there is no significant interaction between the blocks during tipping.
- The vertical pressure exerted on the upper face of the block depends on both the upstream head and the  $\beta$  parameter. For a thin sill, where  $e/P < 1$ , the  $\beta$  has been estimated at around 0.2, while for a wide sill, with  $e/P > 1$ , the  $\beta$  is between 0.6 and 0.65. These values are valid only for blocks with the same geometry as those studied in this work.
- This type of fusible plug is simple and economical, however, the water level at which they tip cannot be determined with great accuracy.
- Furthermore, for real prototypes, the height of the blocks should not exceed 1 m in order to limit the length and weight of the blocks.

### **Master's Thesis of Sekkour (2016)**

In his master's thesis at Mohamed Khider University in Biskra, Sekkour (Sekkour [2016]) determined a formula to design fuse blocks.

Following a theoretical study on block limit stability principle (see the forces diagram in FIGURE 1.11), a relationship between the geometric parameters of fuse plugs and their tilting height has been determined. The mathematical expression established in this research is given by:

$$H_{plug} = \frac{3Pe^2 \left( \frac{\gamma_b - \gamma_w}{\gamma_w} \right) - P^3}{e^2 + 3P^2} \quad (1.5)$$

where

- $H_{plug}$  corresponds to the upstream water depth above the block;
- $\gamma_w$  is the specific weight of water;
- $\gamma_b$  is the specific weight of the concrete fuse plug;
- $P$  is the height of the block;
- $e$  is the length of the block.

In FIGURE 1.11,  $P_H$  is the horizontal hydrostatic pressure,  $P_v$  is the vertical pressure,  $P_U$  is the underpressure and  $G$  is the block self-weight.

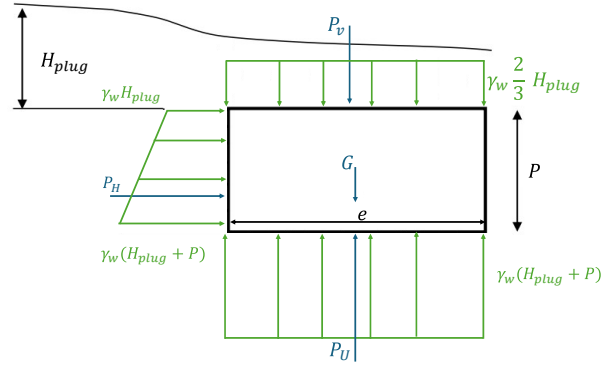


FIGURE 1.11: Diagram of forces applied to the block (inspired by [Sekkour 2016])

To validate this relationship, tests were carried out on model blocks designed in accordance with the theoretical results obtained. The experimental set-up used was a simulated reservoir, a channel 4 metres wide, 5 metres long and 1.5 metres deep. This study involved nine fuse plugs of different widths. The experiments performed were divided into two distinct phases. The first step aimed to confirm the theoretical correlation for a single block, while the second phase consisted of a weir equipped with three blocks.

The initial results of this work indicated that the behaviour of the flow over the blocks was similar to that observed on a conventional weir, as long as the fuse plugs had not tipped over. In addition, the experimental data showed satisfactory consistency with the theoretical correlation.

Sekkour's study revealed that the tipping height increased with the length of the block. Tests carried out on a weir made up of three fuse plugs confirmed the observations made for a single plug, which valid theoretical developments.

### 1.4.3 Conditions of use of concrete fuse block

When it comes to defining the design criteria and determining the tipping rate for each block, the designer must balance two opposing constraints ([ICOLD - CIDGB 2010]):

- **Economy**: It is crucial to minimise frequent tilting of the blocks to avoid excessive water losses.
- **Safety**: It must be ensured that there is an adequate distance between the top of the dam and the water level when the last fuse plug tips over.

These criteria need to be adjusted according to local conditions and specific objectives. However, experience usually suggests the following:

- **Return flood** : Fusible concrete plugs are generally designed to tip over during floods with a return period of between 20 and 100 years, or even more.
- **Raising existing weirs**: When adding height to an existing weir, the height of the blocks must not exceed approximately 25% of the distance between the crest of the dam and the sill.

## 1.5 Construction of fuse plugs

The report of ICOLD [ICOLD - CIDGB 2010] also proposes a method for constructing concrete fuse plugs on the spillway, with two options: using prefabricated blocks or pouring them in situ.

For blocks built in situ on an existing weir, the following steps, illustrated in FIGURE 1.12, can be performed:

- (1) First, level the sill.
- (2) Next, place a layer of material, which can be of any type as long as it is easy to take off afterwards. This material is needed to create the lower chamber and should be removed once the block has been concreted. At the downstream extremity, it is advisable to use clay or clay sand (known as a “clay plug”) to seal any leaks at the joint. Alternatively, a rubber seal can be placed under the downstream end of the block, as shown in FIGURE 1.13.
- (3) Then, a plastic membrane should be laid over the materials installed on the sill.
- (4) The fourth step is to pour the concrete for the block.
- (5) Once the concrete has hardened, the layers of material must be removed, leaving the “clay plug” in place. A few unsealed supports are then placed under the block to ensure its stability.

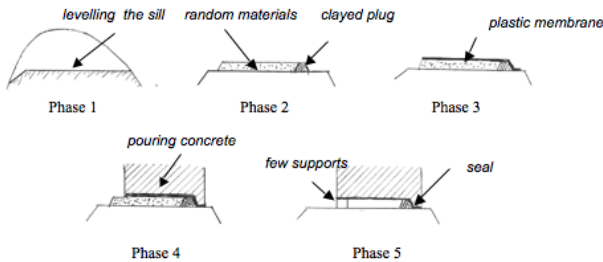


FIGURE 1.12: Steps for the block construction with “clay plug” (drawing from [ICOLD - CIDGB 2010])

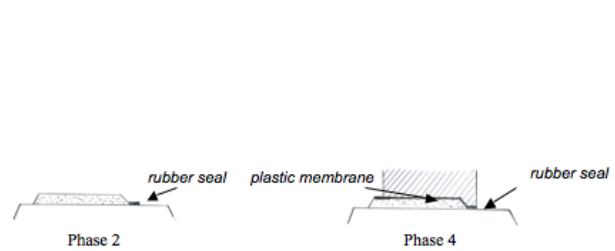


FIGURE 1.13: Steps for the block construction with rubber seal (drawing from [ICOLD - CIDGB 2010])

In addition, a rubber sheet can be used to ensure a vertical seal between the blocks and adjacent elements. This can be embedded or bolted into the block [Lempérière and Vigny 2013].

According to ICOLD [ICOLD - CIDGB 2010], increasing the flow by  $1 \text{ m}^3/\text{s}$  generally requires less than  $1 \text{ m}^3$  of new concrete blocks. For an already constructed weir, it is necessary to remove around  $2 \text{ m}^3$  of existing concrete for every  $1 \text{ m}^3$  of replacement blocks to achieve this flow increase. In the context of future dam construction, the use of blocks rather than a Creager weir results in a net saving of approximately  $1 \text{ m}^3$  of concrete for each additional  $1 \text{ m}^3/\text{s}$  of the flow.

### 1.5.1 After tilting

After blocks have toppled over, it may take some time to replace them with new blocks, resulting in a corresponding loss of water storage capacity [ICOLD - CIDGB 2010].

One solution is to use temporary devices, such as wooden planks supported on steel tubes while waiting for the new blocks to be installed. This method can be implemented quickly, even as

early as the day after the flood, provided that suitable fixing holes for the tubes have been drilled in the weir before the first concrete blocks are laid. Inexpensive pipes and boards also need to be available from stock.

## 1.6 Objectives of this work

The main objective of this work is to focus on blocks with underpressure, in line with Lempérière & Vigny’s recommendations [Lempérière and Vigny 2013], which highlight the effectiveness of the “total underpressure” solution in ensuring accurate tipping. Although this technology requires more concrete, it offers greater precision in terms of the level of water inducing tipping. In addition, it does not necessitate high tolerances in the position of the seal, making it easier to install.

Two design approaches have been proposed for these blocks. Sekkour has developed a formula which not consider the recommended geometry described above. On the other hand, the geometry studied by Hien & Khanh is based on Hydrocoop’s suggestions, but their experiments took place in a canal, which does not faithfully reflect the conditions encountered in a reservoir.

As part of this work, experiments will be performed to assess the correlation between the two design formulas provided and the results of tests carried out under conditions simulating a reservoir with blocks whose geometry follows the above-mentioned indications. These tests will also make it possible to determine whether parameters other than those taken into account in the equations have a significant influence on the behaviour of the fuse plugs. Finally, these analyses will be used to evaluate the potential need to develop a new analytical model.

Once a reliable model has been established, the final objective is to create a sizing table to facilitate the practical use of the blocks. In addition, it will be necessary to summarise the recommendations from the literature and the conclusions drawn from the discussions held as part of this work.

# Chapter 2

## Methodology

The issue can be tackled in three ways: by carrying out experimental tests, by developing an analytical model, or by conducting numerical modeling (CFD). In this work, the first two approaches are executed.

The analytical model is based on examining the physical stability of the block. It consists of determining a formula relating the geometry of the fuse plug to its tilting height. This analysis is described in chapter 4.

The experiments are undertaken for two purposes. They are used to verify the established equation. Moreover, they facilitate identifying the influence of parameters excluded from the theoretical model. These objectives are met through new tests rather than by referring to literature results. Indeed, previous research did not take into account the same block geometry as that chosen in this work and/or were not completed under the conditions envisaged in this study (depicted in the section 2.1).

In this chapter, the experimental setup and measurement devices are described. The protocols for processing data and conducting the tests are also explained.

### 2.1 Experimental setup

The experimental system consists of real fuse blocks, designed on a geometric scale suitable for laboratory use.

The setup must be installed in such a way as to represent reality as closely as possible. Therefore, accurately simulating the reservoir of a dam requires careful control and stabilisation of the water level upstream the fuse plugs.

To achieve this, a basin with relatively large dimensions is used. A photo of the model studied is provided in FIGURE 2.1. The aim is to achieve stationary water level conditions despite variations in discharge released through the weir. These conditions will allow for the neglect of velocity and friction terms in the Bernoulli equation, which describes the conservation of energy in fluid flow. Consequently, regardless of where the height is measured, it will reflect the hydraulic head. The primary challenge lies in maintaining water level as constant as possible, even as the discharged flow varies abruptly after tilting.

The model consists of a 3.6 meters long and 2.4 meters wide tank. As shown in the drawing in FIGURE 2.2, this reservoir is composed of three sides made of metal sheets and closed by a masonry block wall.

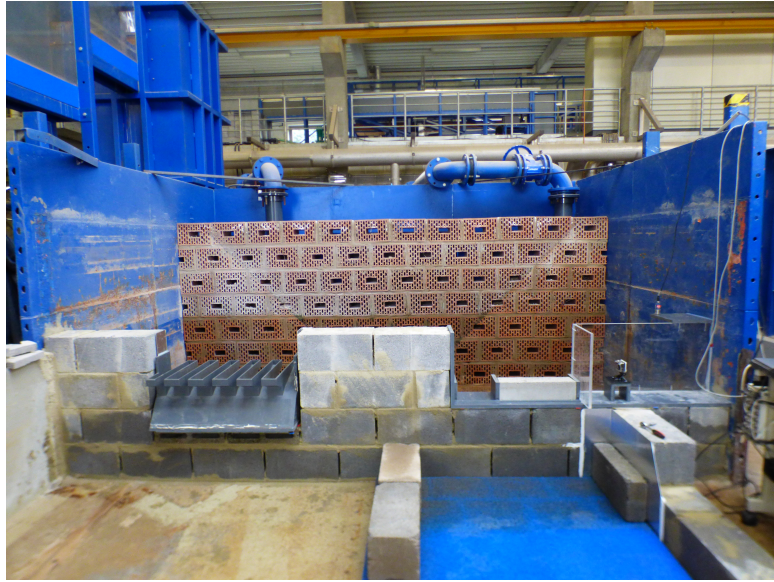


FIGURE 2.1: Photo of the model studied

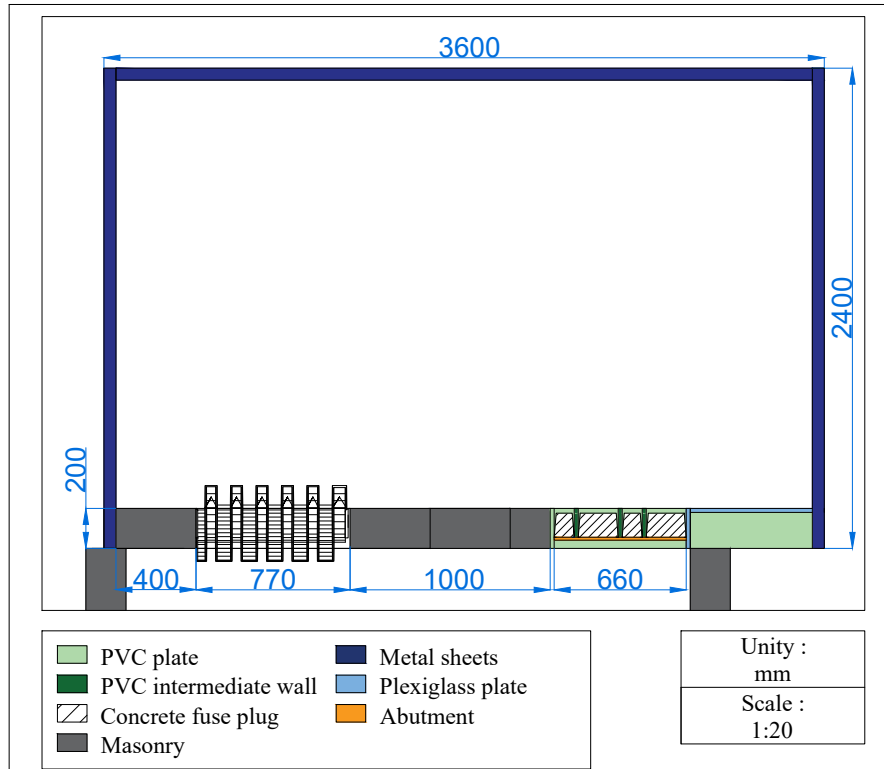


FIGURE 2.2: Plan view of the model studied

In this basin, various elements are installed to carry out experimental tests.

### 2.1.1 Fuse plugs

The sill, on which the blocks are positioned, is located on the left-hand side of the masonry wall. This space extends 66 cm to accommodate the placing of various combinations of the fuse plugs.



In this study, the concrete plugs used were designed by Jean-Baptiste Pachuco for his master's thesis entitled "Contribution à l'étude hydraulique expérimentale des blocs fusibles" ("Contribution to the Experimental Hydraulic Study of Fuse Blocks." in English) [Jean-Baptiste 2014]. It was conducted at the University of Liège in 2014.

### Geometry of the fuse plugs

The geometry features common to all blocks are now examined. The fuse plugs are presented in FIGURE 2.3 and the dimensions are drawn in FIGURE 2.4.

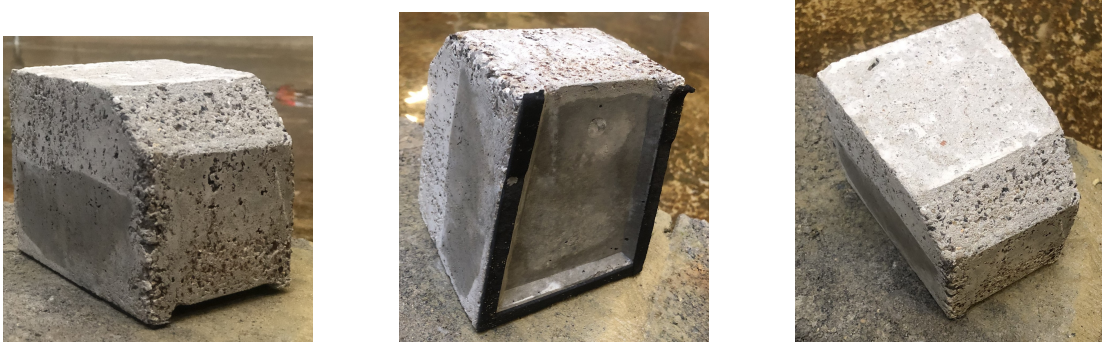


FIGURE 2.3: Photos of a concrete block from several angles

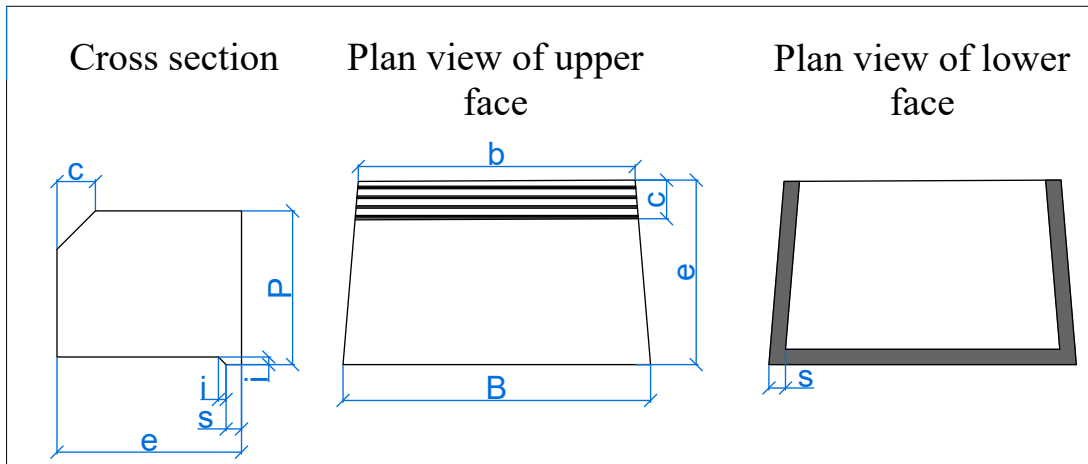


FIGURE 2.4: Geometry of the fuse plugs used

The different fuse plugs share certain dimensions, which are detailed below:

- The height ( $P$ ) is 0.1 m, which represents  $\frac{1}{3}$  of the blocks implemented on the Gaskaye dam in Burkina Faso.
- It was decided to chamfer the upstream face of the plugs with a slope of 1:1 and a width ( $c$ ) of 0.025 m. It facilitates the overflow onto them, as explained in the state of the art.
- It was chosen to use uplifting blocks, as this geometry allows water to be discharged before tipping, thereby increasing tank storage capacity. Hence, in each concrete piece, a 5 mm-high opening ( $i$ , equivalent to  $\frac{1}{20}$  of the total height) is made from its bottom corner. This represents the underpressure chamber. However, on three sides of the block, a 0.01 m-wide ( $s$ ) strip is left intact, serving as a support. In contrast, the upstream face allows water from the reservoir to enter the lower chamber.

- The length of the fuse plug ( $e$ ), defined in the direction of the flow, is 0.12 m.
- The upstream and downstream faces of the block do not have the same width (defined perpendicular to the direction of the flow). In fact, the upstream dimension ( $b$ ) corresponds to the downstream width ( $B$ ) reduced by 0.02 m. This trapezoidal shape prevents friction between the block and adjacent elements.

The concrete fuse plugs are distinguished by their width ( $B$ ), which ranges from 0.1 to 0.6 m.

Regarding the construction of these blocks, firstly, moulds were prepared [Jean-Baptiste 2014]. These were made by assembling 0.018 m-thick boards using screws. The chamfer of the fuse plugs are made by the formwork, and a 0.005 m-thick PVC plate was placed on the bottom. This element creates the lower chamber. This PVC panel was chamfered on the lateral and downstream sides to form a 1:1 slope between the block supports and the upper face of the chamber. Then, concrete was made using two volumes of gravel, one volume of sand and one volume of cement. As for the quantity of water, the mixture was adjusted to ensure that it was not too liquid but still sufficiently workable to be poured into the moulds. Finally, after three days, the blocks were un moulded.

Thus, six types of block, categorised by their width, were produced in 2014. The actual dimensions of the fuse plugs, with an accuracy of 1 mm, are given in TABLE 2.1.

Type of block	Height $P$ [cm]	U/S width $b$ [cm]	D/S width $B$ [cm]	Length $e$ [cm]
B10	$10 \pm 0.1$	$7.9 \pm 0.1$	$10 \pm 0.1$	$12.1 \pm 0.1$
B20	$9.9 \pm 0.1$	$18.3 \pm 0.1$	$20 \pm 0.1$	$12 \pm 0.1$
B30	$9.8 \pm 0.1$	$28.3 \pm 0.1$	$30 \pm 0.1$	$12.1 \pm 0.1$
B40	$10 \pm 0.1$	$38.3 \pm 0.1$	$40 \pm 0.1$	$11.9 \pm 0.1$
B50	$9.8 \pm 0.1$	$48.2 \pm 0.1$	$50 \pm 0.1$	$12 \pm 0.1$
B60	$9.9 \pm 0.1$	$58.3 \pm 0.1$	$59.9 \pm 0.1$	$12 \pm 0.1$

TABLE 2.1: Actual dimensions of the fuse plugs used

For the remainder of this work, additional information concerning the blocks, in particular their density, must be identified.

To begin with, the fuse plugs are weighed, TABLE 2.2. Elements “B10” and “B20” can be measured to the nearest gram. For the others, mass could only be determined to within a tenth of a kilogram.

Type of blocks	B10	B20	B30	B40	B50	B60
Mass [kg]	2.315	4.923	7.2	10	12.5	14.9

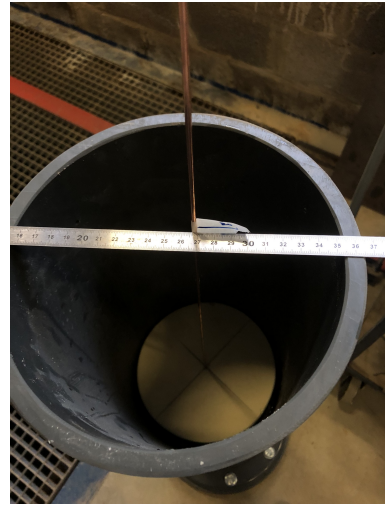
TABLE 2.2: Dry mass of the different types of blocks

Then the volume of the blocks is determined. To do this, given the complexity of their shape, the water displacement method is used. This technique relies on the principle that when a solid object is submerged, it displaces an amount of water equal to its own volume.

Consequently, a tube closed at one end is used to immerse the blocks, a photo of it is provided in FIGURE 2.5a. This tube needs to have a sufficient height to fit all sizes of fuse plugs and a section relatively close to their cross-section. The tube used is neither transparent nor graduated, a float is therefore put in place to identify the water level easily. This circular float, shown in the photo in FIGURE 2.5b, has a diameter relatively close to that of the tube.



(a) Photo of the measuring tube



(b) Photo of the float placed in the tube

FIGURE 2.5: Instruments for measuring block volume

The process of determining the volume begins with the initial step of filling the tube with water (depicted on the left in Figure 2.6). Subsequently, the water level is measured using the float. Next, a block is submerged into the tube, and the water level is once again identified (illustrated on the right in Figure 2.6). Finally, the change in water height is calculated to obtain the volume of water displaced ( $V_D$ ), which consequently equates to the volume of the block.

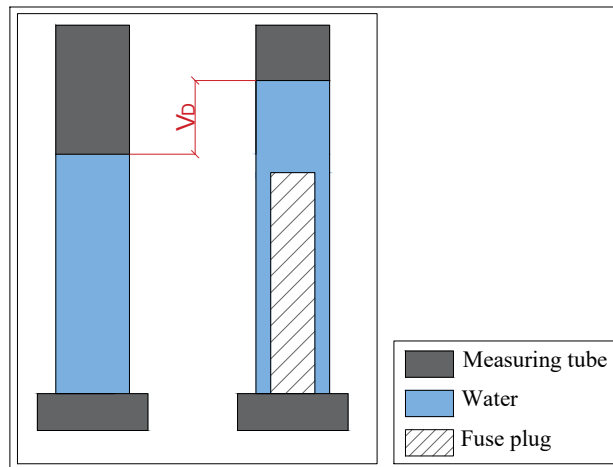


FIGURE 2.6: Scheme illustrating the variation in height ( $V_D$ ) of the water level before and after the installation of a block

In TABLE 2.3, the mass and volume of each of the blocks are listed, along with their corresponding density. Since water levels measured in the tube are accurate to the nearest millimetre, a density range has been determined for each block. This is calculated on the basis of the  $V_D \pm 1$  mm measurement.

Type of block	Mass [kg]	Volume [mm <sup>3</sup> ]	Density [kg/m <sup>3</sup> ]	Density range [kg/m <sup>3</sup> ]
B10	2.315	1006494	2300	2228-2377
B20	4.923	2142857	2297	2263-2333
B30	7.2	3214286	2240	2232-2278
B40	10	4290323	2331	2313-2348
B50	12.5	5422078	2305	2292-2319
B60	14.9	6461039	2306	2295-2318

TABLE 2.3: Summary of block weight, volume, and density range

### Installation of the fuse plugs

Regarding the installation of the blocks on the sill, various elements are put in place to facilitate their utilisation. Firstly, the fuse plugs are placed on a PVC support, as shown in FIGURE 2.7. This flat surface is used to screw in an abutment and intermediate walls. The abutment is a PVC slat 5 mm high and 15 mm wide. Walls separating two adjacent blocks are installed, as suggested in the literature. Different placement configurations will be studied, therefore, several positions of the PVC walls are planned. These separators are the same height as the fuse plugs and are aligned with the upstream edge of PVC support. They have a length of 144 mm, which is defined as 1.2 times  $e$  (recommended relationship in the literature).

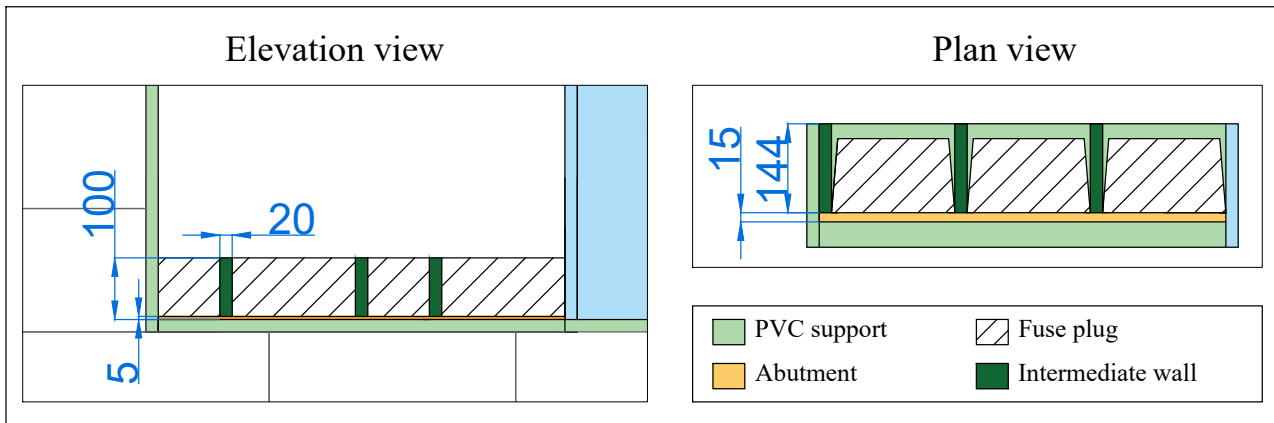


FIGURE 2.7: Elevation and plan view of block installation (Dimensions are given in mm)

A leakage occurs between the blocks and the separating walls when nothing is placed between them, as shown in the photo in FIGURE 2.8a. One solution to this problem is to use folded plastic strips (see photo in FIGURE 2.9a) to avoid the passage of water between the fuse plug and the intermediate wall. Once correctly positioned, as shown in the photo in FIGURE 2.9b, water can no longer infiltrate. In the FIGURE 2.8b, it can be seen that with the sealing strip in place, there's no water ingress. It is important to note that this system is intended to prevent leaks and should not create lateral friction, thus not affecting the tilting of the block.



(a) Photo of water leaks

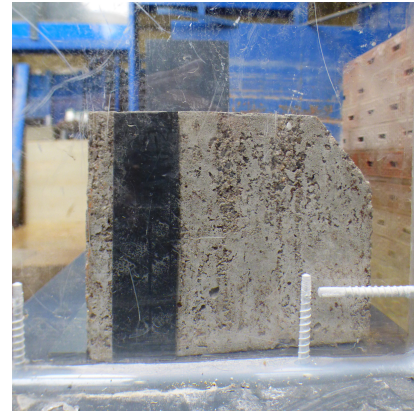


(b) Photo after installation of sealing strip

FIGURE 2.8: Water leaks problem



(a) Photo of folded plastic strip placement



(b) Photo of waterproofing strip in place

FIGURE 2.9: Waterproofing strip

In addition, to cushion the fall of the blocks and avoid damaging them, a deformable panel is put in place downstream of the threshold, as shown in FIGURE 2.10.



FIGURE 2.10: Photo of the deformable panel



### 2.1.2 Piano Key weir

On the wall, to the right, a Piano Key weir (PKW) is placed. This PKW is depicted in the photo in FIGURE 2.11. This labyrinth weir aims to achieve more stable water level in the reservoir. This spillway provides a large evacuation capacity for a small range of height variation. Consequently, if the outflow over the fuse plugs fluctuates, the PKW will absorb these changes. The objective is therefore to minimise the impact of flow variation on the water level when the block begins to destabilise, and then tilt. This principle is implemented to achieve a height that remains as constant as possible during a test.



FIGURE 2.11: Photo of the PKW model

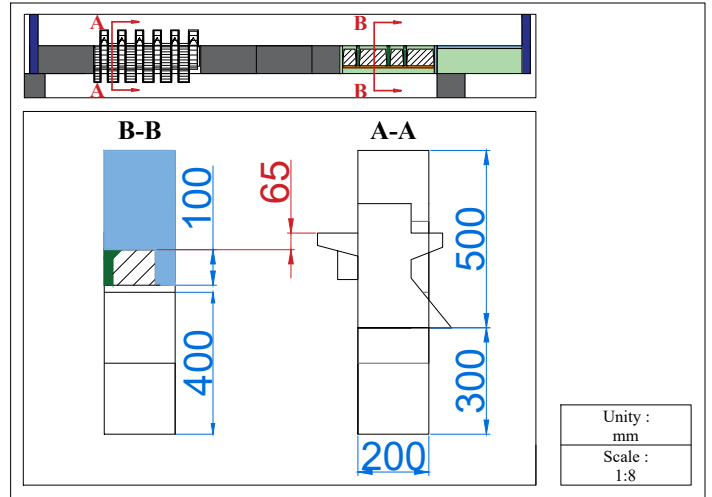


FIGURE 2.12: Cross-sectional drawing of the model: section A-A through the weir and section B-B through a fuse plug

As shown in the cross-sections in FIGURE 2.12, the elevation of the PKW crests and the fuse plugs are not aligned. Indeed, it should only operate when the water levels are close to tipping the blocks. The later the PKW is used (i.e. at high water levels), the more the weir is at the beginning of the head-flow relationship, resulting in minimal variation in head for a fluctuation in the discharge. This head-flow relationship is illustrated in FIGURE 2.13.

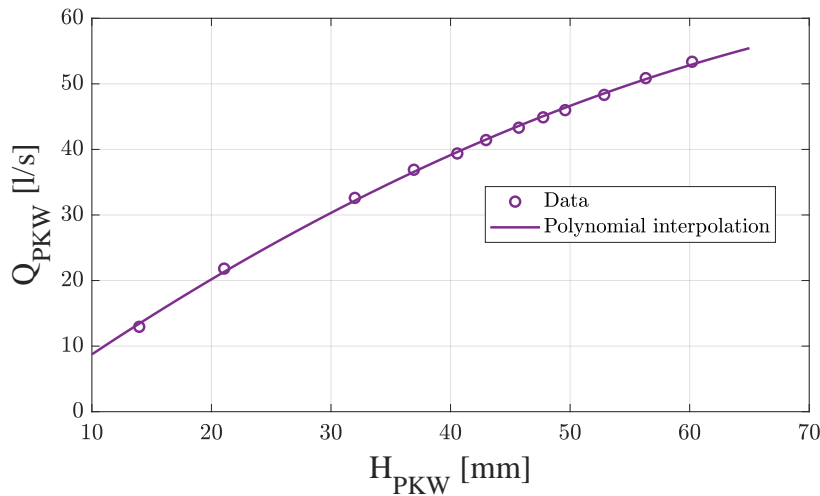


FIGURE 2.13: Head-flow relationship of the PKW model

The relationship was determined by injecting several flows into the model and measuring the as-

sociated head in the reservoir. To do this, the space reserved for the fuse blocks was obstructed, as can be seen from FIGURE 2.14. In this way, the flow entering the model corresponds to that leaving via the weir.

The various measurements are displayed in the graph (using the term “data”) in the figure above. To use this relationship, a polynomial interpolation expressed by the equation (2.1) is established.

$$Q_{PKW} = -0.007 \cdot H_{PKW}^2 + 1.342 \cdot H_{PKW} - 4.021 \quad (2.1)$$

where  $H_{PKW}$  corresponds to the hydraulic head and  $Q_{PKW}$  represents the weir flow.

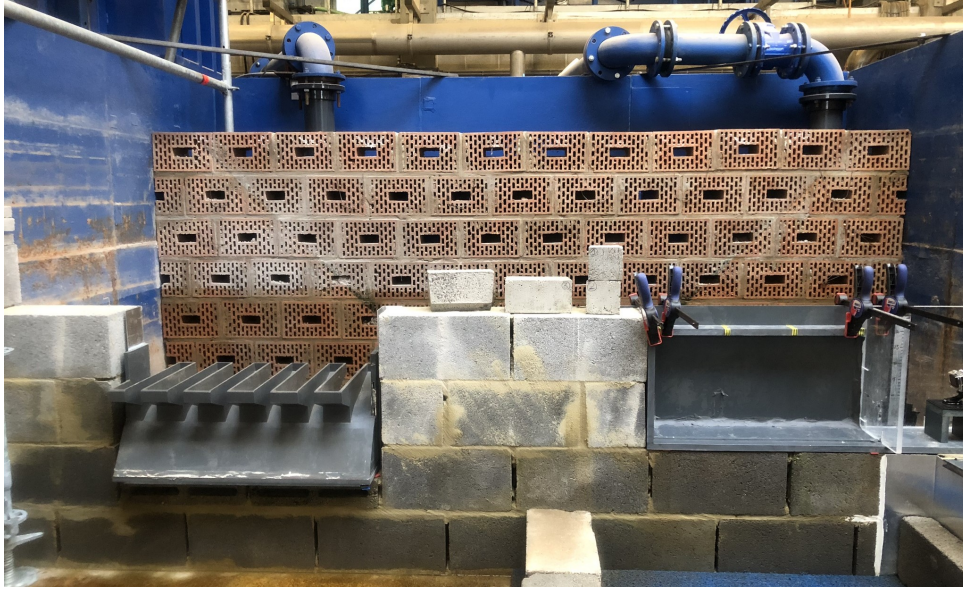


FIGURE 2.14: Photo of the obstruction in the space reserved for the blocks

Furthermore, the flow coefficient of the blocks  $C_d$  can be determined. For this purpose, as for the PKW, several flow rates were injected into the model and the corresponding height was measured. These data are represented on the graph in FIGURE 2.15 by the H-Q relationship. In this graph, the head-flow coefficient relationship is also plotted.

Based on the analysis of the graph, it is observed that for low head values (between 40 mm and 80 mm), the flow coefficient starts to increase significantly, indicating sensitivity of the relationship between head and  $C_d$ . This trend can be attributed to the surface roughness of the blocks, resulting in frictional effects. When the height exceeds approximately 80 mm, the flow coefficient reaches a more stable value, around 0.4. In addition, for heads greater than 120 mm, the coefficient increases, this phenomenon probably being due to the fact that when the water depth exceeds a certain threshold, the sill seems less and less thick in relation to this head.

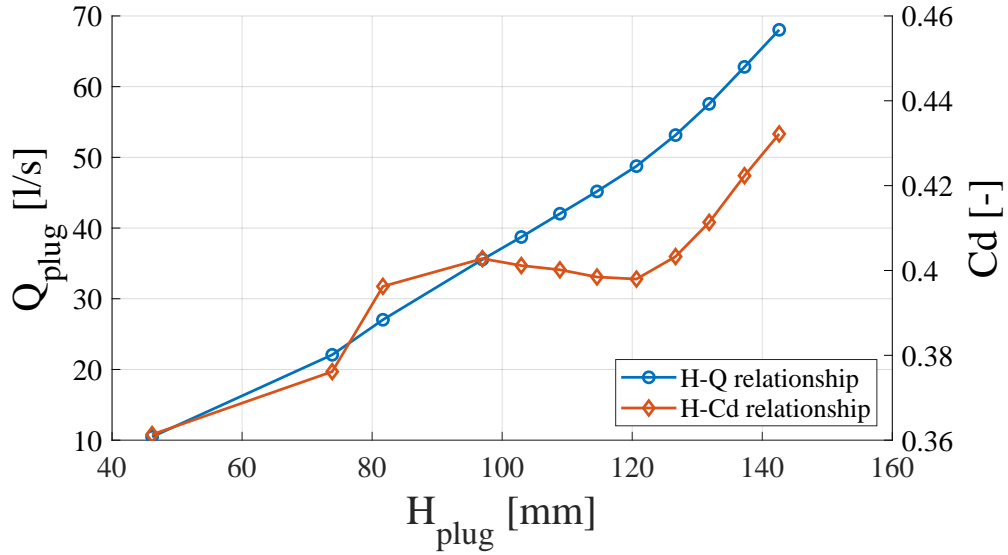


FIGURE 2.15: Head-discharge and head-flow coefficient relationships for the fuse plugs

### 2.1.3 Observable zone

Returning to FIGURE 2.2, it can be seen that an area on the far right of the masonry wall is made of Plexiglas plate. The purpose of this area is to allow observation of the level upstream, in the reservoir, as well as the cross-section of the blocks. This zone is therefore very useful, in particular, for placing a camera (see FIGURE 2.17 below).

## 2.2 Measurement devices

In order to analyse the behaviour of fuse plugs, two essential pieces of information must be collected : the hydraulic head and the discharge on the blocks.

### 2.2.1 Determination of hydraulic head

The hydraulic head is, in other words, the height of water upstream above the concrete blocks. It corresponds to the water depth because the flow velocity in the reservoir is very small. This parameter is noted  $H_{plug}$  and represented in FIGURE 2.16.

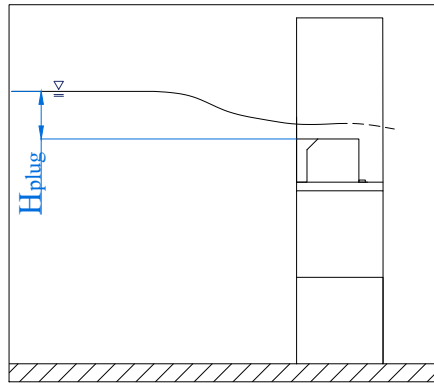


FIGURE 2.16: Representation of hydraulic head  $H_{plug}$



To obtain this data, an ultrasonic sensor is used. This device is placed 25 cm upstream of the fuse plugs as shown in FIGURE 2.17.

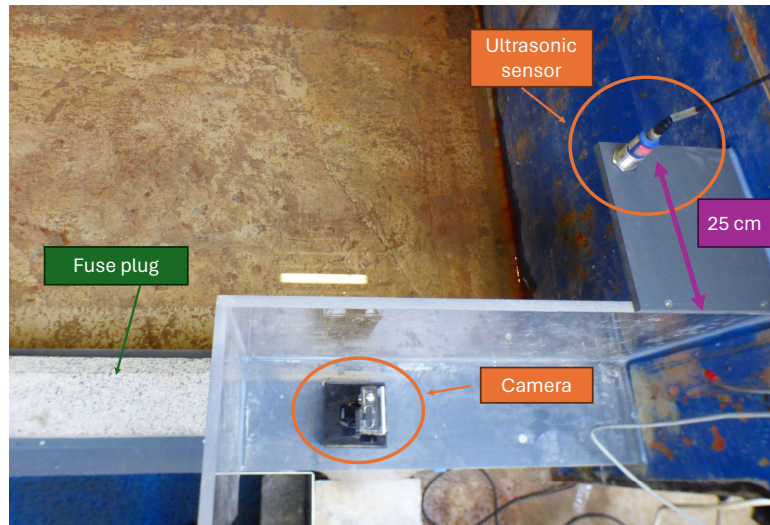


FIGURE 2.17: Photo of ultrasonic sensor and camera location on the model

The measuring instrument emits a pulse that is reflected off the surface of the water. The time taken for the sensor to receive the signal is translated into distance ( $D_{sensor}$ ). The device can detect water levels 65 to 500 mm away with millimetre accuracy. The probe is connected to a box that transmits data to a computer. LabVIEW software captures it at a frequency of 10 Hz, recording 10 values per second. These values are provided in terms of voltage ( $V_{Distance}$ ) rather than distance. The output obtained during a test is illustrated in FIGURE 2.18.

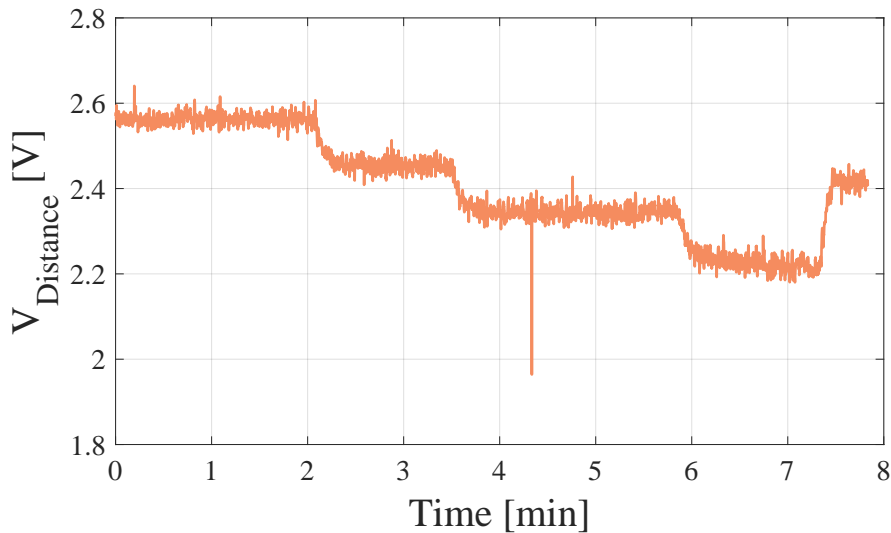


FIGURE 2.18: Signal expressing the distance between the sensor and the water level over time

Therefore, to get distance information, it is necessary to calibrate the sensor. In other words, three measurements are taken to establish a relationship between the voltages obtained by the software and the actual heights. To do this, three PVC shims of different sizes are positioned under the probe, as shown in FIGURE 2.19. Next, the distance is read from the sensor and a 10-second recording is made, voltages are collected. Once the average has been calculated for each

data set, the Voltage-Distance relationship is determined. This is illustrated in FIGURE 2.20 and given by :

$$D_{sensor} = 43.222 \cdot V_{Distance} + 66.687 \quad (2.2)$$

where  $V_{Distance}$  is expressed in volts and  $D_{sensor}$  in millimetres.



FIGURE 2.19: Photo of a shim under the sensor for calibration purposes

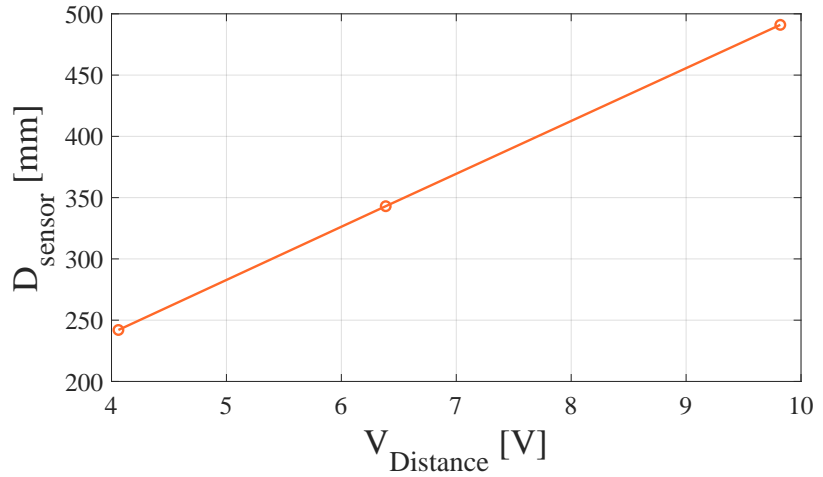


FIGURE 2.20: Distance - Voltage relationship

To ensure the accuracy of the calibration line, a second calibration is carried out several days later. This second relationship is given by :

$$D_{sensor} = 43.321 \cdot V_{Distance} + 66.153. \quad (2.3)$$

This equation is similar to the first one and does not vary by more than 0.5 mm.

Finally, to obtain the hydraulic head of the blocks, the following expression is used :

$$H_{plug} = 370 - D_{sensor} - P \quad (2.4)$$

where the value 370 corresponds to the distance between the sensor and the sill (expressed in millimetres), represented in FIGURE 2.21.

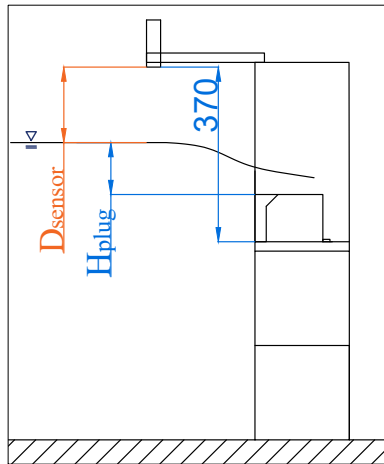


FIGURE 2.21: Representation of distance from sensor to sill and water level (Dimensions expressed in millimetres)

### 2.2.2 Determination of flow rate

The flow rate injected into the basin is the second main measure to capture. In order to determine it, a flowmeter is installed on the water pipe. This device is also connected to the LabVIEW software, so that the incoming flow is collected in terms of voltages. The signal obtained during a test is illustrated in FIGURE 2.22.

A calibration line must also be established. To do this, several flow rates are read from the flowmeter and associated with the recorded measurement. The voltage-flow relationship is plotted on the FIGURE 2.23 and given by :

$$Q_{in} = 34.401 \cdot V_{flow} - 37.728 \quad (2.5)$$

where  $Q_{in}$  is the flow rate injected into the model (expressed in litres per second) and  $V_{flow}$  is the voltage measurement (expressed in volts).

Several days later, the voltage-input relationship was established a second time to ensure its accuracy. The new equation is relatively close to the first and is given by :

$$Q_{in} = 34.439 \cdot V_{flow} - 37.739. \quad (2.6)$$

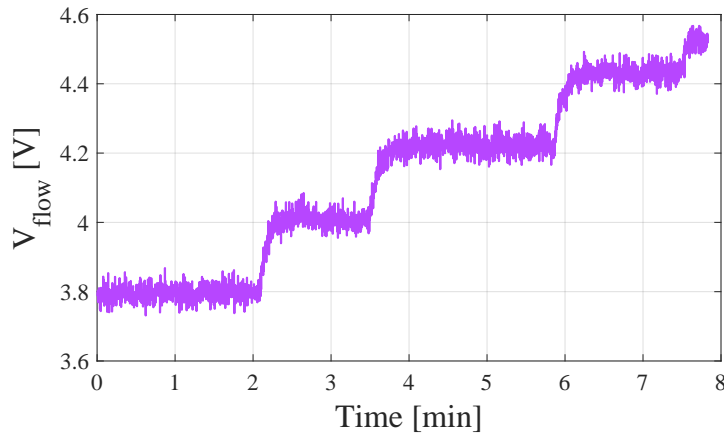


FIGURE 2.22: Signal expressing the flow rate injected into the model over time

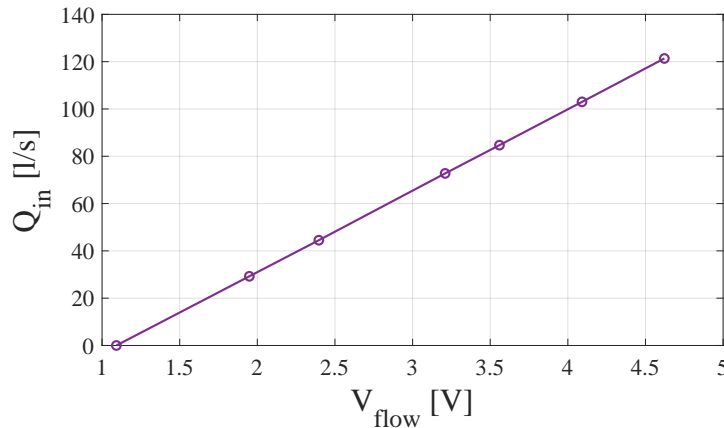


FIGURE 2.23: Voltage - Flow rate relationship

## 2.3 Data processing

The results obtained are noisy. Indeed, even when measuring a level (or flow) that is assumed to be constant, the sensor does not provide a perfectly stable signal. To process this data, an automatic procedure has been set up.

In addition, during the test, the flow rate is increased in stages (resulting in a stepwise increase in the upstream level). For this reason, a method has been developed to determine a value for each plateau of the water level and flow signals provided.

The routine comprises the following four steps:

- (a) **Replacement of outliers** : In a data set, values qualified as “outliers” can be identified. These, induced by the noise, are relatively far outside the average. This type of value should therefore be replaced to match all the others of the same plateau.
- (b) **Signal smoothing** : To reduce measurement noise, the moving average technique is used. This method smoothes the data in order to attenuate irregularities.
- (c) **Identification of plateaus** : The signal consists of plateaus separated by transition intervals. A procedure is used to detect the beginning and the end of a level by comparing values with adjacent ones.
- (d) **Calculation of the average over a level** : For each plateau, the average is calculated in order to have one value representing this measuring stage.

Once each level of measurement is clearly defined by an average value, it is possible to summarise the data from a test in three types of results :

1. **The stable head** : This value is obtained by the hydraulic head given by the last step before tipping. It represents the highest height at which it can be ensured that the block has not yet toppled over during the test.
2. **The tipping head** : This value corresponds to the head that causes the block to tilt during a measurement step.
3. **The unstable head** : This value is calculated to represent the head associated with the final phase of flow rate after the block has tilted. The term “unstable head” thus refers to a water depth indicating that the block has indeed tipped over during the test.

These different stages of data processing are explained below.

### 2.3.1 Replacement of outliers

The first step consists in identifying the outliers. To do so, each value is compared to the previous one:

$$|f(i) - f(i - 1)| = \Delta_{outliers} \quad (2.7)$$

with

- $f(i)$  is the value being examined ;
- $f(i - 1)$  is the previous value already examined ;
- $\Delta_{outliers}$  is the variation between two consecutive values.

The variation between two consecutive data must be limited to avoid including outliers in the results. Nevertheless, it is also important not to impose too strict a limit to prevent considering too many values as outliers.

Concerning water heights, to carefully determine the maximum acceptable value for  $\Delta_{outliers}$ , the graph in FIGURE 2.24 was generated. This shows the amount of data for which  $\Delta_{outliers}$  exceeds a certain value. This relation is determined for four different experimental tests.

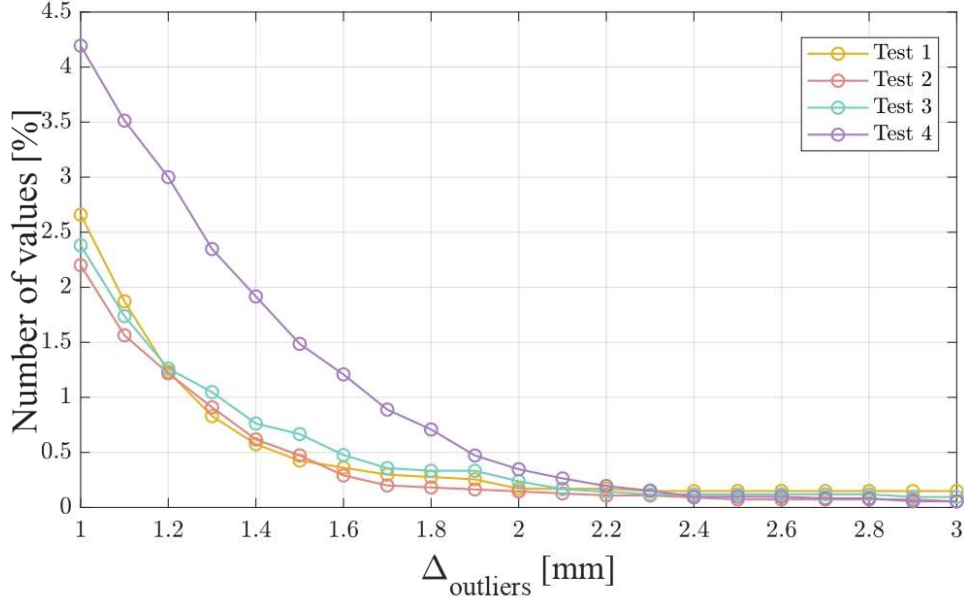


FIGURE 2.24: Percentage of values in a data set for which  $\Delta_{outliers}$  exceeds a certain value. Relationships established based on hydraulic head for four different experimental tests.

Based on this graph (FIGURE 2.24), it can be observed that to have less than 0.5% of data identified as “outliers”, the parameter  $\Delta_{outliers}$  must be greater than 1.6 mm. It also reveals a relative stability of the percentage for values below  $\Delta_{outliers} = 2$  mm, followed by a marked increase above this cutoff. The value of 2 mm is selected as the maximum variation because of this observed change for the hydraulic head.

The same procedure is applied for signals corresponding to the flow rate injected into the model. In this way, the parameter  $\Delta_{outliers}$  is set to 3 l/s.

Then, the second step is the replacement of the extreme values. A linear interpolation is performed for these outliers. This is expressed as :

$$f(i) = f(i-1) + [(f(i+1) - f(i-1))] \cdot \frac{i - (i-1)}{(i+1) - (i-1)}. \quad (2.8)$$

The signal can now be smoothed.

### 2.3.2 Signal smoothing

The second stage of data processing involves smoothing the signal. To do this, the moving average method is applied.

The moving average  $M_M$  is an average calculated for each value  $H_i$  (from the data set  $H$ ) over a window of length  $I$ .

The equation is :

$$M_M(i) = \frac{1}{I} \cdot \sum_{j=i-\frac{I-1}{2}}^{i+\frac{I-1}{2}} H(j). \quad (2.9)$$

The parameter  $I$  can be chosen arbitrarily, but must be odd. It represents the number of data points in the window. The length  $I$  influences the smoothing performed. To illustrate this impact, the curves in FIGURE 2.25 have been drawn. These represent signal smoothing for three different  $I$  of 19, 59, and 119.

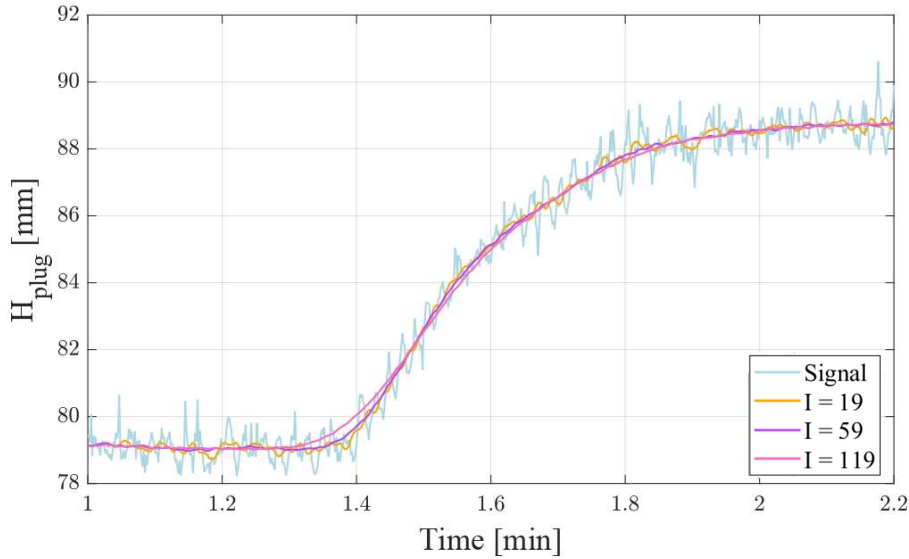
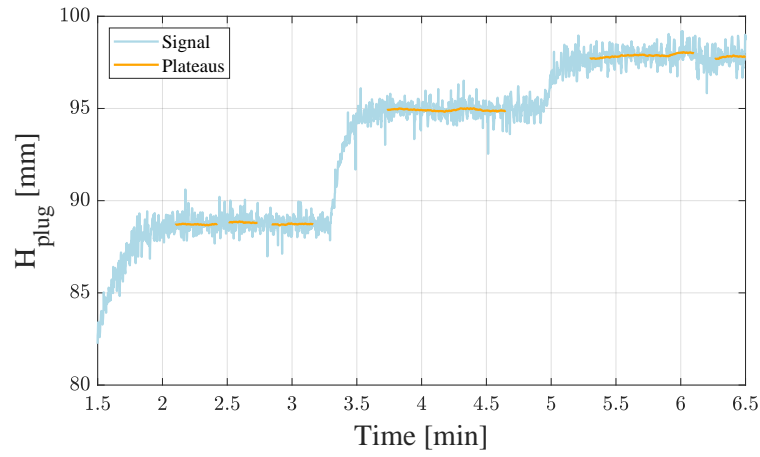
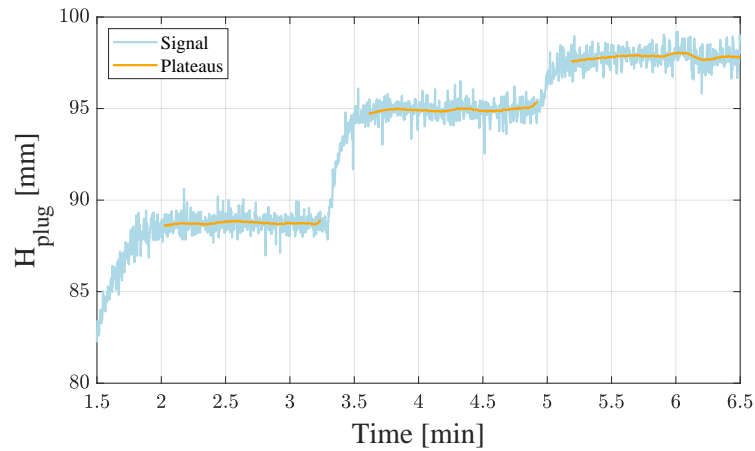
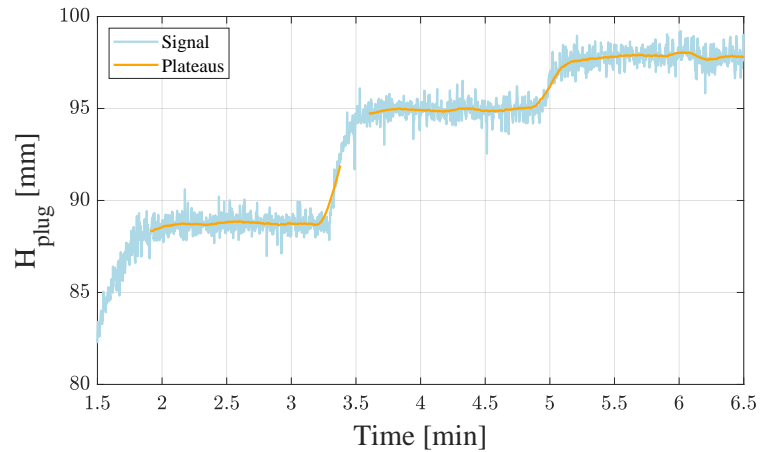


FIGURE 2.25: Hydraulic head ( $H_{plug}$ ) smoothing curves for three different window lengths ( $I=19, 59,$  and  $119$ ).

From this graph, it can be seen that the higher the  $I$  parameter, the smoother the signal (the fewer irregularities there are in the data set). However, it should be noted that the increase in the rising phase between two steps in the data occurs in a softer, more curved manner. As a result, the end of the first level therefore no longer represents the plateau (the same applies to the start of the second level). It was decided to choose  $I$  equal to 119 because even though this value reduces the size of the steps, it allows better smoothing of the signal. Since the objective is to obtain an average value per plateau, it is more advantageous to have a smooth signal than to have a long stage of data.

### 2.3.3 Identification of plateaus

Thirdly, it is important to differentiate between plateau and ascent phases. This distinction is made by comparing values with adjacent ones within a defined interval. This comparison is based on the variation between the value considered and those located in this interval. Thus, a maximum limit of variation ( $\Delta_{plateau}$ ) between the data is established. The impact of the choice of this parameter is demonstrated through the graphs presented in FIGURE 2.26.

(a)  $\Delta_{plateau} = 0.01$  mm.(b)  $\Delta_{plateau} = 0.02$  mm.(c)  $\Delta_{plateau} = 0.05$  mm.FIGURE 2.26: Determination of the plateaus of a signal with different parameters  $\Delta_{plateau}$ 

These graphs highlight that choosing a limit that is too low results in the division of a plateau into several distinct parts, as observed with  $\Delta_{plateau} = 0.01$  mm (FIGURE 2.26a). On the other hand, a limit that is too high makes it difficult to distinguish between the different levels, as shown in the case where  $\Delta_{plateau}$  is 0.05 mm (FIGURE 2.26c). On the contrary, when the parameter value is appropriate, as illustrated in FIGURE 2.26b with  $\Delta_{plateau} = 0.02$  mm, it becomes possible to identify the plateaus in a relatively precise way.

The parameter is therefore chosen to identify the plateaus correctly. However, the value used to distinguish them is not unique. Thus, it is interesting to determine what impact the choice of this parameter might have on the average value calculated for a stage.

For each stage of a test, the average height is determined using parameters  $\Delta_{plateau}$  around the chosen value, as shown in TABLE 2.4. Then, for each level, the maximum variation in head ( $\Delta_{H,max}$ ) between a parameter value and the chosen one ( $\Delta_{plateau} = 0.02$  mm) is calculated.

	Head [mm]				
$\Delta_{plateau}$	Level 1	Level 2	Level 3	Level 4	Level 5
0.017 mm	79.048	88.741	94.952	97.833	100.858
0.018 mm	79.048	88.741	94.952	97.833	100.865
0.019 mm	79.051	88.741	94.952	97.833	100.864
<b>0.02 mm</b>	<b>79.051</b>	<b>88.743</b>	<b>94.973</b>	<b>97.833</b>	<b>100.864</b>
0.021 mm	79.051	88.744	94.961	97.825	100.864
0.022 mm	79.051	88.744	94.965	97.826	100.864
0.023 mm	79.051	88.744	94.978	97.837	100.907
$\Delta_{H,max}$ [mm]	0.003	0.002	0.021	0.008	0.043

TABLE 2.4: Head of every level of a test determined with different values of  $\Delta_{plateau}$  (0.017 mm to 0.023 mm)

From this table, it should be noted that the maximum variation  $\Delta_{H,max}$  is less than five hundredths of a millimetre. It can therefore be concluded that a slight change in  $\Delta_{plateau}$  does not produce a significant difference in the results identified.

To ensure that the choice of  $\Delta_{plateau}$  did not significantly influence the results, this development is carried out for 5 different tests. The maximum variation  $\Delta_{H,max}$  for each test is given in TABLE 2.5.

	Test 1	Test 2	Test 3	Test 4	Test 5
$\Delta_{H,max}$ [mm]	0.043	0.059	0.076	0.034	0.281

TABLE 2.5: Maximum variation  $\Delta_{H,max}$  in head over the stages of different tests

This table shows that a fluctuation in the choice of  $\Delta_{plateau}$  can lead to variations in the results. These do not appear to be greater than a few tenths of a millimetre. Consequently, when the variation limit ( $\Delta_{plateau}$ ) is set (because it allows the different levels of a signal to be identified), the fact that there is no single value for this parameter does not markedly affect the results obtained.

### 2.3.4 Result Types

The first type of data that can be collected is the ‘‘Stable Head’’. This can be identified for all tests, regardless of the fall of the block. On the graph in FIGURE 2.27, a blue area indicates the moment when the fuse plug flipped. The desired height corresponds to the last head level before this blue zone and is represented by the green zone on the graph.



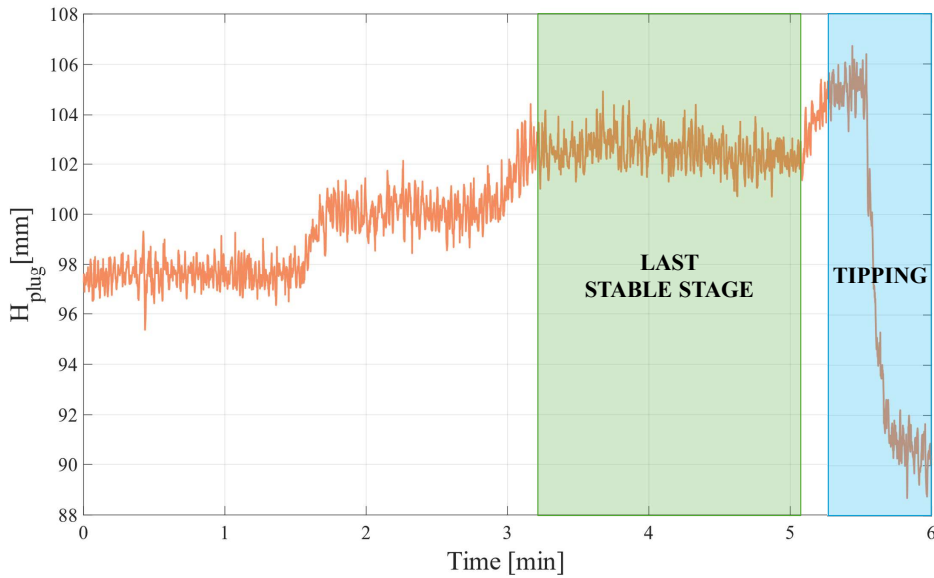


FIGURE 2.27: Representation of the “Stable Head” (last stable stage) on a signal

Then, depending on when the block tips over — whether during a data step or during a rising phase — it is possible to determine either the “Tipping Head” or the “Unstable Head”. In the graph in FIGURE 2.28, it is observed that the fuse plug falls while the plateau is already well established (blue zone), which represents the “Tipping Head”.

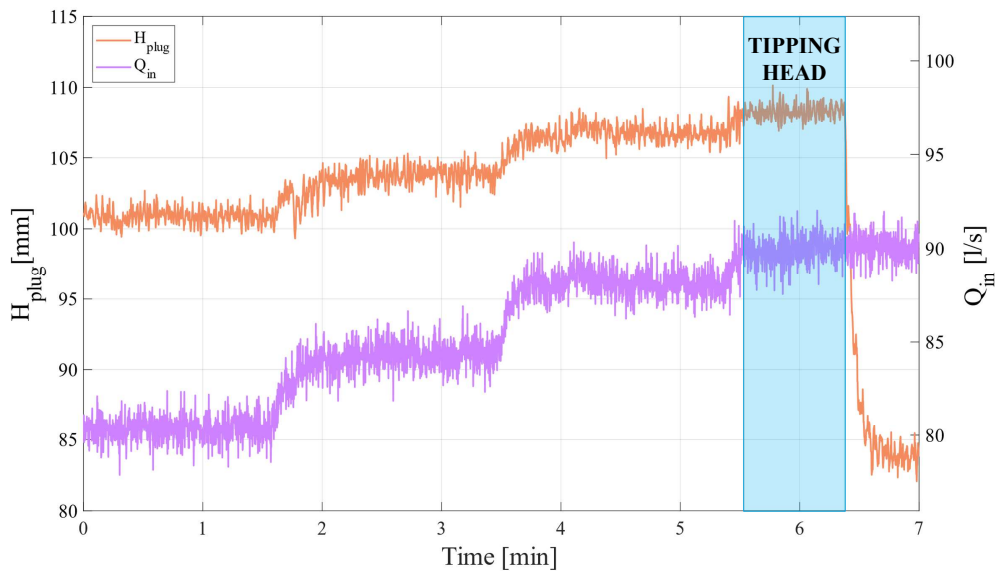


FIGURE 2.28: Representation of the “Tipping Head” on a signal

In contrast, in FIGURE 2.29, the block overturns while the flow rate was increasing. In this case, the height that caused the tilt cannot be directly determined. Consequently, the information collected is the last flow level (after the tipping), represented by the red zone. This flow makes it possible to calculate the associated head (“Unstable Head”), which was previously unknown.

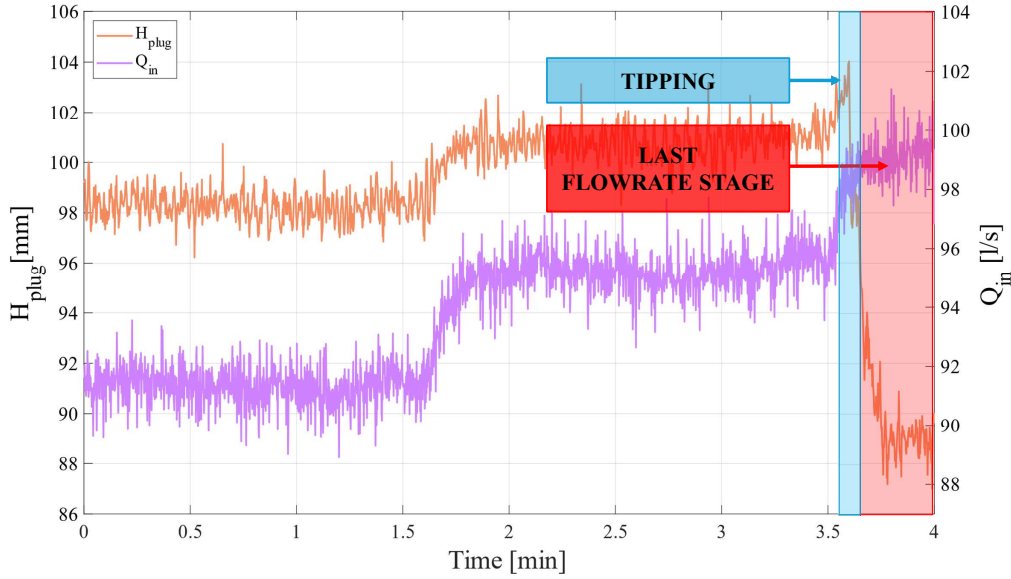


FIGURE 2.29: Representation of the “Unstable Head” (corresponding to the last flow rate stage) on a signal

To calculate the “Unstable Head”, it is necessary to consider that the flow rate spilling over the blocks ( $Q_{plug}$ ) is determined as follows:

$$Q_{plug} = Q_{in} - Q_{PKW} \quad (2.10)$$

where  $Q_{plug}$  and  $Q_{PKW}$  both depend on the head.

Therefore, a numerical method (the MATLAB function *fsolve*) is used to obtain the desired water level. Concerning the discharge  $Q_{plug}$ , it is established that the block behaves like a thick threshold, whose flow rate law is given by:

$$Q_{plug} = C_d \cdot L \cdot \sqrt{2 \cdot g \cdot H_{plug}^3} \quad (2.11)$$

where  $C_d$  is the flow coefficient and  $L$  is the length of the sill where the blocks are placed.

## 2.4 Tests

This section describes the experimental tests carried out in the course of this work.

### 2.4.1 Configurations

Various configurations are studied and described below.

#### Configuration 1 : Adjacent blocks have already tipped

Initially, tests are carried out to determine the hydraulic head that would cause each of the blocks to tip over. To do this, the fuse plugs are tested individually, leaving the rest of the sill empty. In this way, the configuration represents the moment when all the adjacent elements have already tipped over and only the block under consideration remains.

The positions of the blocks in this configuration are illustrated by the photos in FIGURE 2.30.

In the case of the B10 block, two positions are studied. Firstly, it is placed in the middle of the sill, FIGURE 2.30a. Secondly, the block is positioned at one end of the sill, FIGURE 2.30b.

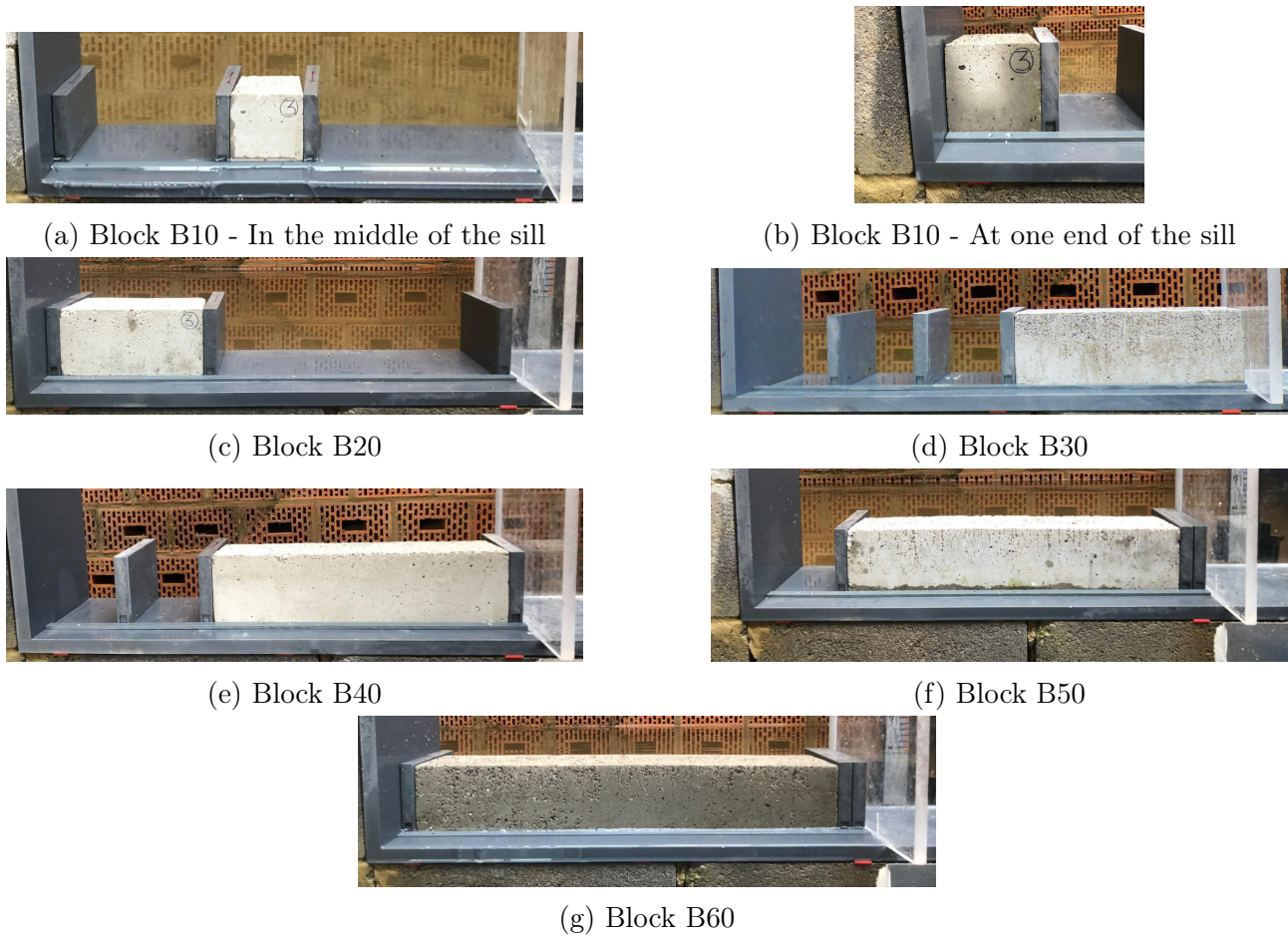


FIGURE 2.30: Configuration 1 : Position of the blocks

**Configuration 2 : First block to tip over**

The second configuration also looks at tilting one block at a time. However, in this configuration, the remaining space on the sill is occupied by other blocks, as the photo in FIGURE 2.31a shows. They are fixed to prevent them from tipping over. These tests therefore represent the situation where the block under consideration is the first to topple over.

Plastiline is used to fix the blocks. This material seals and prevents the blocks from tipping, and has the advantage of being easy to remove. The way the plastiline is placed is shown in the photo in FIGURE 2.31b.

The blocks tested in this second configuration are B10 (in the middle and at the end of the sill), B20 and B30 in the same positions as the first configuration.

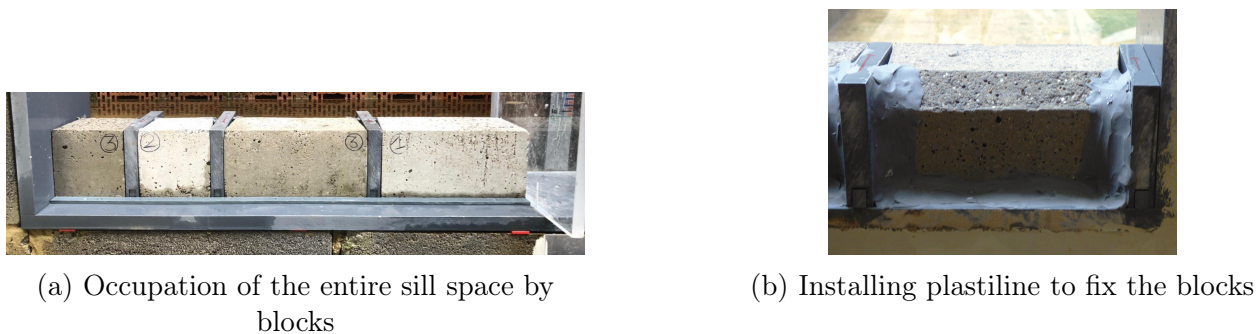


FIGURE 2.31: Configuration 2

TABLE 2.6 below summarises the configurations carried out and the number of test repetitions.

		Config. 1	Config. 2
End of the sill	B10	5	2
	B20	4	5
	B30	3	4
	B40	5	\
	B50	4	\
	B60	5	\

		Config. 1	Config. 2
Middle of the sill	B10	3	5
	B20	3	\

TABLE 2.6: Summary of test repetitions

### 2.4.2 Procedure

The experimental tests consist of working in flow steps (and therefore with a constant hydraulic head) until the block under study tilts.

The following procedure is followed for each of the experimental tests :

- (a) Place the intermediate walls according to the block being studied and its position ;
- (b) Install the studied block and fit the water-proofing plastic strip ;
- (c) For configuration 2, place the remaining blocks and fix them with plastiline ;
- (d) Open the valve and switch on the pump. The pump used can be set between 25 and 50 Hz to the nearest tenth of Hertz. There are therefore 250 possible positions with a maximum capacity of 250 l/s. The test starts with the minimum pump setting and the data is recorded ;
- (e) Increase the flow rate. Data is recorded continuously at a frequency of 10 Hz. The time interval for each flow rate step is defined by a minimum of 1 min. Consequently, after at least 1 min, the flow rate is increased by one unit (1 Hz) in the pump's frequency range (depending on the configuration, it may be necessary to increase the flow rate by 0.5 Hz in terms of pump operating frequency, so that the water level does not rise by more than 2 mm between steps);
- (f) Repeat the previous step until the block tilts ;
- (g) When the block has tipped over, switch off the measurement recorder and the pump. Repeat the previous steps (from point b) 3 to 5 times for each type of test.

# Chapter 3

## Results

This chapter presents and discusses the results of experimental tests carried out.

### 3.1 Presentation of results for configurations 1 and 2

The experimental tests on the tipping of individual blocks were conducted in two configurations: either alone on the sill or alongside adjacent fixed fuse plugs.

In the first configuration, all six types of blocks are studied. Multiple tests were carried out for each block (see the number of test repetitions for each block in TABLE 2.6), leading to the identification of “Stable Head”, “Unstable Head” and “Tipping Head” points.

In the second configuration, only fuse plugs B10, B20, and B30 are studied.

The error bars in the graphs represent the uncertainty associated with the determination of the calibration lines, as described in the methodology.

#### 3.1.1 B10 block

To begin with, the data from the 10 cm block are presented in FIGURE 3.1. The B10 plug was positioned at two separate locations: at one end of the sill (left in FIGURE 3.1) and in the middle of the weir (right in FIGURE 3.1).

Firstly, it is clear that the position of the 10 cm block on the sill, as well as the presence or absence of adjacent blocks, significantly influence the results. Indeed, when the fuse plug is placed in the middle of the weir, it does not tip at the same heights as when it is positioned to one side, regardless of the configuration.

From the graph, it is evident that when the block is situated at one end of the sill, tipping occurs at the same water heights, regardless of nearby fuse plugs. The head ranges of the two configurations overlap, with a relatively wide interval spanning from 105 to 118 mm.

On the other hand, when the block is positioned centrally, the two configurations yield different results, with a variation of more than 25 mm between the tipping head points.

Furthermore, the graph shows that when the fuse plug is installed on the side, the tipping heights fall between the results of the two configurations for the central position.

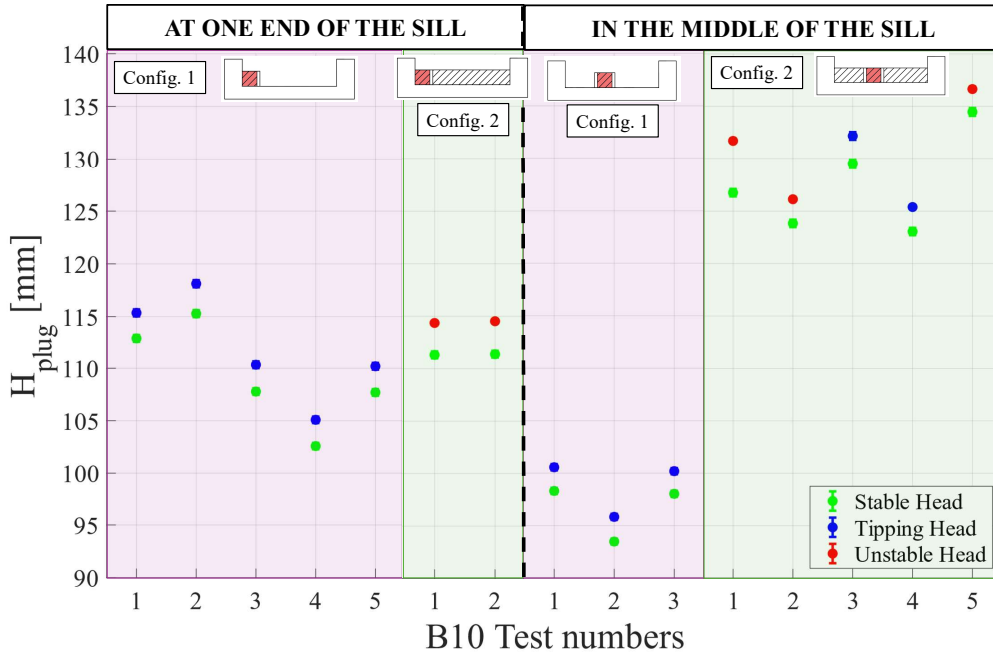


FIGURE 3.1: Comparison of results for the 10 cm block: configuration 1 and 2 for the side and middle positions on the sill

The central position provides insight into the influence of adjacent elements. When the fuse plug is surrounded by others, the tipping height increases compared to when nearby blocks have already fallen. This demonstrates the stabilizing effect of neighbouring elements.

In the first configuration, placing the block at one end of the sill reveals that the absence of the flow on the right (replaced by the wall) increases the tipping height compared to the other position. However, this configuration does not enhance stability as effectively as having fuse plugs on both sides (as the tipping height is lower than observed when the block is placed in the centre of the sill in configuration 2).

One would expect similar results for both positions of the block in the second configuration. However, this is not the case. When the fuse plug is situated at the side of the sill, only two tests were conducted, but they yielded identical heads. The tipping heights are at least 11 mm lower than those obtained when the block is placed centrally.

A notable difference between these two positions lies in the behavior of the surrounding flow. At the edges of the weir, there is an abrupt reduction in the width of the reservoir in the direction of the flow due to the right-angle geometry, resulting in a contraction of the inflow (known as the "effet d'entonnement" in French). This phenomenon is visible in the photo in FIGURE 3.2. The flow tends to concentrate towards the middle of the weir. Consequently, for the same upstream head, there is more water above the block positioned at the centre of the sill than at the edge.



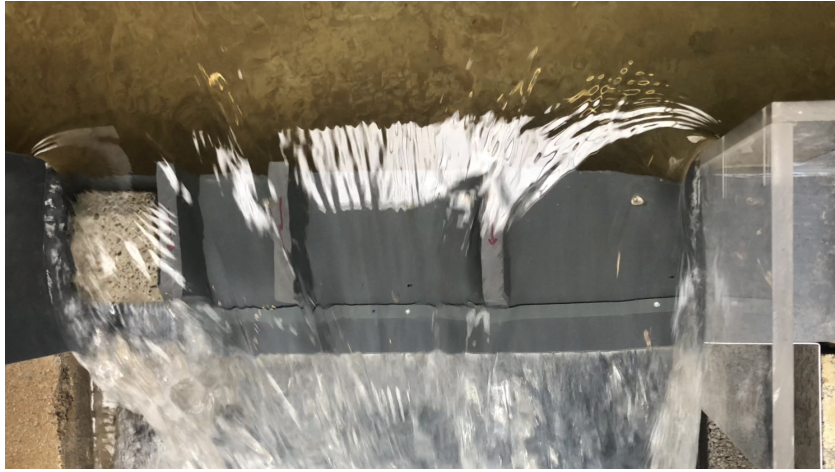


FIGURE 3.2: Photo of flow contraction

In this work, the pressures acting on the blocks are not measured, and this effect is not studied. However, it is possible that pressure differences, resulting from the behaviour of the flow along the weir, justify these variations. Based on this hypothesis, an attempt will be made to explain why the head can be higher when the block is positioned at the centre of the sill, by analysing the pressure balance. This discussion will be addressed in chapter 4, when the theoretical stability of the fuse plug is studied.

### 3.1.2 B20 & B30 blocks

Secondly, the comparison of the two configurations reveals that, for blocks B20 and B30, the presence of adjacent blocks did not significantly affect the results.

From FIGURE 3.3, which depicts the results for block B20, it initially appears that the height range for the second configuration is encompassed within that of the first configuration. However, upon closer examination of the graph, it becomes evident that the tilt interval for the second configuration (109.1 to 114 mm) only falls within the range of test 2 in configuration 1 (109.9 to 114.4 mm). The remaining trials in the first configuration exhibit tilt levels spanning between 104.8 and 109.5 mm. This suggests that the presence of adjacent blocks could indeed influence the overturning moment. Nonetheless, despite the lack of exact overlap between the results, the difference between the two configurations is not significant, as the two ranges are relatively close.

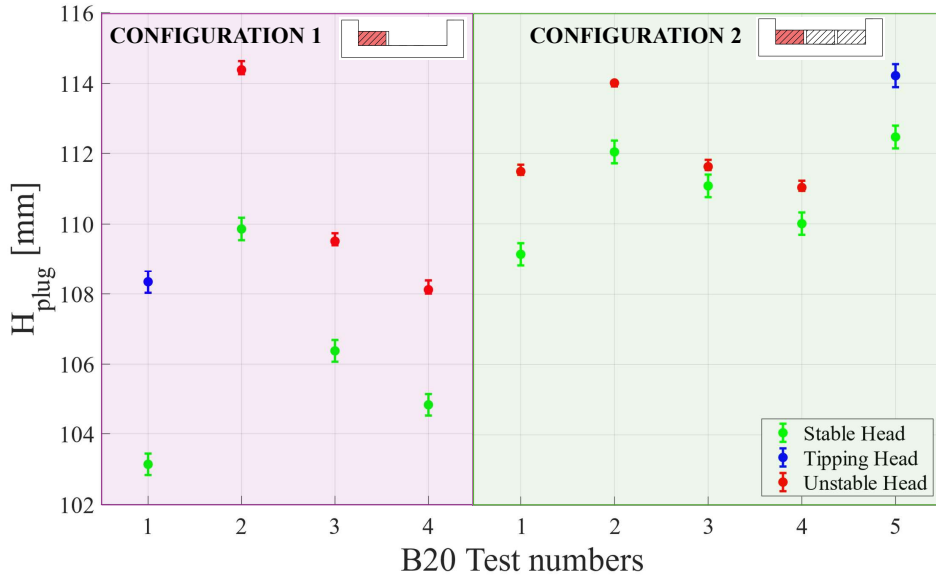


FIGURE 3.3: Comparison of results for the 20 cm block: configuration 1 and 2

The data in FIGURE 3.4 indicates that for block B30, the results of the two configurations overlap relatively well, yielding a common range of 100.5 to 109 mm within which the fuse plug can tip.

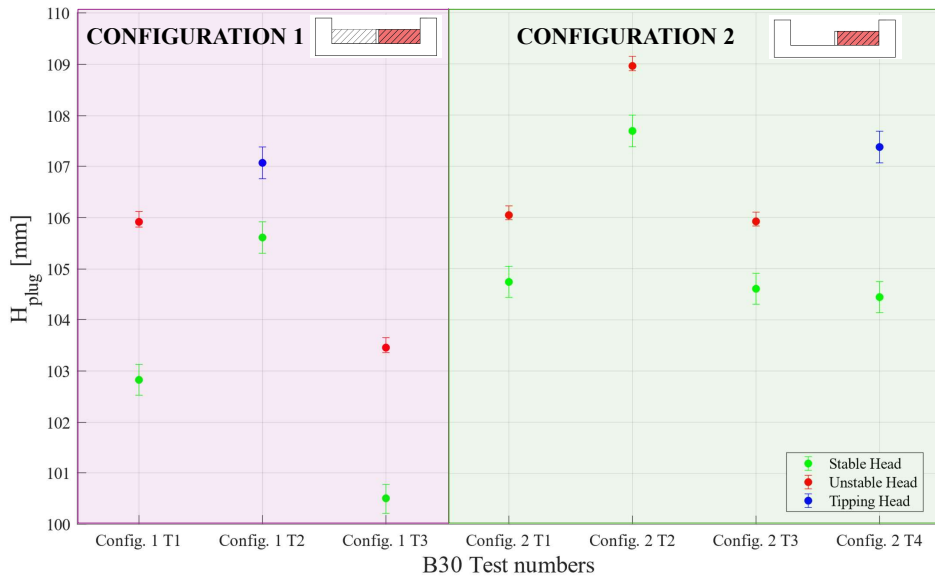


FIGURE 3.4: Comparison of results for the 30 cm block: configuration 1 and 2

### 3.1.3 B40, B50 & B60 blocks

The blocks B40, B50, and B60 were solely tested under the first configuration (with the fuse plug alone on the sill) and at one position (at the side of the sill, except for block B60, which has the same width as the weir).

The results for block B40 are depicted in FIGURE 3.5. The measured tipping heights are 107.4 mm for the first two trials and 104.8 mm for the fourth test. For experiments 3 and 5, unstable heads were calculated, yielding ranges of 101.2 to 105.7 mm and 104.6 to 108.4 mm, respectively.



It is noteworthy that the heads of the first two trials fall within the range of test 3, while the value of test 4 is within the interval of test 5.

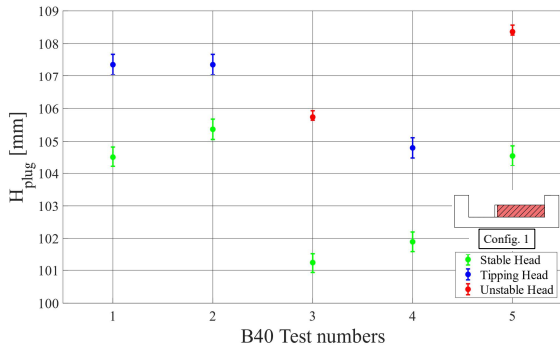


FIGURE 3.5: Configuration 1 : Test results for block B40

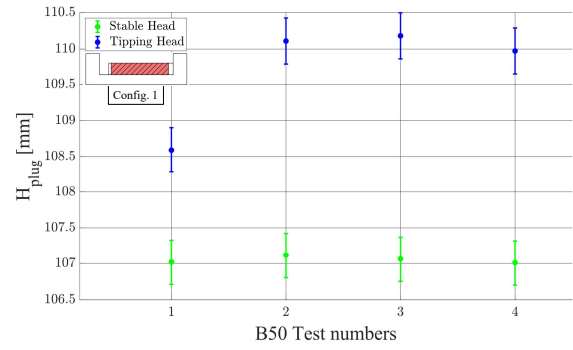


FIGURE 3.6: Configuration 1 : Test results for block B50

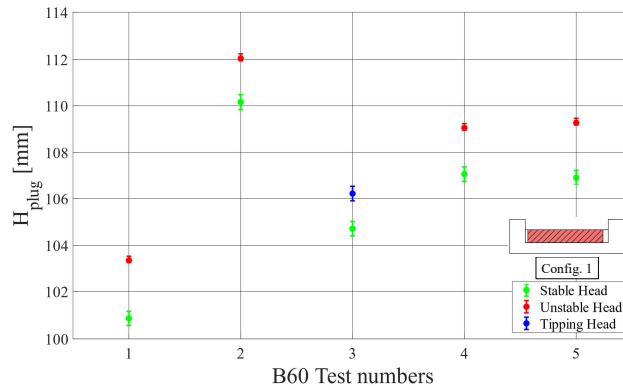


FIGURE 3.7: Configuration 1 : Test results for block B60

Regarding the B50 block, refer to FIGURE 3.6. Out of four tests, three resulted in tipping levels of approximately 110 mm, while the first trial yielded a head of 108.5 mm.

Lastly, the results of block B60 are presented in FIGURE 3.7. A notable variability is observed. Tests 4 and 5 provide similar values ranging from 107 to around 109 mm, while the other trials yield different heights. Test 1 shows a range from 100.9 to 103.4 mm, while Test 2 indicates an interval from 110.1 to 112 mm. Finally, experiment 3 reveals a tipping level of 106.2 mm.

## 3.2 Analysis and discussions

Based on the results of the tests carried out on the various blocks, some points can already be discussed.

### 3.2.1 Influence of the position on the sill

In the methodology section, it was intended to test the 10 cm and 20 cm blocks in two different positions: on the side and in the centre of the weir, while the other fuse plugs were tested only at one end of the sill.

However, the results of block B20 positioned in the middle of the weir were not presented in the previous section. Despite conducting three tests, the fuse plug never tipped over, likely due to excessive friction. This issue will be addressed in the next subsection 3.2.3.

Through the comparison of different results for block B10, it was demonstrated that the position of the fuse plug on the sill played a crucial role in influencing the height of water causing overturning. Given the width of the weir and the planned combinations of blocks and intermediate walls, only plugs B10 and B20 could be placed in the centre of the sill.

As a result, the conducted tests were unable to determine whether this positional factor (or the impact of flow contraction) affects all the blocks, irrespective of their width, or to identify the dimension at which this effect ceases to influence the overturning height.

### 3.2.2 Influence of adjacent blocks

The comparison of results indicates that the width of the block significantly influences its behaviour concerning the surrounding flow, particularly when adjacent fuse plugs are present.

Analysis reveals that block B10 is more susceptible to the presence of nearby fuse plugs in contrast to blocks B20 and B30. The existence of neighbouring elements seems to have a stabilising effect on plug B10, delaying its tilting compared to configuration 1.

For the 20 cm block, the influence of nearby fuse plugs on its tipping remains uncertain. Although the block does not tilt under precisely the same head in both configurations, the impact doesn't seem significant. However, for the 30 cm element, the presence or absence of the flow alongside it does not affect its tilting.

It appears that for a block to tip over independently of adjacent elements, it needs to be 2 to 3 times wider than its height (in this work, the fuse plug height is around 10 cm).

### 3.2.3 Influence of friction

As previously mentioned, the 20 cm unit was positioned in the centre of the weir for three tests, yet it never tipped over. According to the signal from FIGURE 3.8, the head reached 158 mm without any tilting occurring.

The issue stemmed from the planned location for the separating walls, which did not provide sufficient space to properly position block B20 in the middle. Consequently, the plug became wedged between the intermediate panels, resulting in significant friction that prevented overturning. Conversely, for all other fuse plugs and configurations tested, there was adequate clearance between the various components. Thus, it is essentially a construction flaw that led to lateral friction affecting block B20 in the middle of the sill.

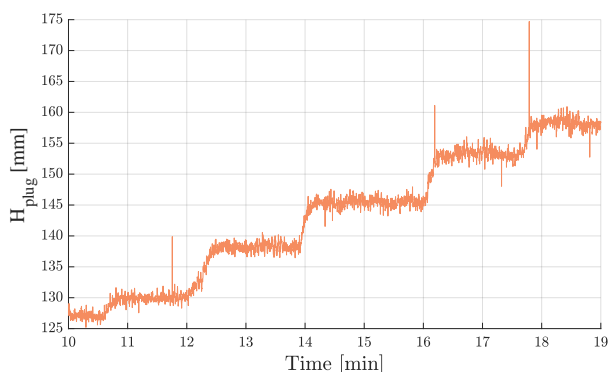


FIGURE 3.8: Head signal of block B20 placed in the centre of the sill



FIGURE 3.9: Photo of a block between the intermediate walls

The trapezoidal shape of the block was intended to minimise friction with the dividing walls. To illustrate the extent of contact between the block and the side walls, refer to the photo in FIGURE 3.9 depicting block B10. It is evident that the blocks only come into contact with adjacent walls along a small portion of the cross-section's length, highlighted by the red rectangle. Consequently, friction between the fuse plug and the intermediate walls emerges as a critical factor influencing system performance. Ensuring adequate clearance between the components is essential for facilitating block overturning. Additionally, sealing this clearance with plastic strips prevents leaks without significantly increasing friction, as observed in cases where the fuse plugs successfully tipped over.

### 3.2.4 Determination of the tilting head

The next step involves determining a single range of heights that trigger block overturning for each fuse plug, crucial for further analysis. This implies selecting pertinent information from the three data points: “Stable Head”, “Tipping Head”, and “Unstable Head”, as well as the intervals identified on various graphs.

The objective is to establish a height range that ensures fuse plugs tipping while adequately mitigating the risk of dams overtopping. Therefore, it is preferable to utilise the “Tipping Head” and “Unstable Head” points for describing block tilting.

The “Tipping Head” points define a lower limit, signifying that smaller heights ensure block stability. Conversely, the “Unstable Head” points within the tipping interval establish an upper limit, indicating that beyond these heights, the fuse plug has tilted.

Between these limits, the system must function effectively to ensure dam safety.

This approach identifies an operational interval during which the block is likely to topple. The data is presented as box plots in FIGURE 3.10, illustrating the distribution of “Tipping Head” and “Unstable Head” points, along with any outliers. The box plots incorporate results from both configurations for fuse plugs B20 and B30, showing overlapping outcomes. Contrastingly, block B10 exhibits distinct cases, with “B10 S” representing configurations with the block on one side of the sill. “B10 M1” and “B10 M2” denote configurations with the block placed in the middle of the weir.

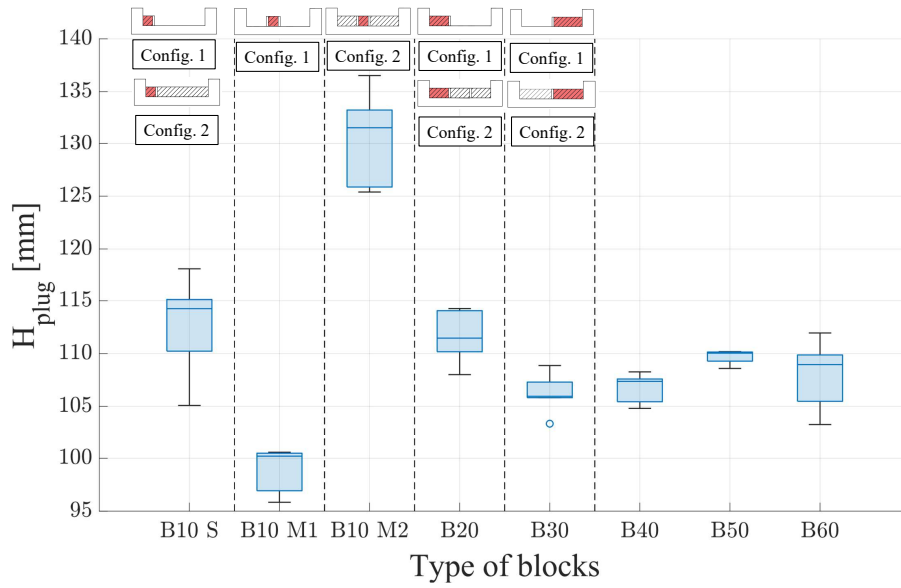


FIGURE 3.10: Box plots of the results (“Tipping Head” and “Unstable Head”) for each block configuration

### Variability of the results

The whisker boxes provide several noteworthy insights.

Firstly, the span between the ends of the whiskers delineates the data extent, essentially defining the interval’s length, i.e., the gap between the maximum and minimum values. This measure allows assessing the experimental result precision. Additionally, the median, depicted by the line within the box, serves as a measure of the data’s central tendency. These values are summarized in TABLE 3.1.

	B10 S	B10 M1	B10 M2	B20	B30	B40	B50	B60
Length of the interval [mm]	13	4.76	11.1	6.3	3.1	3.5	1.6	8.7
Median [mm]	114.3	100.2	131.6	111.5	106	107.4	110	109

TABLE 3.1: Length of interval and median of each box plot

Analysis of this data indicates that, in most instances, ranges of less than 1 cm were observed. Notably, for blocks B30, B40, B50, and the B10 M1 configuration, the variance between results was further reduced to less than 5 mm. Conversely, for cases B10 S and B10 M2, values exhibited greater dispersion, resulting in intervals exceeding 1 cm.

Examining the medians listed in TABLE 3.1 (ranging from 106 to 111.5 mm for blocks B20 to B60), no discernible relationship between tipping level and block width is apparent. Furthermore, the whisker boxes exhibit relatively well overlap.

Lastly, an outlier value of 103.4 mm is notable for block B30, approximately 3 mm below the median.

# Chapter 4

## Analytical model

In this chapter, an analytical model describing the tilting of a concrete fusible plug is established. To do this, the previously developed formulas are analysed. Then, an equation adapted to the block studied is determined.

### 4.1 Formulas from the literature

The first formula present in the literature was developed by Dr. Truong Chi Hien and Mr. Ho Ta Khanh in 2007 ([Hien and Khanh 2007]), it is provided in equation (4.1). The second, equation (4.2), was determined by Ilyese Sekkour in his master's thesis in 2016 ([Sekkour 2016]).

$$H_{2007} = \frac{-6Me + \rho_w(P - i) \cdot [2B(P - i) \cdot (P + 2i) + 3(B + b)e^2]}{3\rho_w \cdot [-2B \cdot (P^2 - i^2) + (\beta - 1)(B + b)e^2]} \quad (4.1)$$

$$H_{2016} = \frac{3Pe^2 \left( \frac{\gamma_b - \gamma_w}{\gamma_w} \right) - P^3}{e^2 + 3P^2} \quad (4.2)$$

where

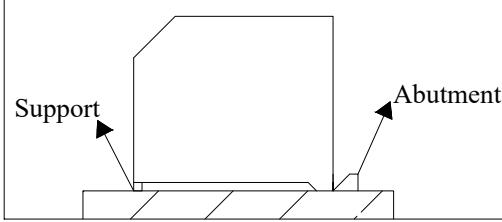
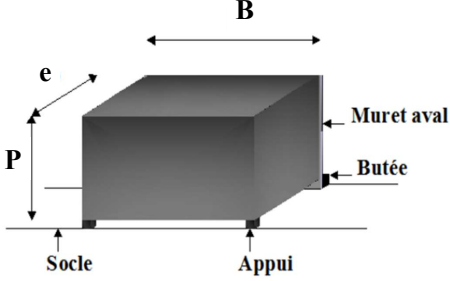
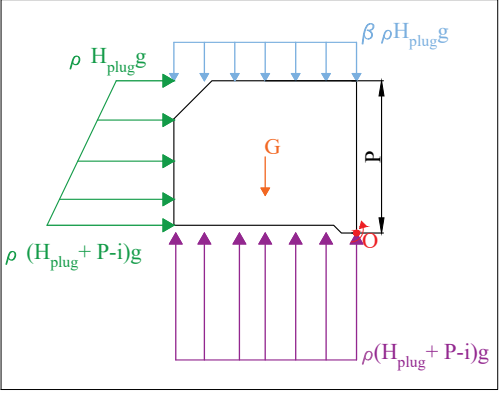
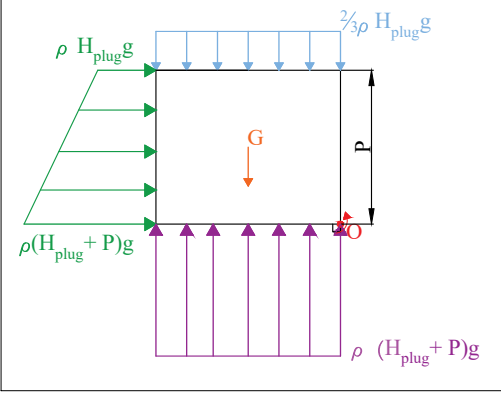
- $M$  corresponds to the mass of the fuse plug [kg];
- $\gamma_w$  is the specific weight of water : 9810 N/m<sup>3</sup>;
- $\beta$  is a reduction factor [-];
- $\gamma_b$  is the specific weight of the concrete fuse plug [N/m<sup>3</sup>];
- $\rho_w$  is the water density : 1000 kg/m<sup>3</sup>.

Theoretical developments are grounded in block stability, where the various loads acting on the fuse plug are categorized into stabilising and destabilising forces. The relationship to be established is therefore a balance of the moments induced by these forces around the block's axis of rotation (point "O" on the following figures). This axis is defined by the position of the abutment.

The stabilising forces include the block's own weight, as well as the vertical pressure applied by the water surface on the upper face of the block.

The destabilising forces are the underpressure and the horizontal hydrostatic pressure applied to the upstream surface.

The different considerations and hypotheses taken to establish these two relationships are presented in the following table (TABLE 4.1).

	Hien & Khanh (2007)	Sekkour (2016)
Block geometry	<p>The geometry considered is identical to that used for the blocks in this study. The only difference lies in the type of abutment. In this case, it requires the fuse plug to tilt along the axis of rotation at its lower downstream corner, as shown in FIGURE 4.1.</p>  <p style="text-align: center;">FIGURE 4.1</p> <p>For the developments, the entire block geometry is considered.</p>	<p>The geometry of the block studied is simply a rectangular parallelepiped with an underpressure chamber, as shown in FIGURE 4.2.</p>  <p style="text-align: center;">FIGURE 4.2: Drawing from [Sekkour 2016] (with modified dimension names)</p> <p>The developments are based on a cross-section.</p>
Pressure distribution	 <p style="text-align: center;">FIGURE 4.3</p>	 <p style="text-align: center;">FIGURE 4.4</p>
Block self-weight ( $G$ )	<p>Calculated using the mass of the fuse plug.</p> <p><u>Hypothesis for the moment induced by <math>G</math></u>: The centre of gravity is approximately <math>e/2</math> from the axis of rotation.</p>	<p>Calculated using the density of the fuse plug.</p>
Vertical pressure	<p><u>Hypothesis</u>: The flow applies a uniform pressure to the upper face, equivalent to a percentage <math>\beta</math> of the head. This coefficient (<math>\beta</math>), which varies according to the shape of the fuse plug, was established during experiments.</p>	<p><u>Hypothesis</u>: Flow over the fuse plug is supposed to be the same as over a broad crest weir. The water depth considered for the hydrostatic pressure is assumed to be the critical height (<math>\frac{2}{3} \cdot H_{plug}</math>).</p>

	Hien & Khanh (2007)	Sekkour (2016)
Horizontal pressure	<p><u>Hypothesis:</u> A hydrostatic pressure is applied to the upstream face of the block.</p> <p>Taking into account the lower chamber in the height of the block (<math>P</math>). Therefore, the lower corner head is <math>H_{plug} + P - i</math>.</p>	<p><u>Hypothesis:</u> A hydrostatic pressure is applied to the upstream face of the block.</p> <p>The lower chamber is not included in the height of the block (<math>P</math>). Therefore, the lower corner head is <math>H_{plug} + P</math>.</p>
Underpressure	<p><u>Hypothesis:</u> The underpressure is considered to be uniform across the entire underside.</p>	<p><u>Hypothesis:</u> The underpressure is considered to be uniform across the entire underside.</p>

TABLE 4.1: Hypotheses used for the developments of the Hien &amp; Khanh and Sekkour formulas

### 4.1.1 Comparison of formulas with experimental results

Now that the assumptions of the two previous formulas are known, it is appropriate to compare the experimental results with the theoretical ones. This comparison will determine whether these equations adequately represent the tests carried out, or whether the development of a new analytical model is necessary.

#### Hien & Khanh (2007)

To begin with, the box plots of the experimental results (“Tipping Head” and “Unstable Head”) obtained for each block are presented in FIGURE 4.5. The theoretical heights, calculated using Hien & Khanh formula, are also plotted.

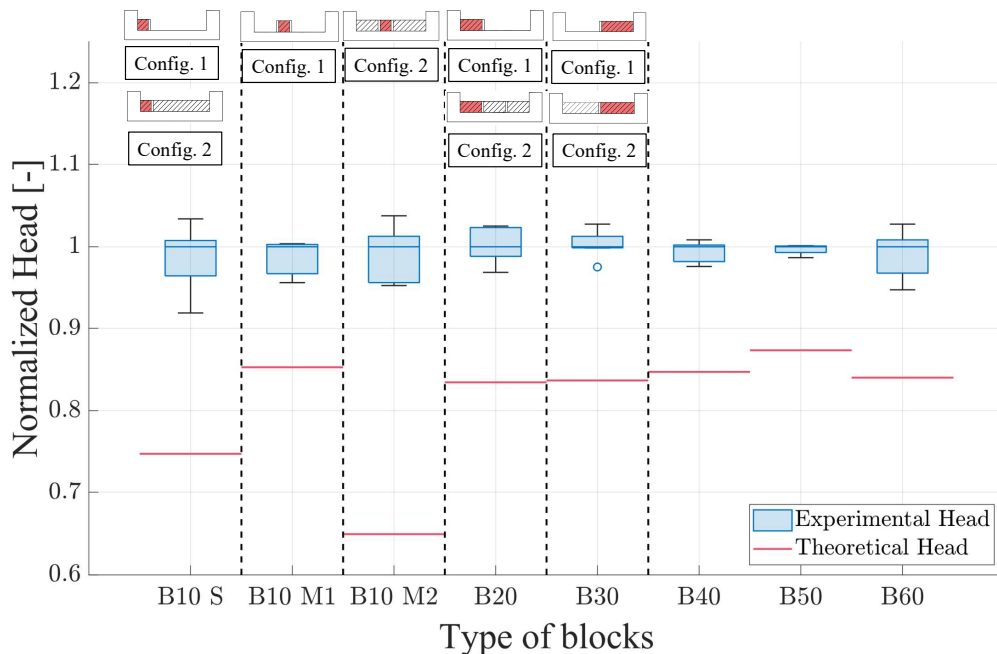


FIGURE 4.5: Box plots of experimental results and theoretical heads from the Hien &amp; Khanh equation, normalized by the median head of each block configuration

In equation (4.1), the parameter  $\beta$  determining the vertical pressure applied to the fuse plug

has been fixed at  $2/3$ . Hien & Khanh demonstrated in their paper ([Hien and Khanh 2007]) that for blocks with an  $e/P$  ratio greater than 1, the factor  $\beta$  was between 0.6 and 0.65. The value of  $2/3$  has been chosen here, corresponding to the critical head of the flow.

To objectively assess the ability of the mathematical expression to accurately represent the experimental data, a head normalisation is undertaken on the graph. The median of the points used for each box charts is calculated, allowing all the results to be divided by this value. In this way, the theoretical height of a block is presented as a percentage of the experimental tipping water level.

The graph reveals an underestimation of the tipping heights according to the formula developed by Hien & Khanh. The difference between the theoretical heads and the experimental data is around 15%. This difference is more pronounced for block B10, which exhibits a greater variation in certain configurations.

This expression does not therefore seem to be in agreement with the tests carried out in this work satisfactorily.

### Sekkour (2016)

Firstly, FIGURE 4.6 depicts the box plots of the previously determined experimental results for each block. Additionally, the theoretical heads, calculated using Sekkour’s formula, and normalised by the median of the box plot, are presented.

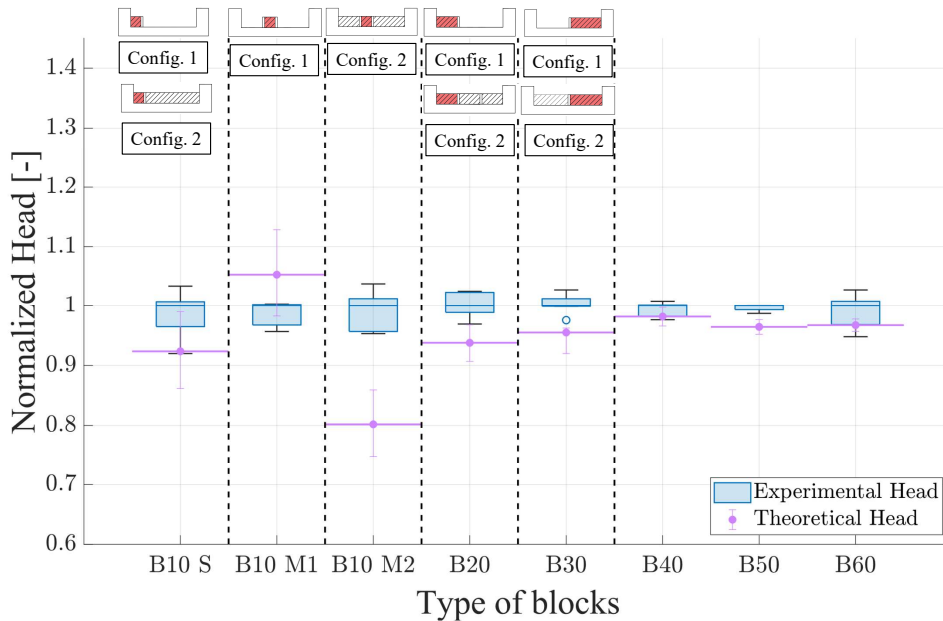


FIGURE 4.6: Box plots of experimental results and theoretical heads from the Sekkour equation, normalized by the median head of each block configuration

The equation (4.2) incorporates the density of the blocks, determined with an uncertainty interval, as explained in the methodology section. Consequently, the theoretical results are presented in the graph by an interval.

Analysis of the graph reveals that the 2016 formula reasonably represents the test results. To verify this, the disparities between the theoretical data ( $H_{th}$ ) and the experimental height ( $H_{exp}$ ) are computed and summarised in TABLE 4.2. The tipping head of the experiments considered



corresponds to the median of the relevant box plot. In this table, the variation does not exceed 10%, except for configuration 2 of block B10 when placed in the middle of the sill. Overall, the equation tends to underestimate the tipping head of the fuse plugs by less than 10%.

	B10 S	B10 M1	B10 M2	B20	B30	B40	B50	B60
$H_{th} - H_{exp}$	-8%	5%	-20%	-6%	-5%	-2%	-4%	-3%

TABLE 4.2: Difference between the theoretical heads ( $H_{th}$  : calculated with Sekkour equation) and the heights determined experimentally ( $H_{exp}$ )

The differences in theoretical heads among the blocks can be attributed to either the dimensions or the density of the fuse plugs. Therefore, it is pertinent to ascertain which factor the equation is particularly sensitive to.

The interval derived for the theoretical head already hints at the impact of density on the calculated values. FIGURE 4.7 illustrates this effect. The relationship established by Sekkour has been plotted as a function of density. Additionally, the theoretical heights determined for each block are represented on the graph, assuming that they all possess precisely the same cross-sectional dimensions.

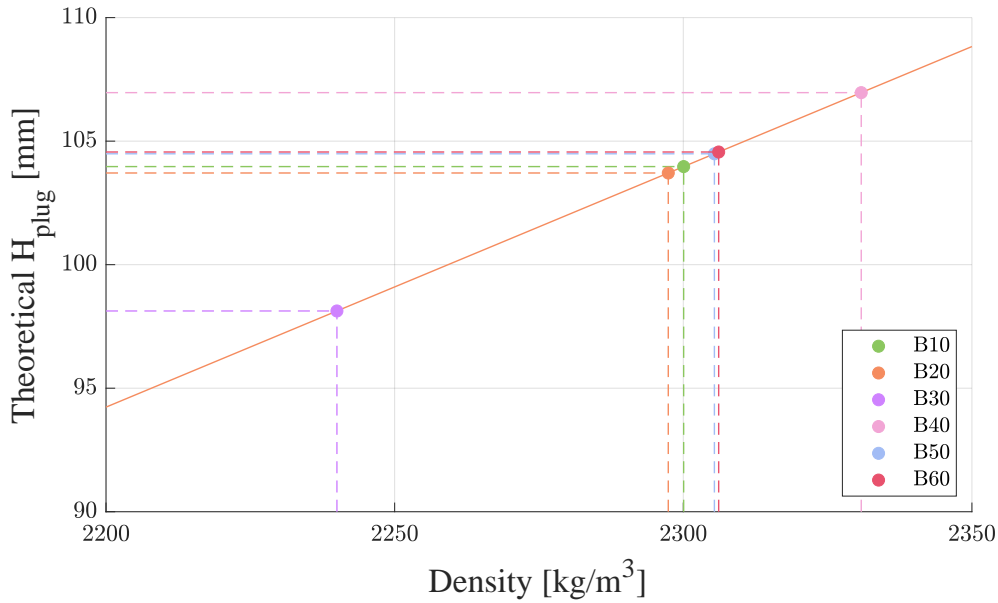


FIGURE 4.7: Relationship between density and theoretical tipping height (based on Sekkour's equation). The theoretical heights of each block, with identical cross-section dimensions ( $e = 120$  mm,  $P = 100$  mm), are highlighted.

From this graph, it is evident that for blocks B20 and B60, with densities of 2297 and 2306 kg/m<sup>3</sup> respectively (a difference of 9 kg/m<sup>3</sup>), the tipping head ranges from 103.7 to 104.6 mm, showing a variation of 0.9 mm. Moreover, between the B10 fuse plug with a density of 2300 kg/m<sup>3</sup> and the B30 with a density of 2240 kg/m<sup>3</sup>, there exists a difference in water height of 5.84 mm (103.97 mm and 98.13 mm respectively). In summary, a change of  $x$  kg/m<sup>3</sup> leads to an alteration of approximately  $x/10$  mm in the theoretical tipping head.

The influence of a slight modification in block dimensions on theoretical tipping heights can also be assessed. In FIGURE 4.8, the correlation between calculated head and plug length ( $e$ )

is depicted, assuming identical density and a constant height for all blocks. This graphical representation illustrates that a variation of 1 mm in length corresponds to an approximate variation of 1.5 mm.

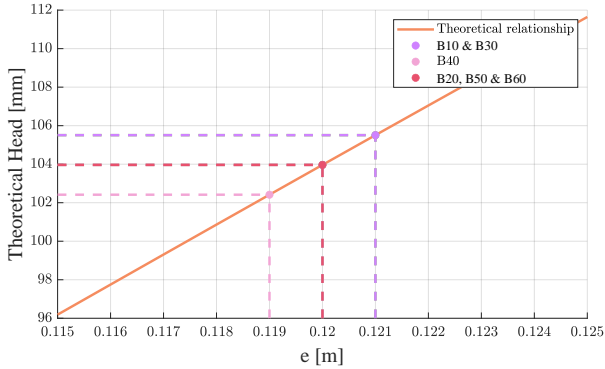


FIGURE 4.8: Relationship between length ( $e$ ) and theoretical tipping height (based on Sekkour's equation). The theoretical heights of each block, with  $P = 0.1$  m and  $\rho_b = 2300$  kg/m<sup>3</sup>, are highlighted.

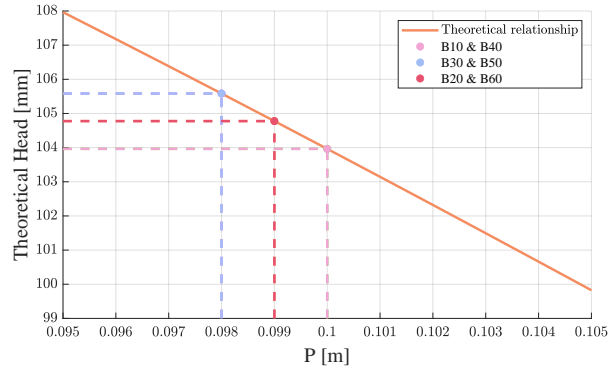


FIGURE 4.9: Relationship between height ( $P$ ) and theoretical tipping head (based on Sekkour's equation). The theoretical heads of each block, with  $e = 0.12$  m and  $\rho_b = 2300$  kg/m<sup>3</sup>, are highlighted.

The graph depicted in FIGURE 4.9 illustrates the correlation between block height and theoretical tipping head. It is observable that a variation of 1 mm in the fuse plug dimension corresponds to an alteration of approximately 0.8 mm.

### 4.1.2 Conclusion

Initially, it was expected that the formula established by Hien & Khanh would best represent the experimental tests due to its reliance on blocks geometry identical to that studied in this work. However, the results indicate otherwise. The formulation based on more simplified assumptions, developed by Sekkour, yields theoretical tilting heights closer to the experimental data. Nonetheless, both equations consistently underestimate the theoretical heads compared to the experimental observations, raising safety concerns.

Although the two equations in the literature share similar assumptions regarding pressure distribution, the Hien & Khanh's formulation offers a more detailed consideration of block geometry. Despite this advantage, it does not adapt the pressure field to the plug's specific geometry, potentially contributing to its greater underestimation compared to the Sekkour's equation.

Consequently, the exploration of a new analytical model is justified. The objective is to incorporate fewer simplifying assumptions about pressures to achieve more accurate results. Subsequently, it will be possible to assess whether adopting simpler hypotheses, such as the Sekkour formula, is more appropriate for determining theoretical heads.

## 4.2 Development of a new analytical model

To develop an analytical model, new assumptions regarding pressure distributions are introduced. These are depicted in FIGURE 4.10. In the calculations, hydrostatic pressure fields are considered, computed using the formula  $P = \rho \cdot g \cdot h$ , where  $\rho$  denotes fluid density,  $g$  represents

the acceleration due to gravity, and  $h$  indicates water height. Water heights are measured relative to the tank level, corresponding to the upstream head, given the negligible velocity in the reservoir studied. While this approach is approximate, it simplifies the system while indirectly incorporating the effect of velocity, also referred to as the “dynamic” effect.

Furthermore, the geometry of the blocks under consideration corresponds to that studied in this work and is detailed in the methodology section. FIGURE 4.11 illustrates the abutment used, with its upper corner situated at a distance  $i$  from the bottom of the fuse plug, representing the point of rotation “O”. The formulation is based on a cross-section of the block, specifically per linear metre of the block.

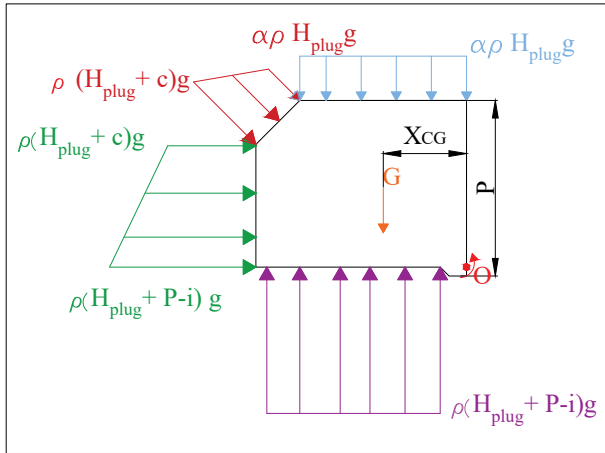


FIGURE 4.10: Pressure distribution considered in the new analytical model

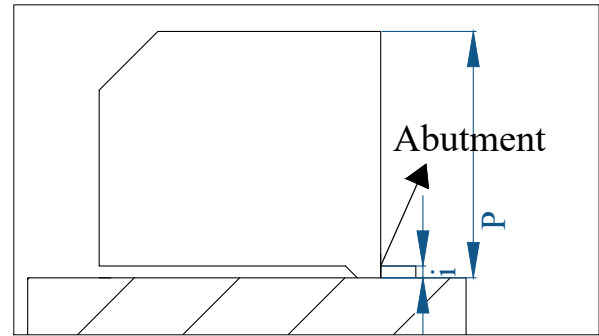


FIGURE 4.11: Block geometry considered for the new analytical model

## Hypotheses

- **Block self-weight ( $G$ )** : Calculated using the density of the fuse plug. The moment induced by  $G$  is determined by locating the centre of gravity ( $x_{CG}$ ), accounting for the presence of the chamfer.
- **Vertical pressure** : The flow exerts a uniform hydrostatic pressure on the block, equivalent to a percentage  $\alpha$  of the head. This coefficient ( $\alpha$ ) is initially assumed to be  $2/3$ , such that the water height corresponds to the critical depth.
- **Horizontal pressure** : A hydrostatic pressure is applied to the upstream face of the block. The lower chamber is considered in the height of the fuse plug ( $P$ ). Hence, the head at the bottom corner is  $H_{plug} + P - i$ .
- **Underpressure** : The underpressure is assumed to be uniform, but not applied over the entire length of the plug. An edge of width  $s$  serves as support for the block, where water cannot apply pressure.
- **Chamfer** : The pressure distribution accounts for the chamfer to maintain pressure continuity on each face of the block. Additionally, the pressure applied to a surface is considered to be orthogonal to it.

Each pressure component generates a rotational moment around the axis O. Therefore, a moment equilibrium must be established to determine the tipping head based on the geometric properties and density of the block. This balance of moments is expressed as follows:

$$M_G + M_v + M_{c,stab} = M_H + M_U + M_{c,destab} \quad (4.3)$$

where :

- $M_G$  corresponds to the self-weight;
- $M_v$  corresponds to the vertical pressure;
- $M_{c,stab}$  corresponds to the stabilising component of the pressure applied to the chamfer;
- $M_H$  corresponds to the horizontal pressure;
- $M_U$  corresponds to the underpressure;
- $M_{c,destab}$  corresponds to the destabilising component of the pressure applied to the chamfer.

The objective is to derive an equation for the head in terms of the block properties. Thus, each moment is expressed as a function of the head, denoted by  $H_{th}$  :

$$M_x = C_x \cdot H_{th} + d_x \quad (4.4)$$

where  $C_x$  is a coefficient and  $d_x$  is a term independent of  $H_{th}$ .

In this way, it can be obtained :

$$H_{th} = \frac{-d^*}{C^*} \quad (4.5)$$

where  $d^* = \sum_x d_x$  and  $C^* = \sum_x C_x$ .

Finally, the tilting head is given by:

$$H_{th} = \frac{-(d_G + d_v + d_{c,stab} - d_H - d_U - d_{c,destab})}{C_G + C_v + C_{c,stab} - C_H - C_U - C_{c,destab}} \quad (4.6)$$

with

$$\begin{aligned} d_G &= \rho_b \cdot g \cdot [(P - i) \cdot e - c^2/2] \cdot x_{CG} & C_G &= 0 \\ x_{CG} &= \frac{e^2 \cdot (P - i) - c^2 \cdot (e - \frac{c}{3})}{2 \cdot e \cdot (P - i) - c^2} & C_v &= \frac{\gamma_w \cdot (e - c)^2 \cdot \alpha}{2} \\ d_v &= 0 & C_{c,stab} &= \frac{\gamma_w \cdot c \cdot (5 \cdot e - 7/3 \cdot c)}{6} \\ d_{c,stab} &= \frac{\gamma_w \cdot (3 \cdot c^2 \cdot e - c^3)}{6} & C_H &= \frac{\gamma_w \cdot (P - c - i)^2}{2} \\ d_H &= \frac{\gamma_w \cdot (P - c - i)^2 \cdot (P + 2c - i)}{6} & C_U &= \frac{\gamma_w \cdot (e^2 - s^2)}{2} \\ d_U &= \frac{\gamma_w \cdot (P - i) \cdot (e^2 - s^2)}{2} & C_{c,destab} &= \frac{\gamma_w \cdot c \cdot [(P - i - c) \cdot 5 + 7/3 \cdot c]}{6} \\ d_{c,destab} &= \frac{\gamma_w \cdot c \cdot [3 \cdot (P - i - c) \cdot c + c^2]}{6} \end{aligned}$$

### 4.2.1 Comparison of the new model with the results

Now that a formula has been established, it can be compared with the experimental results. FIGURE 4.12 displays the box plots for the different blocks, along with the calculated tipping head. The error bars indicate the uncertainty associated with the density of the blocks.

Upon examining this graph, it becomes evident that the formula consistently overestimates the tipping height in comparison to the experimental results (except for situation B10 M2).

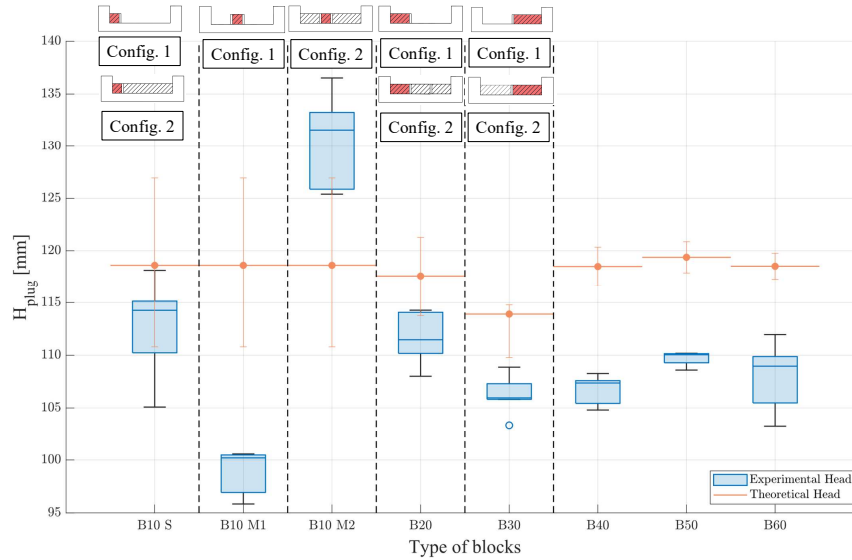


FIGURE 4.12: Box plots of experimental results and theoretical heads from the new analytical model

To quantify this overestimation, the heads depicted in FIGURE 4.12 have been normalised. Each height has been divided by the corresponding median head of the box, thereby conducting individual normalisation for each of the box plots. This is represented in FIGURE 4.13.

For blocks B20 to B60 and configuration B10S, the analytical model overestimates water levels by 4% to 10% compared to the median of the tests. For configurations B10M1 and B10M2, the overestimate is 18% and the underestimate 9% respectively.

Obtaining results slightly higher than those extracted from the tests is favourable for the safety of the dam. However, it is also desirable to optimise the geometry of the blocks by generating an estimate fairly close to the critical tipping level. Consequently, it is possible to adjust and calibrate the formula according to the experimental data.

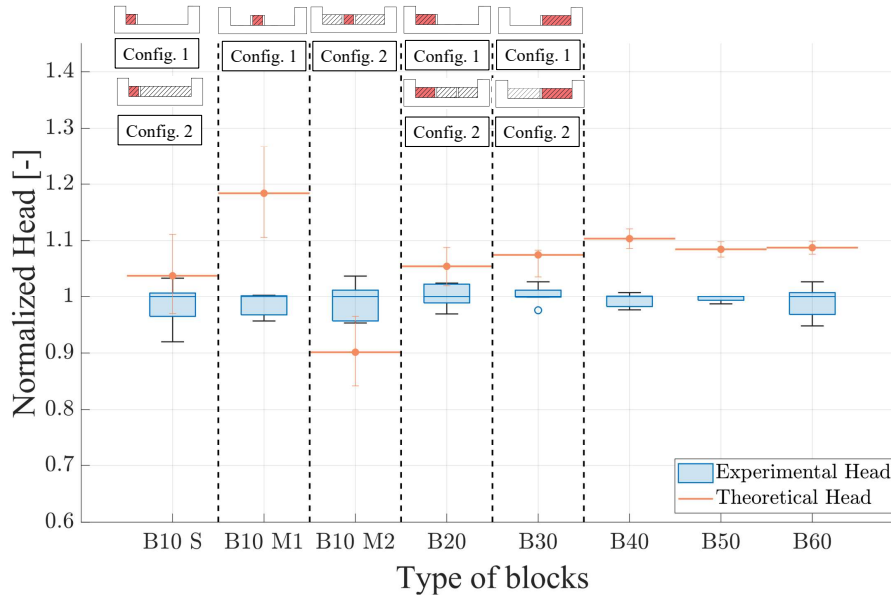


FIGURE 4.13: Box plots of experimental results and theoretical heads from the new model equation, normalized by the median head of each box

### 4.2.2 Adjusting the analytical model based on the results

In order to refine the analytical model, one potential adjustment involves modifying the  $\alpha$  coefficient utilised to compute the vertical pressure exerted by the water on the upper face of the block.

This parameter needs to be tailored to achieve the experimental tipping head for each whisker box. However, despite the necessity for a distinct  $\alpha$  coefficient for each fuse plug to best reflect the tests, it is crucial to establish a singular value. This is because it represents an assumption regarding the pressure that cannot fluctuate based on the block used.

In FIGURE 4.14, a round dot represents the coefficient employed to derive the median head ( $\alpha_{med}$ ), while the lower and upper bounds of the interval correspond to the minimum ( $\alpha_{min}$ ) and maximum ( $\alpha_{max}$ ) heights, respectively.

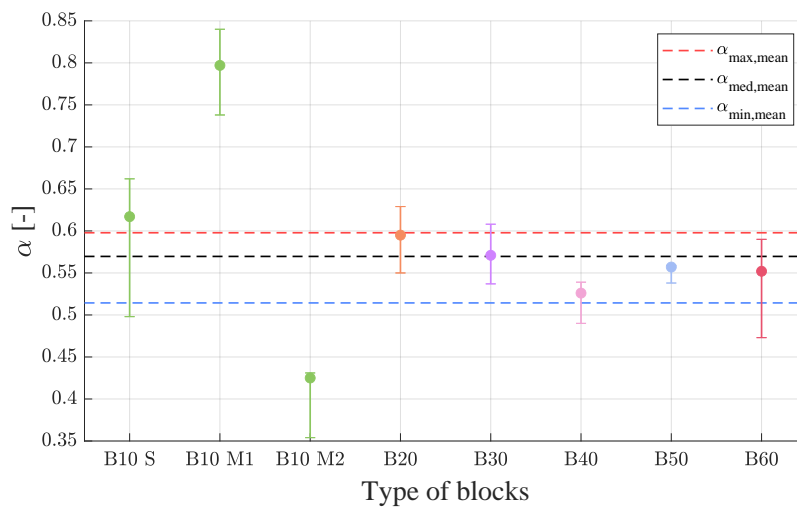


FIGURE 4.14:  $\alpha$  coefficient calculated to obtain the median, maximum, and minimum heads of each box plot

The graph illustrates that the required parameter remains relatively constant for all the fuse plugs, ranging between 0.53 and 0.62 for blocks B20 to B60 and the B10S configuration, in order to achieve the median of the boxes. This consistency is reassuring, as it implies that the selected assumption will be generally suitable for all the fuse plugs, avoiding significant disparities in tipping heights in some cases.

However, the B10 M1 and B10 M2 configurations necessitate extreme coefficient values, specifically 0.8 and 0.43 respectively. This is logical considering the distinct behaviour of these configurations compared to the others studied.

For each block, three different  $\alpha$  coefficients have been identified. Yet, a single value is needed to represent the entire dataset. To address this, the averages of each parameter type ( $\alpha_{med,mean}$ ,  $\alpha_{max,mean}$ , and  $\alpha_{min,mean}$ ) are computed and depicted in FIGURE 4.14. Notably, the B10M1 and B10M2 configurations are excluded from these averages due to their different behaviour.

The value of  $\alpha_{max,mean}$ , which is 0.598, is chosen as an assumption. This value yields theoretical tipping heights exceeding the medians of blocks B20 to B60. Thus, it appears to best represent the various experimental tests.

Initially, a  $\alpha$  coefficient equivalent to  $2/3$  was assumed. Indeed, for a broad crest weir with a rectangular cross-section, the critical depth corresponds to  $2/3$  of the relative specific head of the flow. The critical height is assumed because a spillway is a structure designed to ensure the safety of dams against overtopping. Consequently, its main purpose is to facilitate the rapid evacuation of extreme floods by discharging the maximum flow. The state in which maximum discharge occurs for a given section is characterised by a height equivalent to the critical height.

This critical head represents the height of which the specific energy of the flow is minimal for a given flow rate. A height below the critical height on the weir is obtained by the  $\alpha_{max,mean}$  value. This corresponds to a height where the specific energy is higher than the critical level, which means a less stable state compared with the critical height. This situation is logical compared to observing a height greater than the critical height because the flow tends to maximise the flow with a minimum height.

With this new hypothesis, it is now possible to quantify the disparity between the theoretical heads calculated and the experimentally determined heights. TABLE 4.3 provides these differences in percentage terms.

	B10 S	B10 M1	B10 M2	B20	B30	B40	B50	B60
$H_{th} - H_{exp}$	-1.3%	12.5%	-14.4 %	0%	2%	5%	3%	3.3%

TABLE 4.3: Difference between the theoretical heads ( $H_{th}$ ) calculated with  $\alpha = 0.598$  and the heights determined experimentally ( $H_{exp}$ )

For blocks ranging from 30 cm to 60 cm wide, the calculated theoretical head exceeds the median values of the boxes, with the maximum difference being 5%. Remarkably, for fuse plug B20, the formula closely aligns with the median value of the box.

In FIGURE 4.15, which illustrates the theoretical heads corresponding to each box, it is evident that for blocks B40 to B60, the calculated values also surpass the upper limits. However, for the 30 cm fuse plug, the model yields a result situated between the median and the maximum value. Moreover, the 5% difference observed for the B40 block equates to approximately 5 mm from the median.

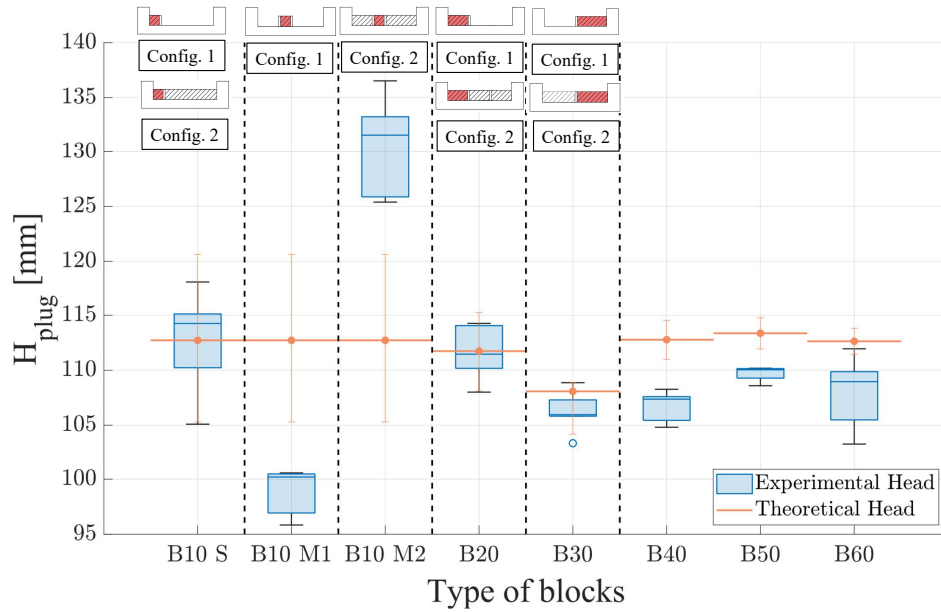


FIGURE 4.15: Box plots of experimental results and theoretical heads from the new model equation. The coefficient  $\alpha$  is taken equal to 0.598.

For the 10 cm block, only one theoretical value is provided, irrespective of the configuration considered, thus failing to accurately represent the three distinct situations. Nonetheless, it is theoretically plausible to approximate the configuration of the fuse plug positioned on the side of the sill.

### 4.2.3 Sensitivity analysis

Now, a sensitivity analysis can be conducted for the newly established analytical model (with the  $\alpha$  assumption set at 0.598).

The purpose of this analysis is to evaluate how variations or uncertainties in the model parameters influence the tipping head results. The goal is to measure the effect of perturbing one of these parameters on the output, thereby discerning which geometric parameter of the block warrants specific attention in its design.

#### Density

The first parameter under examination is the density of the blocks. Indeed, in the various graphs comparing the experimental results with the theoretical tipping heights, error bars are presented to reflect the uncertainty associated with determining the density of the plugs.

For instance, for block B10, which has the widest range of uncertainty in its density (from 2228 to 2377 kg/m<sup>3</sup>), the theoretical uncertainty generated is approximately  $\pm 7.5$  mm, as depicted in FIGURE 4.12. This suggests that the influence of the density on the results plays a significant role.

The graph in FIGURE 4.16 illustrates the variation of the tilting height as a function of the density of the block. In this curve, the densities of each type of block (from B10 to B60) are highlighted. These points are determined based on identical cross-sections, without construction faults (length  $e = 0.12$  m and height  $P = 0.1$  m).



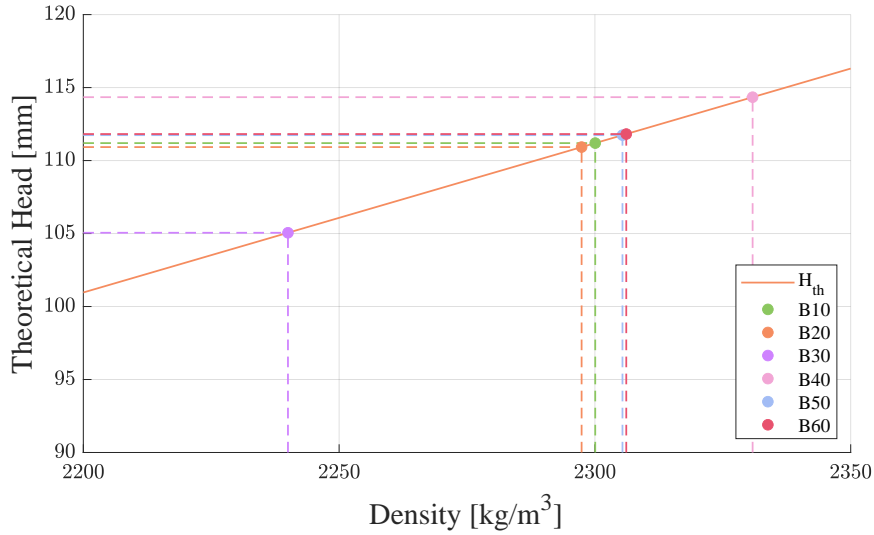


FIGURE 4.16: Relationship between density and theoretical tipping height (based on the new analytical model). The theoretical heights of each block, with identical cross-section dimensions ( $e = 0.12$  m,  $P = 0.1$  m), are highlighted.

Based on this graph, it can be seen that the relationship between theoretical head and density is linear. For example, for a density of  $2300 \text{ kg/m}^3$ , the height is  $111.19 \text{ mm}$ , whereas for a density of  $2240 \text{ kg/m}^3$ , the height is  $105.05 \text{ mm}$ . This indicates that a difference of  $60 \text{ kg/m}^3$  results in a height difference of around  $6.14 \text{ mm}$ .

It can therefore be concluded that, all other things being equal, a difference of  $x \text{ kg/m}^3$  from the expected density results in a deviation of approximately  $x/10 \text{ mm}$  from the desired tipping height.

### Cross-section dimensions

In this section, the impact of variations in block dimensions on the theoretical results will be studied. Given that fuse plugs can have construction defects and may not always have the desired dimensions, it is important to understand how these variations affect the calculated tipping heights. In particular, the effect of block height ( $P$ ) and length ( $e$ ) on these theoretical results is examined.

FIGURE 4.17 and 4.18 illustrate the theoretical evolution of the tipping head as a function of block length and height, respectively. Points have been added to represent the dimensions of the fuse plugs studied. These graphs show a linear relationship between physical dimensions and water height.

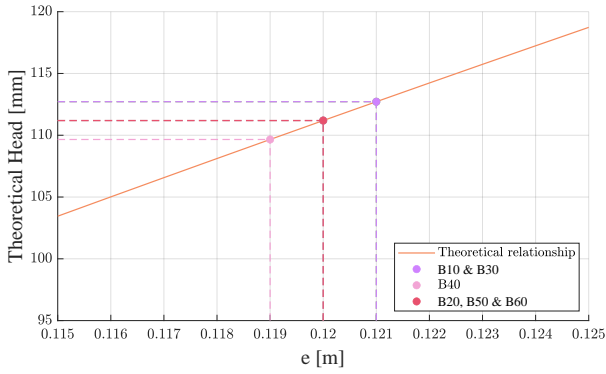


FIGURE 4.17: Relationship between length ( $e$ ) and theoretical tipping height (based on the new analytical model). The theoretical heights of each block, with  $P = 0.1$  m and  $\rho_b = 2300$  kg/m<sup>3</sup>, are highlighted.

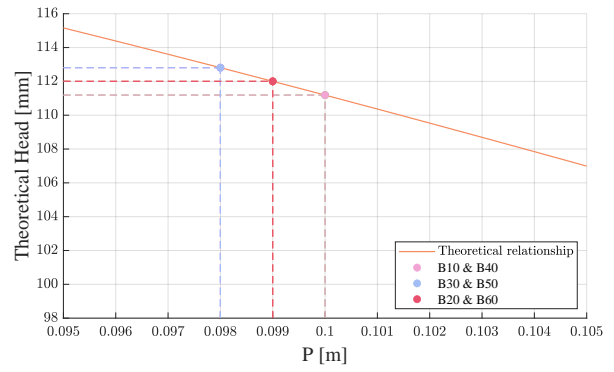


FIGURE 4.18: Relationship between height ( $P$ ) and theoretical tipping head (based on the new analytical model). The theoretical heads of each block, with  $e = 0.12$  m and  $\rho_b = 2300$  kg/m<sup>3</sup>, are highlighted.

These graphs illustrate a direct relationship between the tipping head and block length, alongside an inverse relationship between the tipping head and block height.

For instance, at a length of 120 mm, the corresponding head measures 111.2 mm, whereas at 121 mm, it is 112.7 mm, indicating a difference of 1.5 mm for each millimetre of variation in length.

With regard to the height of the block, for a height of 100 mm the head is 111.2 mm, and for a height of 99 mm it is 112 mm, showing a variation of 0.8 mm for each millimetre of variation in block height.

## Pressure

It is relevant to explore the geometrical parameters that directly impact pressure, such as the chamfer length ( $c$ ), the height of the underpressure chamber ( $i$ ), and the support length ( $s$ ). As these parameters have not been considered in previous studies, assessing their influence on the calculated tipping height is crucial.

Regarding the chamfer length, FIGURE 4.19 illustrates the evolution of the tilting height as a function of  $c$  for a block with characteristics similar to those of the B30 block.

The graph shows a parabolic relationship between the head and dimension  $c$ . As the chamfer size increases, the tilting height rises until it reaches a maximum value  $c_{\max}$ , beyond which the head decreases.

This indicates that, according to the theoretical relationship, a chamfer enhances block stability, and this effect is more pronounced with a larger chamfer. However, this stabilising effect has a limit; beyond a certain point, a larger chamfer becomes destabilising. Notably, the chamfer length chosen for the studied blocks is relatively close to this limit, suggesting an optimisation in terms of block stability.

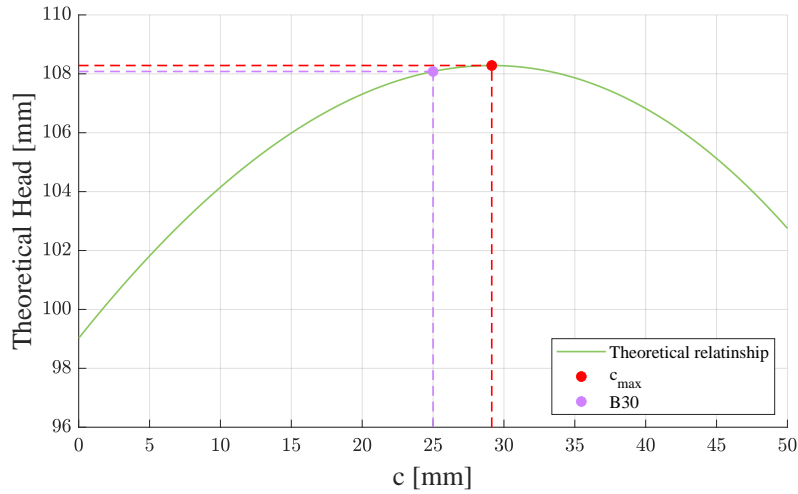


FIGURE 4.19: Relationship between the length of the chamfer ( $c$ ) and theoretical tipping height (based on the new analytical model). The theoretical heights of B30 is highlighted.

The impact of the parameters  $i$  and  $s$  on the tipping height is shown in FIGURE 4.20 and 4.21. Regarding the underpressure chamber, the graph reveals that greater heights have a stabilising effect on the block, leading to a higher head. A similar observation can be made for the length of the block support. A plausible explanation is that longer support reduces the size of the underpressure chamber, resulting in less uplift being applied to the underside of the block.

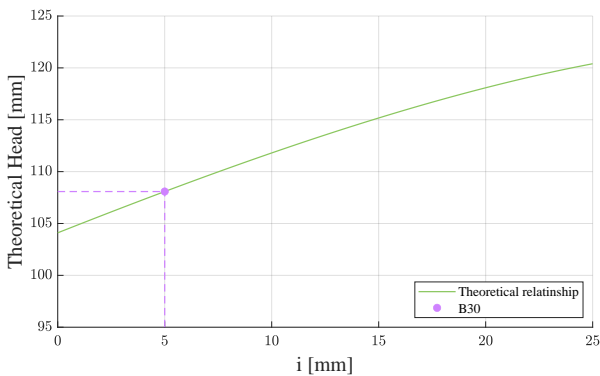


FIGURE 4.20: Relationship between the height of the underpressure chamber ( $i$ ) and theoretical tipping height (based on the new analytical model). The theoretical heights of B30 is highlighted.

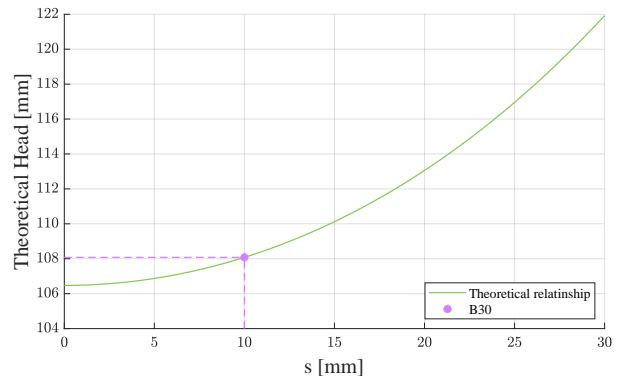


FIGURE 4.21: Relationship between the length of the support ( $s$ ) and theoretical tipping height (based on the new analytical model). The theoretical heights of B30 is highlighted.

### 4.3 Analysis and discussions

The analytical models and the principle of block stability raise a number of points for discussion.

### 4.3.1 Comparison of the new model with previous formulas

It has been previously shown that two formulas are available in the literature. The first, proposed by Hien & Khanh, relates to a block geometry similar to that studied in this work. The second equation established by Sekkour is based on a simple rectangular block, which implies simplifying assumptions with respect to the blocks examined here.

Nevertheless, Sekkour's formula, although simplifying, proves to be the most representative of the experimental tests carried out.

A new analytical model was therefore developed. By adjusting one of the coefficients ( $\alpha$ ) according to the experimental tests, this new formula provides a better match with the observed tipping heights.

A first question emerges: does taking into account the specific geometry of the block studied, while adjusting the assumptions on the pressure fields, allow a better representation of the experimental tests? Indeed, in the new approach, the chamfer is considered and the continuity of the pressures on the different faces is maintained in comparison to the Hien & Khanh's formulation. In fact, the equation developed in this work led to tilting heights closer to the medians of the whisker boxes for blocks B20 to B60. It gives deviations of between 4% and 10%, compared with the formula of Hien & Khanh, which had underestimates of around 15%. An improvement has therefore been made with this new model.

Secondly, given that Sekkour's formula gave results that were relatively close to the actual results, despite very simplifying assumptions in relation to the block geometry used, it is legitimate to wonder whether the new, more complex model really offers an improvement.

Initially, assuming that the height on the blocks was  $2/3$  of the upstream head, the theoretical tipping heights turned out to be 4 to 10 % different for blocks B20 to B60. On the other hand, using the Sekkour formula, the theoretical heads were close to 2 to 6%. It is important to note that the Sekkour's equation systematically underestimates the experimental results, while the new model overestimates them. Of course, excessive overestimation poses a problem in terms of optimising the capacity of a spillway. However, from the point of view of dam safety, it is preferable to have overestimated results, which are therefore safer.

In addition, the formula developed in this work was adjusted in relation to the tests to take an assumption concerning the vertical pressure more appropriate to reality. This adaptation made it possible to obtain theoretical results that were closer to the experimental results and higher than the medians for blocks B20 to B60.

In conclusion, the development of a new analytical model has improved the representation of the tests carried out in this work. However, one key aspect highlighted is the impact of the assumptions concerning pressure distributions. The comparison of the results between the Hien & Khanh's formula and the one developed in this work illustrates the crucial role of these assumptions.

### 4.3.2 Pressure diagrams

The importance of the assumptions concerning the pressure fields has just been highlighted. As far as vertical pressure is concerned, the coefficient determining a uniform height of water over the block has been adjusted to adapt the formula developed in section 4.2. Considering a uniform pressure along the block is one of several assumptions. In the absence of direct measurements of the pressures applied to the blocks during the tests, the actual behaviour of the pressures can only be approximated.

Thus, it is possible to take other hypotheses regarding the vertical pressure field. For example, a triangular pressure could be envisaged as shown in FIGURE 4.22.

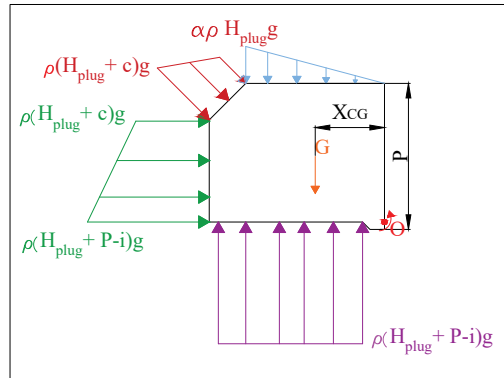


FIGURE 4.22: Pressure distribution with triangular vertical pressure field

Using an  $\alpha$  coefficient of 2/3, the tilting heights are calculated and are presented with whisker boxes in FIGURE 4.23.

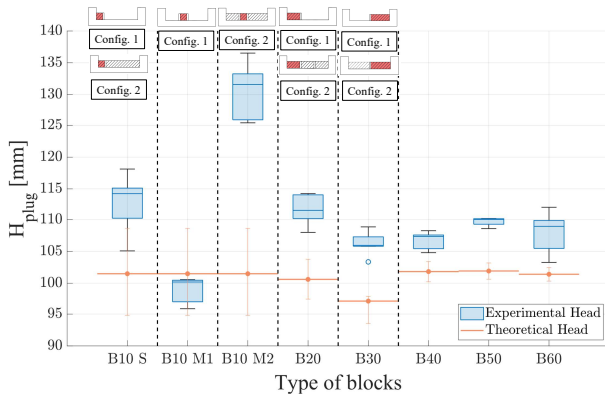


FIGURE 4.23: Box plots of experimental results and theoretical heads from the new model equation with triangular pressure field

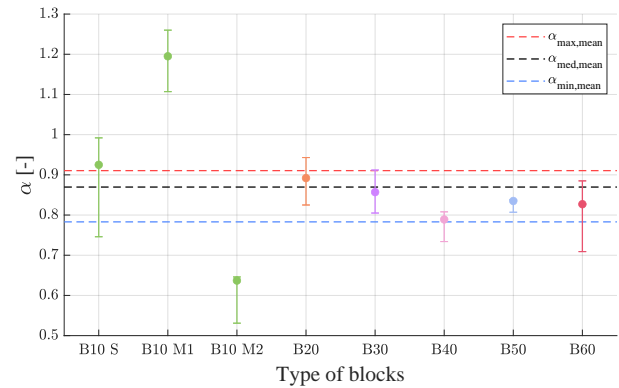


FIGURE 4.24:  $\alpha$  coefficient calculated to obtain the median, maximum, and minimum heads of each box plot (using the triangular pressure field hypothesis)

Looking at this graph, it is clear that this new hypothesis fails to satisfactorily reflect the experimental results, mainly due to their underestimation. However, it should be pointed out that the  $\alpha$  parameter can be adjusted according to the trials. As done in subsection 4.2.2, the  $\alpha$  coefficient is calculated to obtain the median, maximum, and minimum heads for each box plot, as shown in FIGURE 4.24.

It can be seen that the B10 M1 configuration requires a coefficient greater than 1, which is not physically plausible. It is counter-intuitive to see the water height increase as the flow passes over the blocks. On the other hand, the other configurations require a coefficient of less than 1. Therefore, it would be possible to take this hypothesis into account to better represent the tests.

Of course, both the triangular pressure and the uniform pressure assumption represent two extremes. An intermediate option could also be considered. However, until the pressure applied to the block is studied in more detail, it is difficult to determine which hypothesis would be the most appropriate.

### 4.3.3 Influence of geometric and physical parameters

#### Density

In previous analyses, it was observed that the theoretical tipping height calculated was influenced by the density of the blocks. A variation of  $x \text{ kg/m}^3$  in density thus results in a variation of approximately  $x/10 \text{ mm}$  in water height.

It is therefore interesting to see how this relationship changes as a function of block height.

FIGURE 4.25 shows the relationship between the variation in density and the variation in tipping height as a function of block height. It can be seen that this relationship evolves linearly as a function of block height, with a slope of almost 1:1.

The issue can also be reversed: if the desired precision in terms of tipping height is known, it is possible to determine the tolerance to be had in terms of density. This is demonstrated in FIGURE 4.26. For example, for a 1 metre high block, if a tolerance of 1 cm on the tipping head is accepted, then the variation in density between what is planned and what is built must not exceed  $10 \text{ kg/m}^3$ .

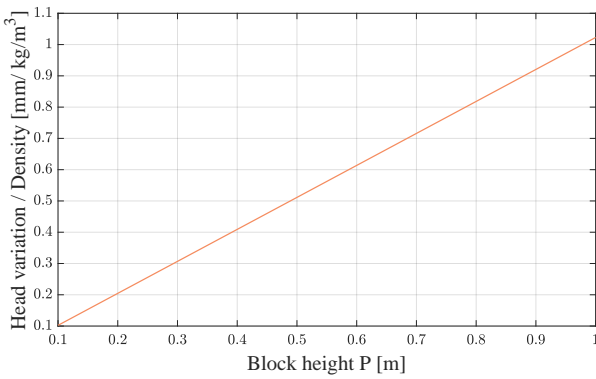


FIGURE 4.25: Evolution of the head variation - density ratio as a function of the height of the block

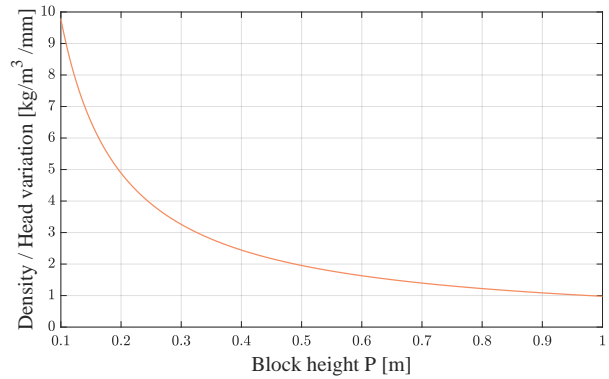


FIGURE 4.26: Evolution of the density - head variation as a function of the height of the block

The accuracy of the density must be carefully considered, especially when the height of the block is significant. It is therefore necessary to pay particular attention when making the concrete mix and/or to produce sample blocks whose density will be measured to ensure accuracy.

#### Dimensions

Regarding the dimensions of the cross-section of the block, it was determined that a variation of 1 mm in length leads to a variation of 1.5 mm in the results, while a difference of 1 mm in block height leads to a variation of 0.8 mm in the theoretical head calculated. FIGURE 4.27 and 4.28 illustrate the evolution of the relationship between the variation in head and the variation, respectively, in length and height. These relationships are not influenced by the height of the block: whether the block is 10 cm or 1 metre high, a tolerance of 1 cm on the actual dimensions of the block would result in an uncertainty of 1.5 cm or 0.8 cm, depending on the dimension considered.

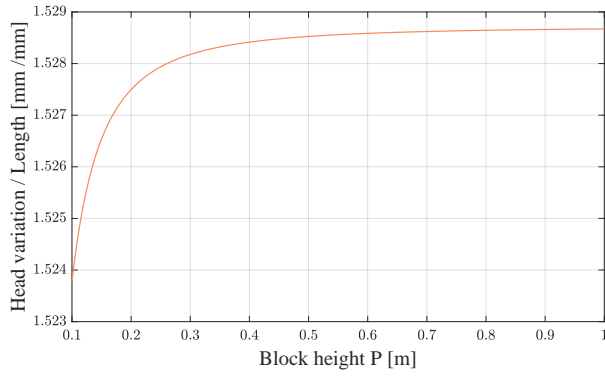


FIGURE 4.27: Evolution of the head variation - length ratio as a function of the height of the block

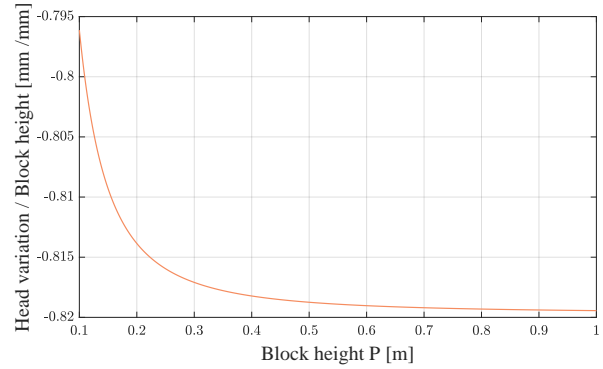


FIGURE 4.28: Evolution of the head variation - block height as a function of the height of the block

#### 4.3.4 Analysis of block B10 results

Based on the graphs comparing the whisker boxes to the calculated tipping heads, the representation of the different configurations for the 10 cm wide block was complex. The results showed significant variation depending on the configurations and positions of the fuse plug. Since the analytical model only provides a single value for a cross-section, it was challenging to account for external factors such as position on the sill or the influence of adjacent elements.

With a better understanding of the types of pressure to which the block is subjected and their effect on fuse plug stability, it is now possible to analyse the influence of these pressure fields on the experimental results.

The first notable aspect concerns the size of the underpressure chamber. As previously observed, an increased width of the support ( $s$ ) leads to a reduction in the length of the underpressure chamber, resulting in a higher tipping height. This relationship is intuitive because a diminution in the space for the application of uplift to the block decreases the destabilising forces, thereby delaying tipping.

In the cross-sectional plane, the underpressure chamber appears to be of uniform size relative to the other blocks. However, a longitudinal consideration of the plug reveals that the width affects the proportion used as an underpressure chamber. FIGURE 4.29 illustrates this relationship: for a 10 cm wide element, where each side is supported by a 1 cm wide structure, the support represents 20% of the total width of the block. On the other hand, for a 20 cm block, the proportion corresponds to 10%. So the wider the fuse plug, the less of its width the support takes up.

For block B10, this 20% also represents the portion of the plug that is not used as a lower chamber. In other words, block B10 is less affected by underpressure and is therefore susceptible to tipping under greater heads than the others. This observation partly explains why, for both the B10 S configuration (where the block is placed on the side of the sill) and the B10 M2 configuration (where the block is positioned in the centre of the sill, surrounded by adjacent elements), the median of the whisker boxes exceeds that of the other fuse plugs.

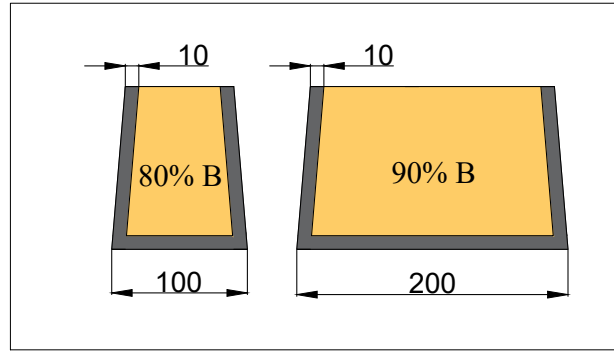


FIGURE 4.29: Representation of the size of the underpressure chamber (Dimensions in millimetres)

Secondly, in the previous discussion, the probable difference in pressure induced by the contraction of the flow was pointed out. As mentioned earlier, this contraction leads to a variation in the water level over the blocks. At the ends of the weir, as the flow is drawn towards the centre, the water height is less than at the middle.

As indicated, the pressure exerted on the upper face of the block is one of the stabilizing forces in its equilibrium. Consequently, a lower height of water on the fuse plug means less stabilizing pressure. As for the other types of pressure applied to the block, it is difficult to determine with certainty the impact of the flow contraction.

However, it is reasonable to assume that the underpressure remains constant along the weir. As for the horizontal pressure and that applied to the chamfer, if they are influenced by the behaviour of the flow, this variation cannot be as significant as that of the vertical pressure. It is therefore plausible to understand that the effect of flow contraction is mainly reflected by a reduced stabilising pressure. Consequently, it leads to a diminution in the tilting head. This observation could explain why, in configuration 2, the block tilts faster when it is positioned at the end of the weir.



# Chapter 5

## Application

In this chapter, the newly developed analytical model is applied to create a practical design table. In addition, recommendations are provided for the use of the blocks, based on previous discussions.

### 5.1 Practical design table

The aim is to create a practical design table for the blocks. To do this, the analytical model developed in chapter 4 is simplified into an easy-to-use equation.

#### 5.1.1 Simplified equation

To simplify the analytical model, each dimension of the block can be expressed as a function of its height. This approach reduces the dependence of the equation to one geometrical parameter and the density of the fuse plug.

The decision to retain height as a variable is motivated by the need to consider the maximum head of the dam ( $H_{dam}$  in FIGURE 5.1) for proper system sizing. While the use of blocks aims to enhance the reservoir's water storage capacity, it's vital to prioritize the dam's safety, especially considering its role as a spillway.

Preventing overflow caused by the presence of fuse plugs is imperative. Therefore, formulating an equation based on block height appears to be the most suitable approach among the various geometric dimensions. This will facilitate expressing the formula as a function of the tank's maximum water level ("Highest water level" in FIGURE 5.1).

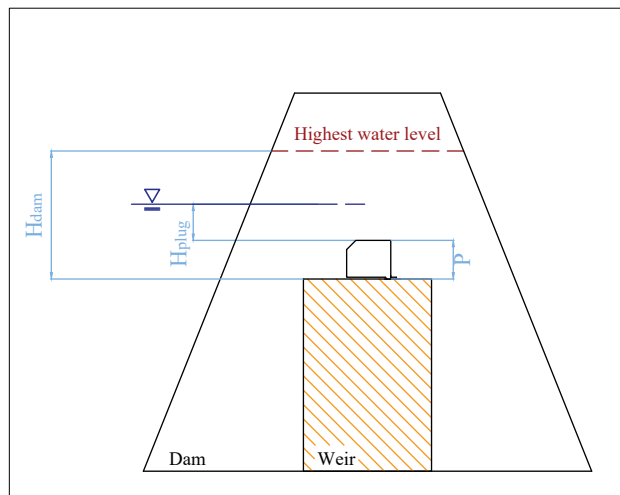


FIGURE 5.1: Diagram of a block on a weir

Therefore, the different dimensions of the fuse plug can be expressed as follows:

$$e = \frac{12}{10} \cdot P \quad (5.1)$$

$$c = \frac{1}{4} \cdot P \quad (5.2)$$

$$s = \frac{1}{10} \cdot P \quad (5.3)$$

$$i = \frac{1}{20} \cdot P. \quad (5.4)$$

These equations are based on the blocks studied in this work.

By injecting these expressions into equation (4.6), it can be obtained a simplified design formula:

$$H_{tilting} = P \cdot (1.022 \cdot 10^{-3} \cdot \rho_b - 1.2404). \quad (5.5)$$

### Error brought by simplification

The simplification process may introduce deviations from the previously developed expression. To assess these errors, it is possible to analyse the difference between the head ( $H_{th}$ ) obtained using equation (4.6) and that derived from the new formula ( $H_{tilting}$ ) as a function of the fuse plug height (refer to FIGURE 5.2).

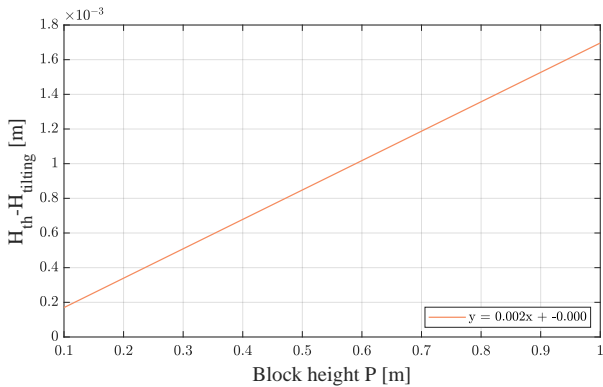


FIGURE 5.2: Difference between  $H_{th}$  (equation (4.6)) and  $H_{tilting}$  (equation (5.5)) as a function of the fuse plug height (for a density of  $2300 \text{ kg/m}^3$ )

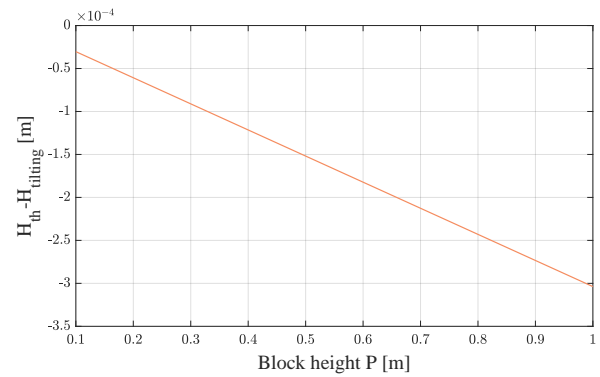


FIGURE 5.3: Difference between  $H_{th}$  (equation (4.6)) and  $H_{tilting}$  (equation (5.6)) as a function of the fuse plug height (for a density of  $2300 \text{ kg/m}^3$ )

From FIGURE 5.2, it can be seen that the difference is generally in the order of a millimetre and tends to increase the higher the block. Moreover, the analysis indicates a consistently positive deviation, suggesting that the simplified equation yields slightly lower results.

The relationship between the error caused by the simplified equation and the block height is estimated to be  $0.002 \cdot P$  and can be incorporated into the equation :

$$H_{tilting} = P \cdot (1.022 \cdot 10^{-3} \cdot \rho_b - 1.2404) + 0.002 \cdot P \quad (5.6)$$

With the inclusion of this error term into the equation, a notable change can be observed, as illustrated in FIGURE 5.3. The deviation is now on the order of a tenth of a millimeter. This level of accuracy is quite acceptable.

### Influence of the parameters on the equation

It is now possible to quantify the impact of a variation in the geometric and physical parameters of the block on the results provided by the simplified equation.

The relationship between density variation and the corresponding change in tipping height, as a function of block height, is depicted in FIGURE 5.4. This relationship varies linearly with block height, exhibiting a slope of 1.022 consistent with the previously developed model.

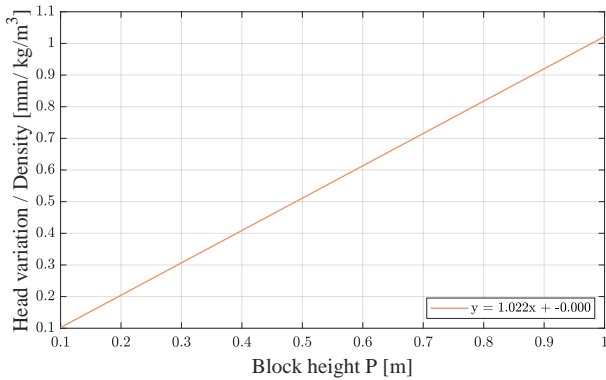


FIGURE 5.4: Evolution of the head variation - density ratio as a function of the block height (from the simplified equation)

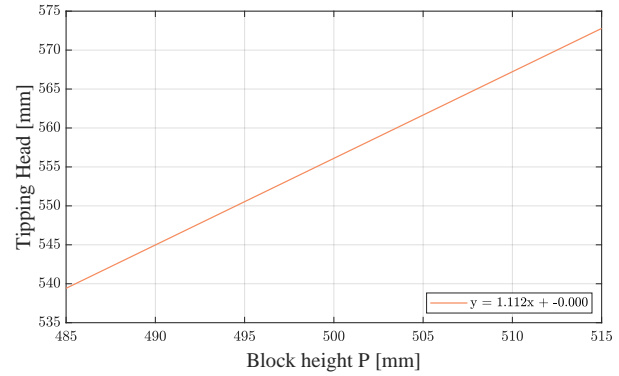


FIGURE 5.5: Evolution of the tipping head as a function of the block height (from the corrected version of the simplified equation)

Next, the impact of the block height can be observed in FIGURE 5.5, which illustrates the relationship between the tipping head and fuse plug height. This graph demonstrates a linear trend, with a ratio of 1.112 mm/mm between height variation and tipping head fluctuation. Unlike density, this relationship differs from that observed in section 4.3.3. This disparity is easily comprehensible, as the height encompasses multiple geometric dimensions.

Therefore, to deduce construction tolerances for various geometric parameters of the block, it is advisable to rely on sensitivity analysis of the analytical model before simplification. This approach enables a clear understanding of each property's influence independently of others.

### 5.1.2 Design chart definition

#### Definition of the maximum head of water in the dam

The maximum water level in the dam  $H_{dam}$  is defined as the distance between the crest of the spillway and the highest water level (i.e. the maximum altitude of the water body for the project flood), which is illustrated in FIGURE 5.6.

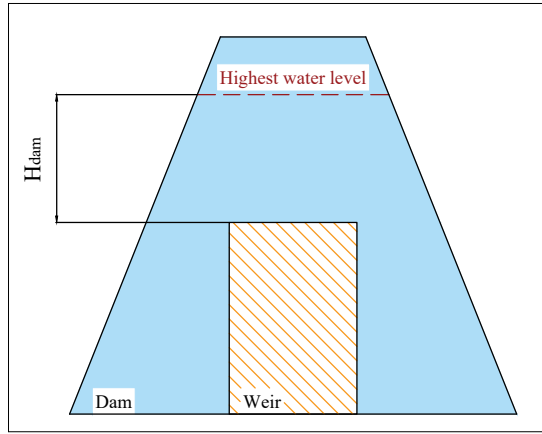


FIGURE 5.6: Diagram representing the maximum water level in a dam  $H_{dam}$

### Determining the block height

The simplified formula presented in the previous section relies exclusively on the height and density of the blocks. Consequently, it is feasible to construct a block sizing table based on these two parameters, as provided in TABLE 5.1.

To create a comprehensive table adaptable to various dams and their corresponding maximum water levels, the height of the blocks is expressed as a percentage of  $H_{dam}$ , denoted as  $P_{dam}$  in the table. The tipping height is then calculated using this percentage and a specific density. While the table does not directly provide the tipping height, it offers a percentage indicating the available distance ( $H_{safe}$ ) in relation to  $H_{dam}$  when the water level reaches the tipping threshold ( $H_{plug}$ ). A schematic representation of  $H_{safe}$  is depicted in FIGURE 5.7.

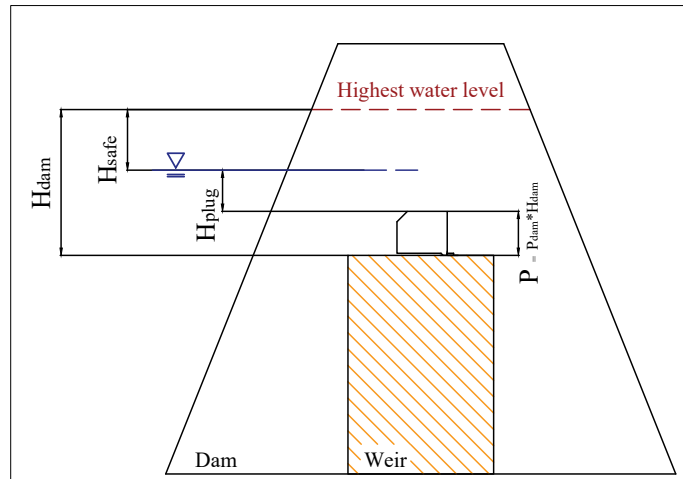


FIGURE 5.7: Diagram representing  $H_{safe}$

Thus, the table facilitates the determination of the required block height considering density, while allowing the designer to select the desired safety margin concerning the highest water level.

		Density ( $\rho_b$ ) [kg/m <sup>3</sup> ]												
		2200	2225	2250	2275	2300	2325	2350	2375	2400	2425	2450	2475	2500
Percentage of $H_{dam}$ ( $P_{dam}$ )	50%	-0.50	-1.78	-3.06	-4.33	-5.61	-6.89	-8.17	-9.44	-10.72	-12.00	-13.28	-14.55	-15.83
	45%	9.55	8.40	7.25	6.10	4.95	3.80	2.65	1.50	0.35	-0.80	-1.95	-3.10	-4.25
	40%	19.60	18.58	17.56	16.53	15.51	14.49	13.47	12.45	11.42	10.40	9.38	8.36	7.34
	35%	29.65	28.76	27.86	26.97	26.07	25.18	24.28	23.39	22.50	21.60	20.71	19.81	18.92
	30%	39.70	38.93	38.17	37.40	36.63	35.87	35.10	34.33	33.57	32.80	32.04	31.27	30.50
	25%	49.75	49.11	48.47	47.83	47.20	46.56	45.92	45.28	44.64	44.00	43.36	42.72	42.09
	20%	59.80	59.29	58.78	58.27	57.76	57.25	56.73	56.22	55.71	55.20	54.69	54.18	53.67
	15%	69.85	69.47	69.08	68.70	68.32	67.93	67.55	67.17	66.78	66.40	66.02	65.63	65.25
	10%	79.90	79.64	79.39	79.13	78.88	78.62	78.37	78.11	77.86	77.60	77.35	77.09	76.83
	7.5%	84.93	84.73	84.54	84.35	84.16	83.97	83.78	83.58	83.39	83.20	83.01	82.82	82.63
	5%	89.95	89.82	89.69	89.57	89.44	89.31	89.18	89.06	88.93	88.80	88.67	88.54	88.42
	2.5%	94.98	94.91	94.85	94.78	94.72	94.66	94.59	94.53	94.46	94.40	94.34	94.27	94.21
	1%	97.99	97.96	97.94	97.91	97.89	97.86	97.84	97.81	97.79	97.76	97.73	97.71	97.68

TABLE 5.1: Distance available ( $H_{safe}$  [%]) with regard to the maximum water level in the dam ( $H_{dam}$ ) when the water level reaches the tipping head ( $H_{plug}$ )

## 5.2 Recommendations for the design and installation of concrete fuse blocks

Recommendations for the design and installation of the fuse block system can now be made. These are based on the observations and discussions throughout this work, as well as the information presented in the background section.

One of the aims of this work was to develop a user-friendly sizing table for designers, along with recommendations to facilitate the use of fuse blocks. the following is a summary of the key information discussed in this work, providing a concrete overview of how fuse blocks can be used. This report is presented in a manner that allows a designer wishing to install fuse blocks on a weir to easily understand the necessary steps and points requiring particular attention.

The recommendations presented in this summary refer to the corresponding section of this work, where they are discussed in detail.

# Recommendations for the design and installation of concrete fuse blocks

## I Block geometry

The geometry of the blocks is detailed in Figure 1 by a cross-section and plan views of the top and bottom faces.

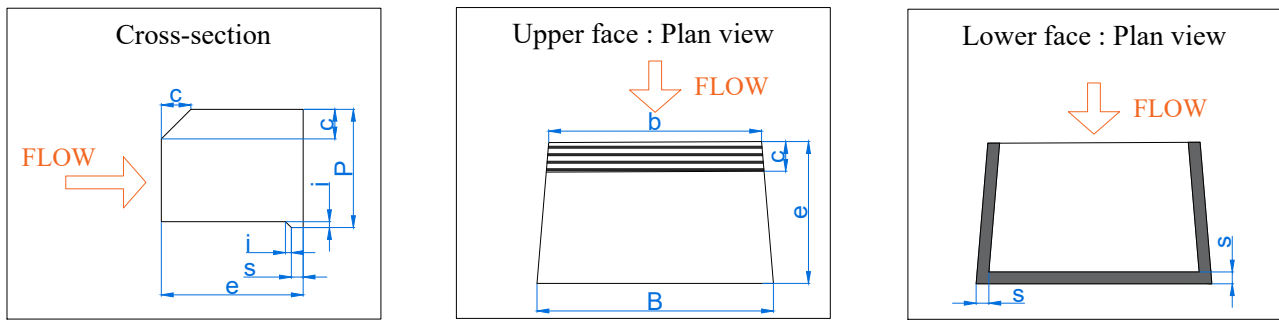


Figure 1: Block geometry

Photos of a block are provided in Figure 2 for a better understanding of the geometry.

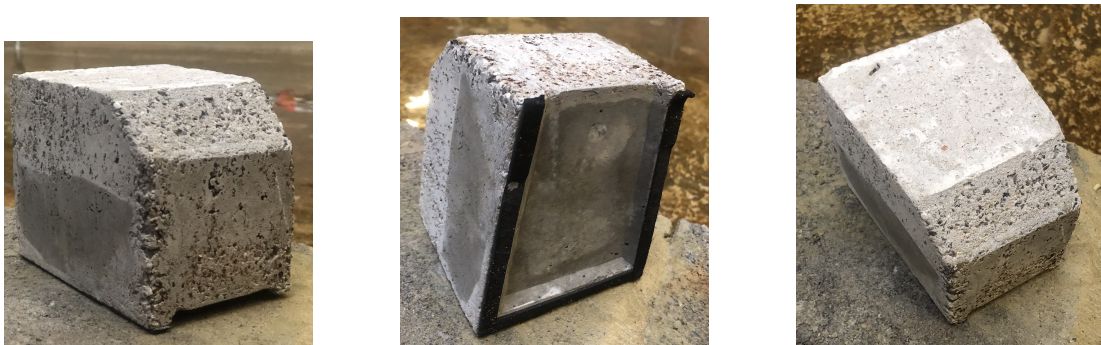


Figure 2: Photos of a concrete block from several angles

The dimensions are described below:

- (1)  $P$  is the block height.
- (2)  $b$  and  $B$  are the upstream and downstream widths of the block, defined perpendicular to the direction of flow.

The upstream width ( $b$ ) is 0.02 m less than the downstream width ( $B$ ). This trapezoidal shape prevents friction between the block and adjacent elements.



The importance of avoiding friction between blocks and adjacent elements is discussed in section 3.2.3 “Influence of friction”.

- (3)  $e$  is the block length, defined in the direction of the flow.

# Recommendations for the design and installation of concrete fuse blocks

---

- (4)  $c$  is the width of the chamfer.  
The upstream face of the block has a chamfer with a 1:1 slope and width  $c$ , facilitating the overflow.
- (5)  $i$  is the height of the opening created for the lower underpressure chamber (see Figure 3).  
This uplifting block design allows water to be discharged before the block tips, thereby increasing the tank's storage capacity.

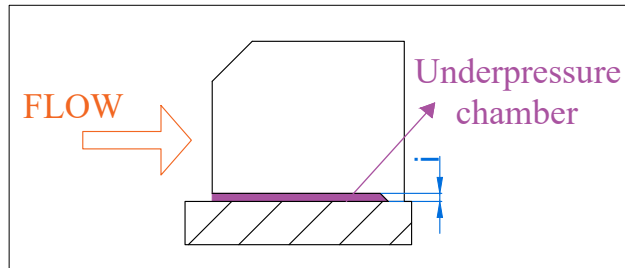


Figure 3: Block underpressure chamber

- (6)  $s$  is the width of the support under the block.  
A strip of concrete on three sides of the block serves as support, while the upstream face allows reservoir water to enter the lower chamber.

## II Design of the blocks

### II.i Definition of the maximum head of water in the dam

The maximum water level in the dam, denoted as  $H_{dam}$ , is defined as the distance between the crest of the spillway and the highest water level (i.e., the maximum altitude of the water body during the project flood), as illustrated in Figure 4.

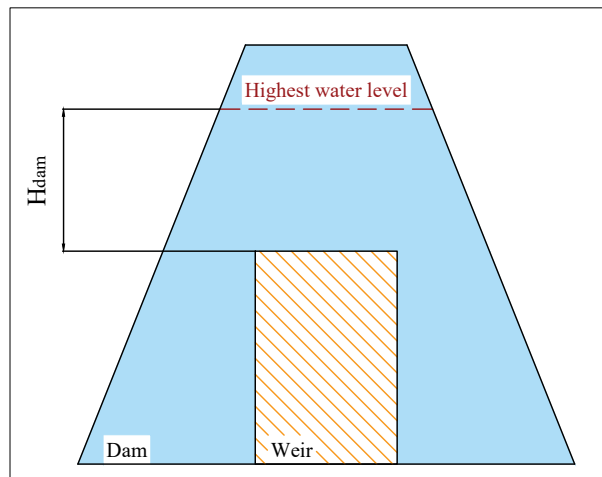


Figure 4: Diagram representing the maximum water level in a dam  $H_{dam}$



# Recommendations for the design and installation of concrete fuse blocks

## II.ii Determining the height of blocks

The height of the blocks ( $P$ ) can be determined using the sizing table provided in Table 1 below.

The dimensioning table has two axes: the horizontal axis corresponds to the density of the blocks, while the vertical axis represents a percentage  $P_{dam}$ . This percentage reflects the proportion of the height  $H_{dam}$ , which is the maximum head of the dam.

By consulting the table with these two parameters, a percentage can be obtained. It represents the distance  $H_{safe}$  (see Figure 5) available between the tipping level of the blocks ( $H_{plug}$ ) and the maximum water level in the dam ( $H_{dam}$ ). This data indicates the acceptable safety margin regarding the highest water level.

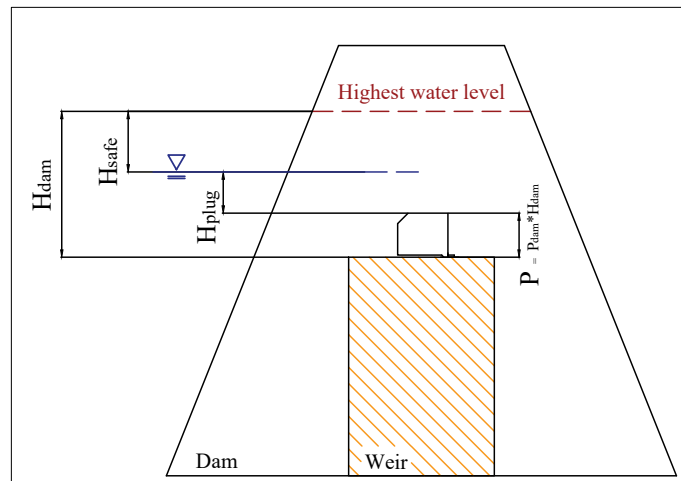


Figure 5: Diagram representing  $H_{safe}$

To determine the height of the blocks, the designer must select a density and define the necessary safety margin for the dam, expressed as an absolute value of  $x$  mm. Then, based on these choices, the percentage  $P_{dam}$  can be used to calculate the height of the block as follows:

$$P = P_{dam} \cdot H_{dam}. \quad (1)$$

With regard to the height of the blocks, the following recommendations should be followed:

- (1) Avoid using blocks that exceed 1 metre in height;
- (2) Maintain a uniform height for all blocks installed on the weir.



These recommendations come from the background section.

		Density ( $\rho_b$ ) [kg/m <sup>3</sup> ]												
		2200	2225	2250	2275	2300	2325	2350	2375	2400	2425	2450	2475	2500
Percentage of $H_{dam}$ ( $P_{dam}$ )	50%	-0.50	-1.78	-3.06	-4.33	-5.61	-6.89	-8.17	-9.44	-10.72	-12.00	-13.28	-14.55	-15.83
	45%	9.55	8.40	7.25	6.10	4.95	3.80	2.65	1.50	0.35	-0.80	-1.95	-3.10	-4.25
	40%	19.60	18.58	17.56	16.53	15.51	14.49	13.47	12.45	11.42	10.40	9.38	8.36	7.34
	35%	29.65	28.76	27.86	26.97	26.07	25.18	24.28	23.39	22.50	21.60	20.71	19.81	18.92
	30%	39.70	38.93	38.17	37.40	36.63	35.87	35.10	34.33	33.57	32.80	32.04	31.27	30.50
	25%	49.75	49.11	48.47	47.83	47.20	46.56	45.92	45.28	44.64	44.00	43.36	42.72	42.09
	20%	59.80	59.29	58.78	58.27	57.76	57.25	56.73	56.22	55.71	55.20	54.69	54.18	53.67
	15%	69.85	69.47	69.08	68.70	68.32	67.93	67.55	67.17	66.78	66.40	66.02	65.63	65.25
	10%	79.90	79.64	79.39	79.13	78.88	78.62	78.37	78.11	77.86	77.60	77.35	77.09	76.83
	7.5%	84.93	84.73	84.54	84.35	84.16	83.97	83.78	83.58	83.39	83.20	83.01	82.82	82.63
	5%	89.95	89.82	89.69	89.57	89.44	89.31	89.18	89.06	88.93	88.80	88.67	88.54	88.42
	2.5%	94.98	94.91	94.85	94.78	94.72	94.66	94.59	94.53	94.46	94.40	94.34	94.27	94.21
	1%	97.99	97.96	97.94	97.91	97.89	97.86	97.84	97.81	97.79	97.76	97.73	97.71	97.68

Table 1: Distance available ( $H_{safe}$  [%]) with regard to the maximum water level in the dam ( $H_{dam}$ ) when the water level reaches the tipping head ( $H_{plug}$ )

# Recommendations for the design and installation of concrete fuse blocks

---

The tilting height of the blocks, used as a basis for the dimensioning table, is as follows:

$$H_{tilting} = P \cdot (1.022 \cdot 10^{-3} \cdot \rho_b - 1.2384) \quad (2)$$



This relationship was established in chapter 4 and simplified in section 5.1.1.

However, this tipping height can be determined from the table as follows:

$$H_{tilting} = H_{dam} - P - \frac{H_{safe}}{100} \cdot H_{dam}. \quad (3)$$

## II.iii Determining block dimensions

The dimensions of the block shown in Figure 1 are determined by the following equations:

$$e = \frac{12}{10} \cdot P \quad (4)$$

$$c = \frac{1}{4} \cdot P \quad (5)$$

$$s = \frac{1}{10} \cdot P \quad (6)$$

$$i = \frac{1}{20} \cdot P. \quad (7)$$

As far as the width of the blocks is concerned, there are no restrictions on placing blocks of different widths side by side.

The width of the blocks can be determined according to the width of the sill. However, it is recommended to use block widths two to three times greater than their height.



This recommendation follows on from the test observations discussed in the section 3.2.2 “Influence of adjacent blocks”.

## II.iv Considerations on construction precision

The previous sections have outlined the dimensions of the blocks to be used. However, it is important to consider certain tolerances regarding the constructional accuracy of the blocks' geometric and physical properties.

### II.iv.1 Density

For density, the ratio between the accuracy of the tipping head ( $\Delta_{Tipping}$ ) and the accuracy of the density ( $\Delta_{Density}$ ) is:

$$1.023 \cdot P = \frac{\Delta_{Tipping}}{\Delta_{Density}}. \quad (8)$$

# Recommendations for the design and installation of concrete fuse blocks

---

where the units of these parameters are :

- $P$  : [m];
- the coefficient 1.023 :  $[\frac{\text{mm}}{\text{kg/m}^3} \cdot \frac{1}{\text{m}}]$ ;
- $\Delta_{Density}$  :  $[\text{kg/m}^3]$ ;
- $\Delta_{Tipping}$  : [mm].

For example, for a 1 metre high block, the ratio is

$$1 \cdot 1.023 = \frac{\Delta_{Tipping}}{\Delta_{Density}}.$$

In other words, if a tolerance of 1 cm of uncertainty on the tipping height is accepted, the density of the block must be accurate to  $(10/1.023) = 9.78 \text{ kg/m}^3$  of the predicted value.

The accuracy of the density must be carefully considered, especially when the height of the block is significant. It is therefore advisable to pay particular attention when making the concrete mix and/or to produce sample blocks whose density will be measured to ensure accuracy.



The ratio and this recommendation are discussed in the section 4.3.3 “Influence of geometric and physical parameters”.

## II.iv.2 Height of the block $P$

For the height of the block, the ratio between the accuracy of the tipping head ( $\Delta_{Tipping}$ ) and the accuracy of the height ( $\Delta_P$ ) is:

$$-0.82 = \frac{\Delta_{Tipping}}{\Delta_P}. \quad (9)$$

where the units of these parameters are :

- the value 0.82 :  $[\frac{\text{mm}}{\text{mm}}]$ ;
- $\Delta_P$  : [mm];
- $\Delta_{Tipping}$  : [mm].

For example, if an uncertainty of 1 cm on the length is likely, the tipping head inaccuracy is about 0.82 cm.



This relationship is presented in the section 4.3.3 “Influence of geometric and physical parameters”.

# Recommendations for the design and installation of concrete fuse blocks

---

## II.iv.3 Length of the block $e$

For the length of the block, the ratio between the accuracy of the tipping head ( $\Delta_{Tipping}$ ) and the accuracy of the length ( $\Delta_{length}$ ) is:

$$1.53 = \frac{\Delta_{Tipping}}{\Delta_{length}}. \quad (10)$$

where the units of these parameters are :

- the value 1.53 :  $\left[\frac{\text{mm}}{\text{mm}}\right]$ ;
- $\Delta_{length}$  : [mm];
- $\Delta_{Tipping}$  : [mm].

*For example, if an uncertainty of 1 cm on the length is likely, the tipping head inaccuracy is about 1.53 cm.*



This relationship is presented in the section 4.3.3 “Influence of geometric and physical parameters”.

## III Additional elements to install on the sill

Additional elements must be present on the weir for the system to work properly.

### III.i Intermediate wall

To facilitate the use of fuse plugs, installing thin concrete walls between two adjacent blocks is advisable. These walls are typically fixed in the weir and do not need to be large. They are generally the same height as the blocks and 1.2 times the length of the blocks, as illustrated Figure 6.

Providing sufficient clearance between the intermediate walls and adjacent blocks is recommended to prevent them from touching. This clearance aims to avoid any risk of friction that could hinder the block from falling.



The influence of friction on the tipping is discussed in section 3.2.3 “Influence of friction”.

# Recommendations for the design and installation of concrete fuse blocks

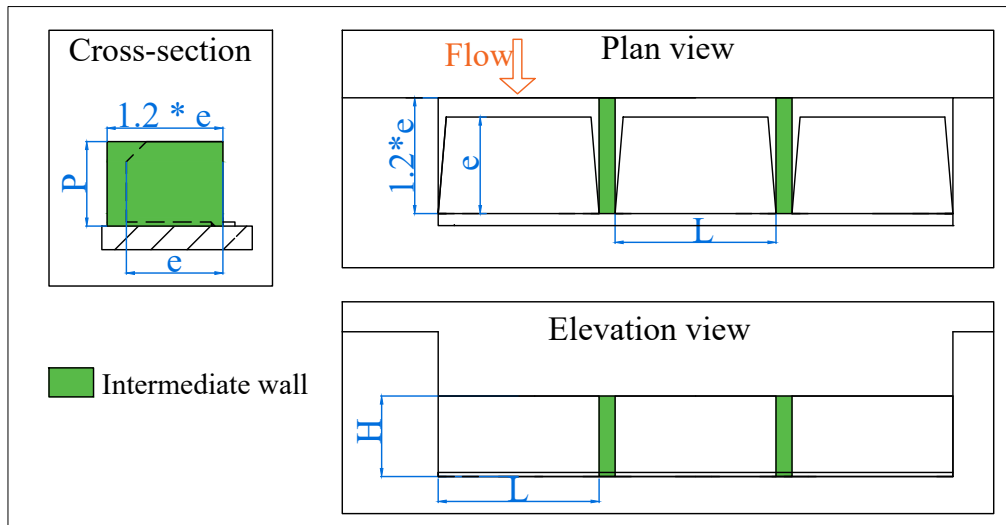


Figure 6: Diagram of general dimensions of intermediate walls



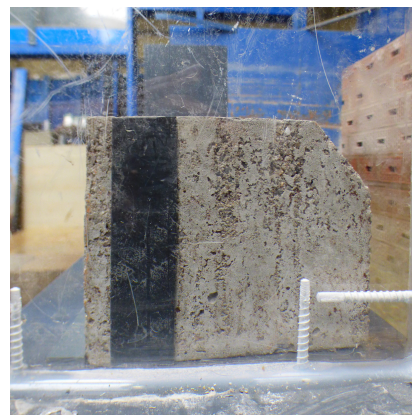
The importance of the presence of walls is explained in the background section.

To ensure a watertight seal, it is recommended to use a sealing strip such as thick plastic or rubber. This strip should be positioned to prevent leaks between adjacent elements while allowing the block to tilt freely.

An example of the positioning of the sealing strip is shown in the photos in Figure 7.



(a) Photo of folded plastic strip placement



(b) Photo of waterproofing strip in place

Figure 7: Waterproofing strip

## III.ii Abutment

To enable the blocks to tilt, it is essential to place them upstream of the abutments. These elements prevent the blocks from sliding under the effect of external stresses. It is recommended

# Recommendations for the design and installation of concrete fuse blocks

---

to use a bar of height  $i$ , as displayed in the drawings in Figure 8.

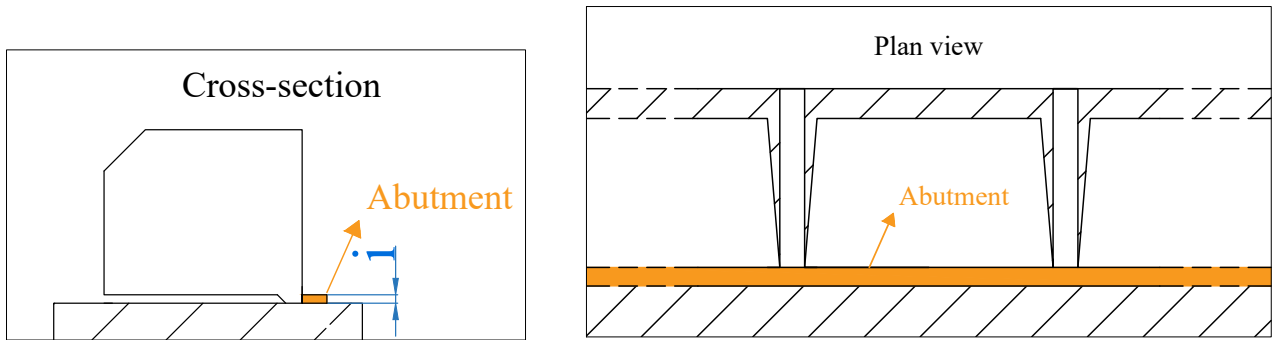


Figure 8: Drawings of the abutments

# Conclusion

In the introduction, it was pointed out that the concrete fuse plugs represent a promising solution for enhancing dam safety and increasing water storage capacity. Developed by the HydroCoop association, this technology addresses the critical needs of regions in Africa, particularly Burkina Faso. Many small dams in this country have been constructed to handle water resources. However, over time, these infrastructures have faced issues such as reduced storage capacity and the inability to properly discharge large flood flows. Effective water management is crucial for the country's development and the vital activities of local communities. These significant challenges necessitate an efficient solution, and fuse blocks, which are cost-effective and easy to install, fulfil this requirement. Therefore, formulating practical methods to facilitate the implementation of these plugs is essential. The primary aim of this project was to contribute to this research.

To achieve the final objective of this work, several stages were necessary.

Firstly, a literature review provided insights into the advancements in the field and identified areas for exploration in this study. Valuable practical recommendations drawn from experiences were uncovered. Furthermore, previous tests have been conducted, leading to the development of design formulas, notably by Hien and Khanh in 2007, and by Sekkour in 2016.

The methodology applied in this work consisted of carrying out experimental tests and developing an analytical model.

The tests aimed to achieve two objectives: first, to validate the correlation of the obtained results with the equations established in existing literature, and secondly, to discern the impact of parameters not accounted for in the theoretical model. To accomplish these objectives, new tests were performed rather than relying on previous research findings. It is to be noted that prior studies either did not consider the same block geometry as selected in this work or were not undertaken under specific conditions envisaged herein.

The experiments were conducted by means of a scale model and a basin designed to simulate reservoir conditions. Six blocks with underpressure of varying widths were studied. This project implemented two test configurations for individual block tilting: placed alone on the sill, and with adjacent blocks fixed beside them.

Several parameters influencing the overturning heights of the blocks were revealed by the tests:

- The position of the block on the sill influences the results for block B10, likely due to flow contraction at the weir ends.
- The presence of adjacent blocks acted as a stabilizer, delaying the overturning of block B10. However, this influence was less evident for block B20, while block B30 was unaffected by the change in configuration.
- Additionally, the absence of friction between the fuse plug and the intermediate walls proved crucial for the proper functioning of the system, requiring sufficient clearance between the various elements to ensure block overturning.



- It was concluded that no relationship between block widths (20 to 60 cm) and the results could be identified. The medians of the results for block B10 are higher than those of the other blocks. This phenomenon can be partly explained by the relative size of the underpressure chamber compared to its width.

Then, height intervals causing block overturning were determined for further analyses.

Next, the two formulas available in the literature were compared with the experimental results to assess their ability to model the overturning of the fuse plugs of this work. The first formula, put forward by Hien & Khanh, concerns a block geometry similar to that studied, while the second, proposed by Sekkour, is based on a simple rectangular block, implying simplifying assumptions in relation to the plugs examined. Despite its simplicity, Sekkour's formula proved to be the most representative of the experimental tests, although it systematically underestimated the observed data. To remedy this problem, a new analytical model was developed and fitted to the experimental tests, demonstrating better agreement with the observed overturning heights than the existing formulas. This new model improved the representation of the tests carried out, and highlighted the importance of pressure distribution assumptions in modelling such phenomena.

Lastly, a practical design table for block was developed. This table enables a person wishing to size fuse plugs to determine, based on their density and the permissible safety margin between the tipping level and the highest water level, the height of the plugs. Simple relationships are then used to calculate the other dimensions as a function of their height. The geometry of these plugs is derived from that of the studied blocks. Additionally, a summary of important points for the design and installation of blocks on a weir is provided, based on recommendations in the literature and discussions in this work.

Continuing the discussion, it is important to mention the limitations of this study and the prospects for future research.

One limitation is that the influence of block position on the sill and the potential role of flow contraction have not been fully explored. Although this observation has been made for the 10 cm wide fuse plug, tests on different positions of the others have not been carried out. It would therefore be advisable to extend this analysis in order to determine at what width relative to the weir the effect of flow contraction becomes negligible. In addition, it would be beneficial to explore different flow entry configurations on the weir, such as replacing angular ends with more gradual changes, or installing an entry corridor.

Another avenue of research would be to study in greater depth the pressure distributions applied to the blocks. As demonstrated above, the choice of these assumptions can have a significant influence on the results obtained by the analytical model. Consequently, it would be relevant to collect experimental data on the pressures actually applied to the plugs. This experimental approach would provide a better understanding of the interactions between the blocks and the flow, and help improve the accuracy and reliability of the analytical models used in the design of fusible plugs.

Moreover, this study focused on analysing blocks of different widths but consistent lengths. Consequently, the recommendations regarding the sizing did not consider the potential placement of fuse plugs with varying lengths on the same sill. Yet the literature suggests the advantage of placing elements of varying lengths to create multiple tipping level landings, although this is not essential. The analytical model developed in this work takes block length into account, enabling a tipping height to be determined. However, no experiments have been conducted to verify if the established mathematical expression accurately predicts results for

blocks of different lengths. It would be valuable, therefore, to experimentally validate this relationship.

This study could prove beneficial for designers seeking to improve the capacities of their spillways by providing a simple method for designing concrete fuse blocks. Finally, it could serve as a foundation for the development of a comprehensive practical guide for the use of this technology, offering explanations of its utility and design possibilities.

# Bibliography

- Philippe Cecchi. Les petits barrages au burkina faso : un vecteur du changement social et de mutations des réalités rurales. 01 2006.
- J.M. Durand, Paul Royet, and P. Mériaux. *Technique des petits barrages en Afrique sahélienne et équatoriale*. 01 1999.
- Truong Chi Hien and Michel Ho Ta Khanh. Report on fuseplugs without uplift model tests. Technical report, Ho Chi Minh city University of Technology, Faculty of Civil engineering, Department of Water resources engineering, 2006.
- Truong Chi Hien and Michel Ho Ta Khanh. Report on fuseplugs with uplift model tests. Technical report, Ho Chi Minh city University of Technology, Faculty of Civil engineering, Department of Water resources engineering, 2007.
- HydroCoop. Concrete fuse plugs, 2013. URL <http://www.hydrocoop.org/concrete-fuse-plugs/>.
- ICOLD - CIDGB. Appendix 3 - concrete fuse plugs. *Cost savings on dams - Economies dans les barrages*, (144):191–196, 2010.
- Pachuco Jean-Baptiste. Contribution à l'étude hydraulique expérimentale des blocs fusibles. Master's thesis, Université de Liège, 2014.
- Moussa Kabore, Founemé Millogo, Aïssa Nacanabo, and Jean Pierre Vigny. Implementation of concrete fuse plugs on gaskaye dam to increase the reservoir capacity. *ICOLD*, 2015.
- Sara Khezzar. Contribution à l'étude des déversoirs auto-stables. Master's thesis, Université Mohamed Khider, Biskra, 2019.
- Solomon Kibret, Matthew Mccartney, Jonathan Lautze, Luxon Nhamo, and Guiyun Yan. The impact of large and small dams on malaria transmission in four basins in africa. *Scientific Reports*, 11, 06 2021. doi: 10.1038/s41598-021-92924-3.
- Johan Lagerlund. Can a laboratory scale test replace a field test ? *FUSE PLUG BREACH TESTS ENERGIFORSKRAPPORT*, 465, 2018.
- F. Lempérière. Dams and floods. *Engineering*, 3:144–149, 02 2017. doi: 10.1016/J.ENG.2017.01.018.
- F. Lempérière and J.P. Vigny. Économie et sécurité des déversoirs du burkina faso. Publication by HydroCoop France, juillet 2013. URL <http://fr.hydrocoop.org/economie-securite-barrages-deversoirs-burkina-faso/>. Presented at the 1er Congrès National des Barrages, Burkina Faso. Accessed on 29.11.2023.
- Serge Marlet, Sidiki Sanogo, and Mariam Keita. Evaluation finale du "projet de réduction de la vulnérabilité des petits barrages aux changements climatiques (prvpb-cc)". Decentralised Evaluation 2017:16, Sida, Swedish Embassy in Burkina Faso, Février 2016.
- Mr. Reid. Hydraulic fuses. URL <http://wordpress.mrreid.org/2014/08/13/hydraulic-fuses/>.

- Lukas Schmocker, Esther Höck, Pierre André Mayor, and Volker Weitbrecht. Hydraulic model study of the fuse plug spillway at hagneck canal, switzerland. *Journal of Hydraulic Engineering*, 139(8):894–904, 2013. doi: 10.1061/(ASCE)HY.1943-7900.0000733.
- Ilyese Sekkour. Contribution à l'étude des déversoirs auto-stables. Master's thesis, Université Mohamed Khider, Biskra, 2016.